EARLY LIFE STRESS REGULATES EXPRESSION OF RISK GENES FOR MAJOR DEPRESSIVE DISORDER

DISSERTATION DER FAKULTÄT FÜR BIOLOGIE DER LUDWIG-MAXIMILIANS-UNIVERSITÄT MÜNCHEN

Prepared at

MAX PLANK INSTITUTE OF PSYCHIATRY

DEPARTMENT OF TRANSLATIONAL RESEARCH IN PSYCHIATRY

Christoph Andreas Zimmerman

München 2016

Erstgutachter: PD Dr. Carsten Wotjak

Zweitgutachter: Prof. Dr. Wolfgang Enard

Tag der Abgabe: 24.08.2016

Tag der mündlichen Prüfung: 28.04.2017

"Imagination is more important than knowledge.

For knowledge is limited."

Albert Einstein

Für meine Eltern

Abstract

Early life stress (ELS) is an important risk factor for the development of various mental disorders later in life. The hypothalamic-pituitary-adrenal (HPA) axis is the major physiological stress system and ELS during sensitive windows of development can induce long-lasting changes in its activity. Here, the long-term regulation of the HPA axis was investigated by two approaches. First, the expression and promoter methylation of corticotropin releasing hormone (CRH), the main stress hormone of the HPA axis, was analyzed in a maternal separation mouse model of early life stress. CRH expression was estrous cycle dependent in female controls, but not in females with a history of early life stress. As underlying mechanism, CRH promoter methylation was investigated but no significant changes were found. Second, a group of genes identified in a human study was evaluated in a translational approach in ELS mice. Since glucocorticoid receptors (GR) play an important role in the negative-feedback control of the HPA axis, genetic variation in GR-dependent gene networks is hypothesized to modulate the long-term effects of ELS. Recent work discovered a subgroup of GR-response expression quantitative trait loci (eQTLs) in humans, which mapped to chromosomal regions identified in previous GWAS studies for major depressive disorder (MDD) as well as schizophrenia (SCZ). These eQTL genes were tightly connected in a literature-based co-expression network. To investigate the long-term regulation of this network in response to ELS, we used two experimental models, namely postnatal maternal separation and limited nesting material. In adult mice (3 month), the interaction of ELS with either an acute pharmacological treatment (corticosterone injection) or a sustained social stressor (chronic social defeat) were analyzed. Network analysis revealed specific co-expression networks in brain regions associated with the stress response, whereby the PVN and CA1 regions formed the most connections. A central gene in two of the networks was Pds5a, a cohesin regulatory factor, which is involved in the modulation of long-range enhancer interactions established by CTCF. Taken together, our results suggest brain region specific regulation of the identified eQTL genes in two independent mouse models of ELS, which strengthens a possible role for the development of psychiatric disorders in men.

Zusammenfassung

Frühkindlicher Stress (FS) ist ein wichtiger Risikofaktor für die Entwicklung psychiatrischer Erkrankungen (u.a. Depression, Schizophrenie und Angsterkrankungen) im Jugendlichen- und Erwachsenenalter. Die Hypothalamus-Hypophysen-Nebennieren (HPA)-Achse ist das zentrale physiologische Stress-System in Säugern und FS in kritischen Entwicklungsphasen kann nachhaltige Veränderungen der HPA-Achsen Aktivität auslösen. In dieser Arbeit wurden langfristige Anpassungen in der Regulation der HPA-Achse in Folge von FS in zwei Tiermodellen untersucht. Im ersten Abschnitt wurden die Expression und die Promotor-Methylierung von Corticotropin-Releasing-Hormon (CRH), welches eine herausragende Rolle in der Regulation der HPA-Achse einnimmt, in einem Mausmodell für FS analysiert. Die CRH-Expression hing in weiblichen Kontrollmäusen, aber nicht in Weibchen mit FS, vom Geschlechtszyklus ab. Als möglicher Mechanismus wurden Veränderungen in der CpG Methylierung des proximalen Promoterabschnittes des CRH Genes untersucht. Hierzu wurden in verschieden, voneinander unabhängigen experimentellen Kohorten keine Hinweise gefunden. Im zweiten Abschnitt der Arbeit wurde in einem translationalen Ansatz ein humanes, Glukokortikoid-Rezeptor (GR) abhängiges eQTL (*engl*. expression quantitative loci) Netzwerk in FS Mäusen untersucht. Der GR spielt eine wichtige Rolle in der negativen Rückkopplung der HPA-Achse und genetische Variationen in GR-abhängigen Gen-Netzwerken könnten daher die langfristigen Auswirkungen von FS beeinflussen. Besonderes Interesse fand hierbei eine Untergruppe von GR-eQTLs, die in chromosomalen Bereichen lokalisierten, die in genomweiten Assoziationsstudien (GWAS) für Depression (MDD) und Schizophrenie (SCZ) identifiziert wurden. Diese MDD/SCZ-assoziierten eQTL Gene formten in einer Literatur-basierten Analyse ein enges Co-Expressions-Netzwerk. Um die langfristige Regulation dieses Netzwerks durch FS zu untersuchen, wurden zwei experimentelle Stressmodelle verwendet. Postnatale Trennung der Neugeborenen vom Muttertier oder mütterlicher Stress infolge von unzureichendem Nestmaterial. In erwachsenen Mäusen wurde die Interaktion von FS mit der akuten Gabe eines GR-Antagonisten oder chronischem sozialen Stress getestet. Netzwerk-Analysen zeigten, dass spezifische Co-Expressions-Netzwerke in ausgewählten Gehirnregionen mit der Stressantwort verknüpft sind, wobei im PVN und der hippocampalen CA1 Region die höchste Verknüpfungsdichte erreicht wurde. Ein zentrales Gen in zwei der Netzwerke war Pds5a, ein Cohesin-regulierender Faktor, der die Chromatin-organisierende Funktion von CTCF und dessen Interaktion mit distalen regulatorischen Elementen beeinflusst. Zusammenfassend zeigen diese Ergebnisse eine Hirnregion-spezifische Regulation der identifizierten eQTL Gene in zwei unabhängigen Mausmodellen für FS, welcher somit eine Rolle in der Entwicklung von psychiatrischen Erkrankungen zukommen könnte.

Contents

List of Figures

List of Tables

1 Introduction

1.1 Psychiatric disorders

Psychiatric disorders are on the rise worldwide. According to the Global Burden of Disease Study 2010 the highest number of years lived with disability worldwide can be attributed to mental and substance use disorders. Worryingly, the amount of disability-adjusted life years (DALYs) increased by over one third between 1990 and 2010 for mental and substance use disorders due to population growth and aging. Depressive disorders were hereby accounting for 40.5% of DALYs (Whiteford et al. 2013). Table 1 summarizes the features, prevalence and heritability of the nine most common psychiatric and substance use disorders.

Table 1: Defining features of nine psychiatric and substance use disorders (adapted from Sullivan et al. 2012)

Name	Life prevalence	Heritability	Essential characteristics	Notable feature
Alzheimer's disease	0.132	0.58	Dementia, defining neuropathology	Of the top ten causes of death in the United States, Alzheimer's disease alone has increasing mortality
Attention-deficit hyperactivity disorder	0.053	0.75	Persistent inattention, hyperactivity, impulsivity	Costs estimated at ~US$100 × 10^9 per year
Alcohol dependence	0.178	0.57	Persistent ethanol use despite tolerance, withdrawal, dysfunction	Most expensive psychiatric disorder (total costs exceed US$225 × 10^9 per year)
Anorexia nervosa	0.006	0.56	Dangerously low weight from self-starvation	Notably high standardized mortality ratio
Autism spectrum disorder	0.001	0.80	Markedly abnormal social interaction and communication beginning before age 3	Huge range of function, from people requiring complete daily care to exceptional occupational achievement
Bipolar disorder	0.007	0.75	Manic-depressive illness, episodes of mania, usually with major depressive disorder	As a group, nearly as disabling as schizophrenia
Major depressive disorder	0.130	0.37	Unipolar depression, marked and persistent dysphoria with physical and cognitive symptoms	Ranks number one in the burden of disease in the world
Nicotine dependence	0.240	0.67	Persistent nicotine use with physical dependence (usually cigarettes)	Major preventable risk factor for many diseases
Schizophrenia	0.004	0.81	Long-standing delusions and hallucinations	Life expectancy decreased by 12–15 years

Despite major efforts to understand the molecular nature of psychiatric disorders, only minor advances have been made. The most widely used antidepressant treatments are still selective serotonin reuptake inhibitors (SSRIs) like Citalopram, Fluoxetine or Paroxetine. Nevertheless, their exact

mechanism of action is still unclear. Therefore, psychiatric conditions are still referred to as `disorders´ in contrast to `diseases´, where the pathophysiological mechanisms are well established (Sullivan et al. 2012).

The most common psychiatric disorder with a lifetime prevalence ranging from 8% to 16% worldwide is major depressive disorder (MDD) (Kessler et al. 2003; The WHO World Mental Health Survey Consortium 2004). MDD is characterized by severely depressed mood which lasts for at least two weeks (American Psychiatric Association and American Psychiatric Association 2000) and is commonly accompanied by the loss of interest in normally enjoyable activities as well as a low self-esteem. Major depressive disorder shows comorbidity with various diseases with more than 50% of patients suffering from a comorbid anxiety or other psychiatric disorder. The presence of a comorbid disease results in increased severity and worse treatment outcome (Hirschfeld 2001).

One psychiatric disorder that frequently manifests with comorbid depressive symptoms is schizophrenia (SCZ). Häfner et al. report a lifetime prevalence of depressive mood in 83% of first admission schizophrenia cases. As discussed later, there is also a substantial genetic risk overlap between major depression and SCZ. In this line of thought, they propose that depressive symptoms preceding schizophrenia are an early, mild manifestation of the same malfunctioning neurobiological processes (Häfner et al. 2005).

1.2 Early life stress as risk factor for psychiatric disorders

It is well recognized that adverse early life events result in an increased risk for the later development of psychiatric disorders (Heim and Nemeroff 2001, 2002; Lupien et al. 2009; Green J et al. 2010). Numerous epidemiological studies have investigated the prevalence of child maltreatment and its influence on the development of psychiatric disorders.

1.2.1 Prevalence of early life adversities

Child maltreatment is a global societal challenge with a prevalence of 9.2 per 1000 children in the US population in 2012 (U.S. Department of Health and Human Services et al. 2013). Nearly four fifth of all maltreatment cases correspond to neglect followed by physical and sexual abuse (Figure 1). Even though the overall rate of maltreatment declined slightly (by 3.3 % over 5 years), the proportion of different types of maltreatment remained unchanged.

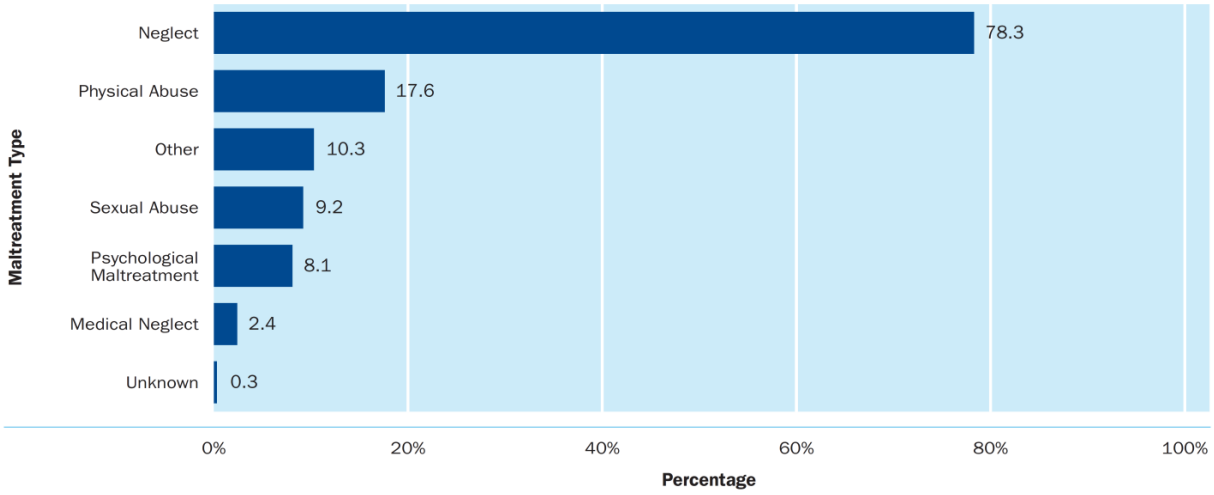

Figure 1: Types of child maltreatment. Percentage of maltreatment types for children in the US population (U.S. Department of Health and Human Services, et al. 2011).

Surveys conducted in the US population revealed that 14.2% of men and 32.3% of women experienced sexual abuse as well as 22.2% of men and 19.5% of women experienced physical abuse during childhood (Briere and Elliott 2003). Another study found similar numbers with sexual abuse being reported by 4.3% and 12.4% of men and women respectively as well as 29.9% of men and 21.2% of women reporting physical abuse (MacMillan et al. 2001). The latest National Survey of Children's Exposure to Violence also reports sexual assault in the past year in 3.7% of men and 4.6% of women between 14-17 years old (Finkelhor et al. 2015). The slight discrepancies between the numbers result from different definitions of the abuse types, the interview procedure, and the investigated time period among other variables. Generally, these retrospective interviews have several limitations. The response rate is typically rather low and thus a bias is expected. It can be argued that families which refuse participation are more likely to suffer from adverse social conditions and thus higher rates of abuse. Additionally, children may not be able to recall all of the adverse situations or caregivers may understate their children's exposures. On the other hand, interviews may be suggestive and situations recalled as more aversive than actually experienced. In conclusion, children are exposed to a substantial amount of maltreatment during their childhood, but this can only be assessed incompletely by psychological studies.

1.2.2 Relationship between early life adversities and psychiatric disorders

A strong relationship between all kinds of early life adversities and mental disorders has been established by numerous epidemiological and clinical studies. A dose-response relation between physical and sexual abuse as well as the witnessing of maternal battering in early life and adult mental health has been reported (Edwards et al. 2003). The Adverse Childhood Experiences study assessed childhood exposures like psychological, physical, and sexual abuse as well as several measures of household dysfunction. They found a graded relationship between the number of categories of adverse experiences and general health (summarized in Figure 2). For mental disorders, the risk

increased at least 4-fold when experiencing four or more categories of adverse childhood experiences (Felitti et al. 1998).

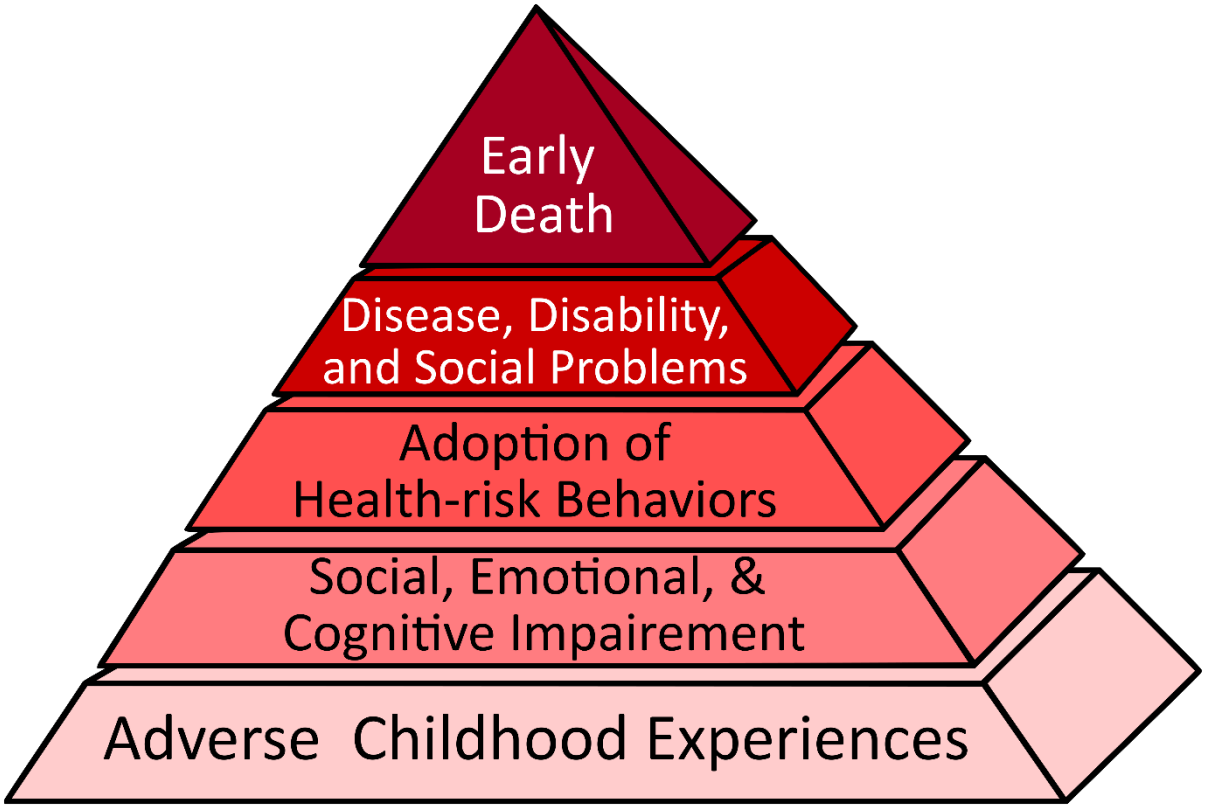

Figure 2: Long-term effect of adverse childhood experiences on physical and mental health.
Adverse childhood experiences often results in a vicious circle of health-risk behaviors. Low self-esteem abets smoking, alcohol or drug abuse. Anxiety, anger and depressed mood are risk factors for obesity and sleep disturbances. The relationship between these behaviors and the development of organic diseases are often overseen. Further, heart attacks, stroke and suicide can lead to preemptive death. (adapted from Felitti et al. 1998).

A strong dose-response relationship between adverse childhood experiences and the probability of lifetime or recent depressive disorders has also been reported by another study (Chapman et al. 2004). Childhood adversities also showed a graded relationship with suicide attempts; any adverse childhood experience increased the risk to attempt suicide by 2- to 5-fold (Dube et al. 2001). Concordant findings were also reported by the Ontario Health Survey (MacMillan et al. 2001). Conclusively, there is a strong association between early life adverse experiences and the development of depressive disorders in later life (Heim and Binder 2012).

1.3 Genetic heritability of psychiatric disorders

A large number of epidemiological studies support the genetic contribution to psychiatric disorders. Meta-analysis of twin studies estimated the genetic heritability of major depressive disorder to 37-38% (Sullivan et al. 2000; Kendler et al. 2006). Interestingly, the heritability differed greatly between men and women with 29% and 42%, respectively (Kendler et al. 2006). In light of the high heritability, there was great anticipation in genome-wide association studies (GWAS) to unravel the genes

responsible for these common disorders. However, up to now, with the exception of schizophrenia, GWAS could not fulfil their promises (Figure 3).

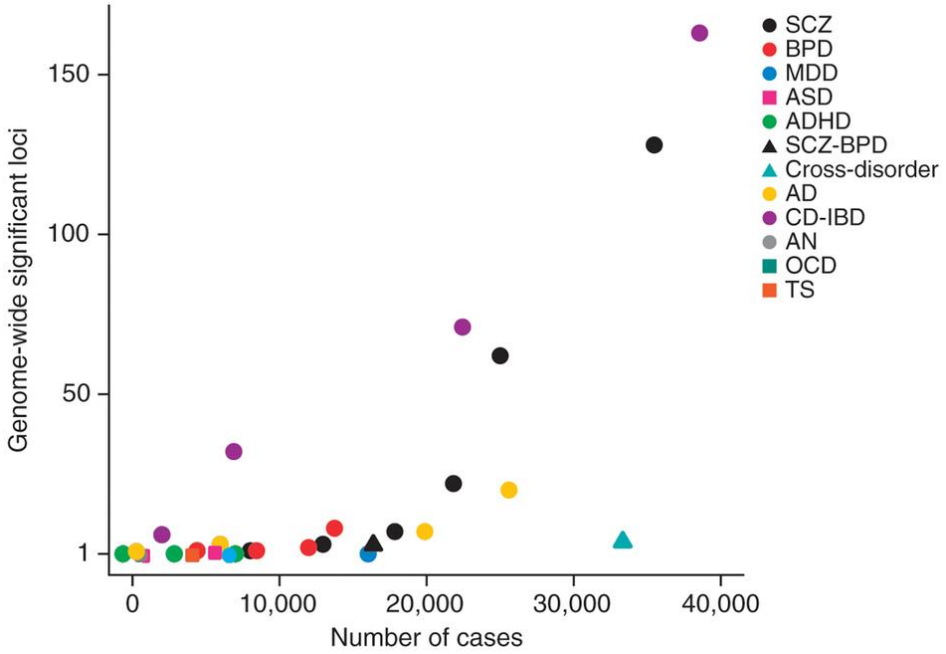

Figure 3: Number of genome-wide significant hits in GWAS studies for various psychiatric disorders in comparison to Crohn's disease and inflammatory bowel disease.
The number of genome-wide significant loci is plotted against the number of cases in genome-wide association studies (GWAS). For psychiatric disorders, the number of identified genome-wide significant hits is very low despite the high number of cases investigated. The only exception is schizophrenia (SCZ). BPD: bipolar disorder; MDD: major depressive disorder; ASD: autism spectrum disorder; ADHD: attention deficit hyperactivity disorder; Cross-disorder: broad psychiatric phenotype spanning ASD, ADHD, BPD, MDD, SCZ; SCZ-BPD, SCZ and BPD; AD: Alzheimer's disease; CD-IBD: Crohn's disease and inflammatory bowel disease; AN: anorexia nervosa; OCD: obsessive compulsive disorder; TS: Tourette's syndrome. (modified from Gratten et al. 2014)

For MDD, a recent Chinese study confined to women with recurrent MDD detected two significant hits (Converge Consortium 2015) while other studies were lacking any significant hits at all (Ripke et al. 2013). A possible explanation for the malperformance could be the high level of etiological heterogeneity among patients diagnosed with MDD. Additionally, the sample size (9240 MDD cases) was still far from the latest schizophrenia analysis which included 36,989 cases (Schizophrenia Working Group of the Psychiatric Genomics Consortium 2014). In the SCZ study, 108 genetic loci reached genome-wide significant levels (Figure 4) whereby 83 loci had not been reported previously.

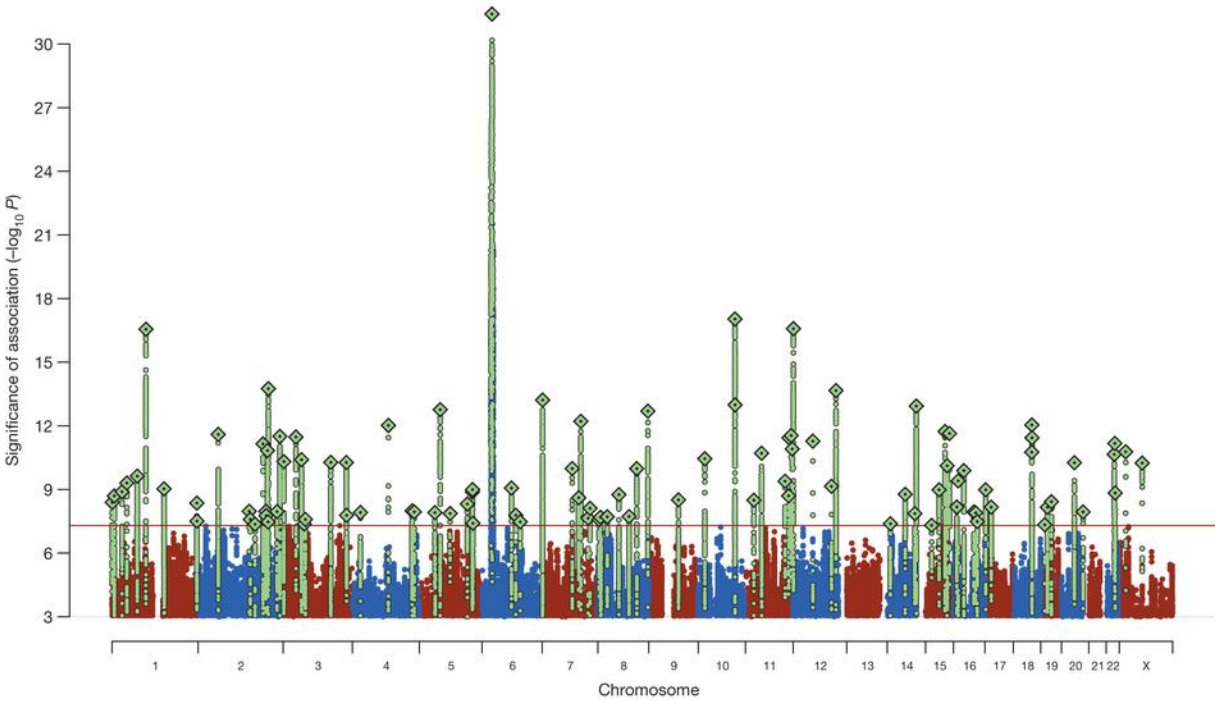

Figure 4: Manhattan Plot of the latest GWAS for schizophrenia with 108 genome-wide significant loci.
The distribution of genome-wide significant hits across the genome is plotted. The red line marks the level of genome-wide significance (5×10^{-8}). Green diamonds mark independent genome-wide significant index SNPs (Schizophrenia Working Group of the Psychiatric Genomics Consortium 2014).

Comparisons between the GWAS of different psychiatric disorders revealed substantial SNP-based coheritabilities and correlations. The highest correlation has been reported between schizophrenia and bipolar disorder (0.68) followed by schizophrenia and major depressive disorder (0.43) and bipolar disorder and major depressive disorder (0.47) (Cross-Disorder Group of the Psychiatric Genomics Consortium 2013). Moreover, a pathway analysis including GWAS data from schizophrenia, bipolar disorder, and major depressive disorder found an accumulation of risk genotypes in specific biological pathways which overlap between these disorders (The Network and Pathway Analysis Subgroup of the Psychiatric Genomics Consortium 2015). These findings highlight common genetic influences across psychiatric disorders.

1.4 Gene × environment interactions

Beside genetic factors, another critical factor for the development of psychiatric disorders are environmental influences throughout life, especially in early life. The interplay between environmental and genetic influences ultimately determines an individual's susceptibility to stressful experiences and thus their risk to develop psychiatric disorders.

1.4.1 Windows of Sensitivity

Every living being is exposed to various kinds of stressors throughout lifetime. These can differ in quantity and quality and are perceived differently on an individual basis. A healthy organism normally responds to these challenging situations with long-term and short-term physiological adaptions aiming

at reinstating homeostasis and preparing for further situations alike. However, there are periods in lifetime during which an organism is more susceptible to aversive exposures (Figure 5). Especially the brain passes through various critical periods prenatally and postnatally. Childhood as well as puberty comprise periods characterized by substantial rewiring and reorganization in the brain. Later in life, age-related mental decline can occur in adult and aged individuals.

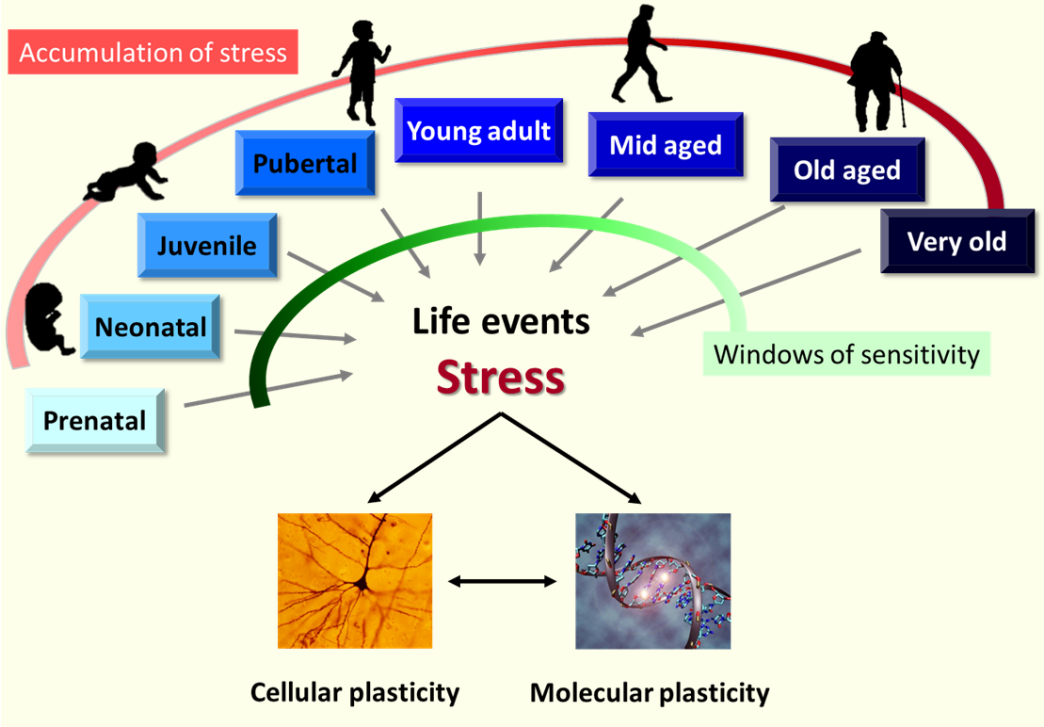

Figure 5: Windows of sensitivity and the accumulation of stress throughout life.
Throughout life, humans face various stressful life events. The impact of these events depends on the developmental stage of the individual and shapes the responsiveness to later events. The brains capability to adapt to environmental cues by cellular and molecular plasticity declines over lifetime. On the other hand, stressful experiences accumulate. The predictive value of early life events is thus influencing the stress-coping capability in later stages (Zimmermann et al. 2016).

Developing brain regions are most vulnerable to stressful disturbances (Lupien et al. 2009). Both positive as well as negative aversive experiences can influence activity-dependent plasticity and lead to permanent structural changes in brain circuitry as well as regulatory differences (Katz and Shatz 1996). Brain regions regulating HPA axis activity like the hippocampus, the frontal cortex, and the amygdala are especially affected by stress during their development in the perinatal period. In these brain regions, alterations can lead to long-lasting changes persisting into adulthood. The frontal cortex undergoes further major refinements during adolescence, which makes it sensitive to stressful experiences during this stage of life. Other brain regions, however, are more vulnerable to the effects of aging and thus affected by stress in later life. Vulnerability for stress-related disorders is therefore dependent on various experience-dependent adjustments throughout the brain in a stressor- and tissue-related manner (Murgatroyd and Spengler 2011).

1.5 Sex differences in psychiatric disorders

Sex differences in the prevalence of psychiatric disorders, especially major depressive disorder, are well known (Dohrenwend and Dohrenwend 1976; Kessler et al. 1993; Weissman et al. 1993). Overall, major depressive disorder was found to be twice as common in females compared to males (Figure 6). On the other hand, men are more severely affected by schizophrenia, attention deficit hyperactivity disorder, and autism (Holden 2005; Menger et al. 2010). Despite these differences between males and females, most studies, especially in animals, still fail to include females (Beery and Zucker 2011).

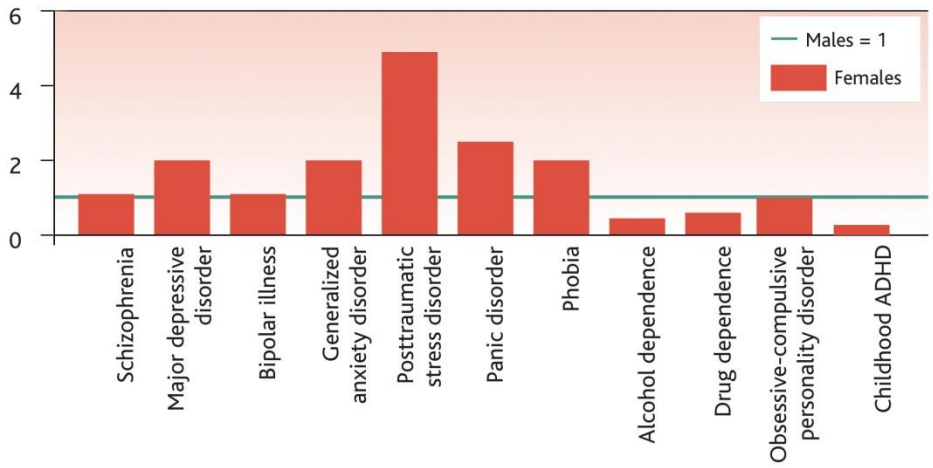

Figure 6: Sex ratio of various psychiatric disorders.
The incidence of various psychiatric disorders in females compared to males (=1) (modified from Holden 2005).

Also on the molecular level, there are differences in the response to stress between sexes. For example, the brain circuits involved, the effects on synaptic and neuronal plasticity, and the cognitive and emotional behavioral effects differ (Hodes et al. 2015). Taken together, there are pronounced sexual differences in the stress response but neuroscience research has so far fallen short in examining the molecular underpinnings in much detail.

1.6 Epigenetic modifications

Although the DNA sequence of all somatic cells of an organism is the same, various developmental processes result in the manifestation of a vast variety of cell types. The so-called epigenetic mechanisms, which do not alter the DNA sequence but alter the accessibility and three dimensional structure of the genome, result in specific expression patterns determining individual cell identities (Armstrong 2014). Besides histone modifications, the so far best studied epigenetic mechanism is DNA methylation, which we will focus on herein. Other epigenetic mechanisms include microRNAs and other non-coding RNAs as well as chromatin remodeling factors (Allis et al. 2015).

1.6.1 DNA methylation

DNA methylation is commonly referred to as the stable, covalent binding of a methyl group (CH_3) at a cytosine nucleotide. It is best studied in the context of CpG dinucleotides, which are normally depleted from the genome but can also form stretches of relatively high abundance, so-called CpG islands (Jeltsch and Jurkowska 2014; Schübeler 2015). CpG islands are often found in promoter regions and generally remain methylation free, whereas other CpGs are mostly methylated (Saxonov et al. 2006; Gibney and Nolan 2010). With the advent of whole genome bisulfite sequencing, it has been established that also non CpG methylation is present on the genome, but its function still remains to be elucidated (Lister et al. 2013).

DNA methyl transferases (DNMTs) catalyze the transfer of a methyl group onto the cytosine nucleotide. This family of enzymes is comprised of DNMT1, DNMT3A, DNMT3B, and DNMT3L (Ooi et al. 2009). DNMT1, the maintenance methyltransferase, recognizes hemimetylated DNA and ensures the conservation of methylation marks during DNA replication in the S phase. In contrast, DNMT3A and DNMT3B, the de-novo methyltransferases, recognize unmethylated DNA and catalyze new methylation marks in concert with other DNA binding proteins. One of these is DNMT3L, which has no catalytic activity itself but plays a role as scaffold (Kareta et al. 2006).

DNA methylation is generally associated with transcriptional repression (Bell et al. 2011; Thurman et al. 2012). Recent studies have however shown that this does not hold true on a genome-wide level. The effect of DNA methylation strongly depends on the sequence context and can be associated with both repression and activation of gene expression (Weber et al. 2007; Lister et al. 2009, 2013; Maunakea et al. 2010).

Historically, DNA methylation has first been studied in the context of imprinted genes, silencing of transposable elements, and cell lineage decisions (Hoffmann et al. 2015). However, the traditional view of DNA methylation as a stable modification which is established during differentiation had to be revised due to the recent discovery of active demethylation (Wu and Zhang 2014). Accordingly, DNA demethylation cannot only occur passively during cell division but also in mature cells like neurons. The core of the demethylation machinery is comprised of the ten-eleven translocation (Tet) family of enzymes (TET1-3). These enzymes catalyze the stepwise oxidation of 5-methylcytosine (5mC) to 5-hydroxymethylcytosine (5hmC) (Tahiliani et al. 2009; Ito et al. 2010) and further to 5-formylcytosine (5fC) and 5-carboxylcytosine (5caC) (He et al. 2011; Ito et al. 2011) (Figure 7). These oxidation products can then be recognized by various other enzymes. 5hmC can be directly deaminated by AID/APOBEC proteins, which generates 5-hydroxyuracil (5hmU). On the other hand, 5fC and 5ca are excised by the DNA glycosylase TDG (thymine DNA glycosylase). The enzymes of the base excision and/or nucleotide excision repair machinery (BER/NER) are then repairing the DNA at this position (Cortellino et al. 2011).

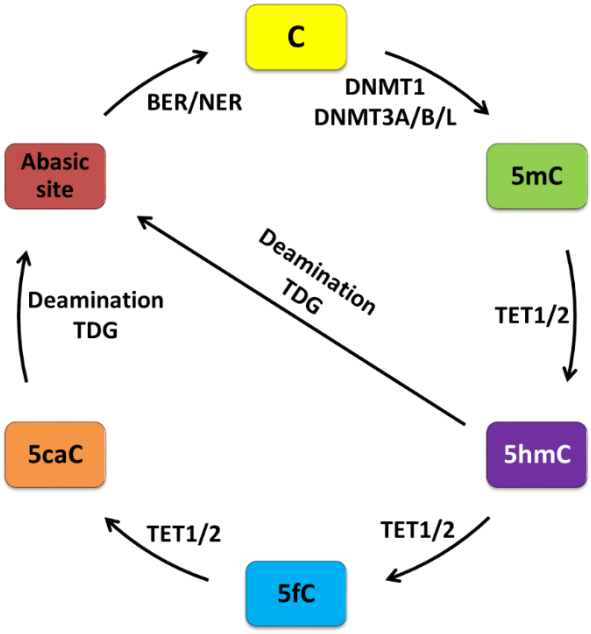

Figure 7: Iterative cycles of methylation and active demethylation.
Cytosine (C) nucleotides are methylated by DNA methyltransferases (DNMTs). Active demethylation by ten-eleven translocation (Tet) enzymes proceeds from 5-methylcytosine (5mC) via 5-hydroxymethylcytosine (5hmC) and 5-formylcytosine (5fC) to 5-carboxylcytosine (5caC). These cytosine derivatives are deaminated to thymine, removed by thymine DNA glycosylase (TDG) and subsequently repaired by the base excision and/or nucleotide excision repair machinery (BER/NER) (Zimmermann et al. 2015).

It has been proposed that not only methylation but also hydroxymethylation and its derivatives at cytosine nucleotides have various functions. They are present at regulatory sites throughout the genome (Lister et al. 2013) and specific reader proteins have been found for each of them (Spruijt et al. 2013). In summary, DNA methylation is a dynamic epigenetic mark, which is involved in many different processes. Active demethylation as well as the recruitment of specific reader and effector proteins is involved in its regulation.

1.7 The HPA axis

The hypothalamic-pituitary-adrenal (HPA) axis is well known for its central role in the neuroendocrine stress response. It is activated by a broad variety of physiological and psychological stressors and coordinates the cognitive, behavioral, and metabolic stress response of the organism. Extrinsic and intrinsic stressors trigger the release of corticotropin-releasing hormone (CRH) and arginine vasopressin (AVP) from the paraventricular nucleus (PVN) of the hypothalamus (Figure 8).

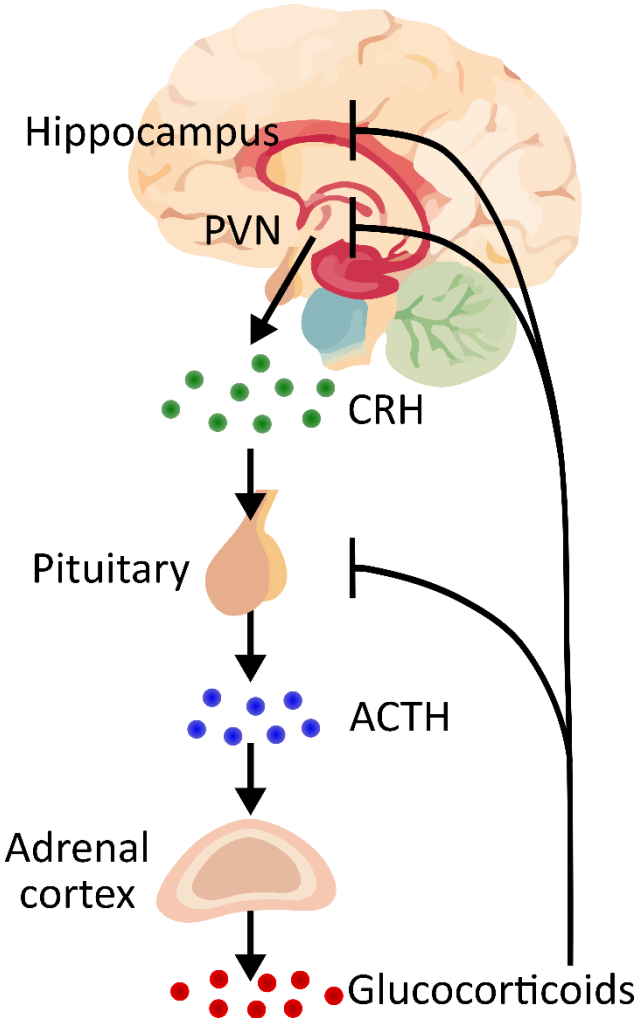

Figure 8: The hypothalamic-pituitary-adrenal axis.
Upon stress, corticotropin-releasing hormone (CRH) is released from the paraventricular nudeus (PVN) which results in the release of adrenocorticotropic hormone (ACTH) from the pituitary. ACTH stimulates the release of glucocorticoids from the adrenal cortex. Negative feedback by glucocorticoids occurs in the hippocampus, the PVN and the pituitary.

CRH and AVP are transported through the median eminence to the anterior pituitary where they bind their respective receptors. This triggers transcription of pro-opiomelanocortin (POMC) which is processed postranslationally to adrenocorticotropic hormone (ACTH). ACTH binding at the adrenal cortex, in turn, stimulates the production and secretion of glucocorticoids (cortisol in humans and corticosterone in humans, rats, and mice). These glucocorticoids orchestrate the bodies peripheral stress response, which includes the release of glucose from the liver and the suppression of the immune system. However, the stress response is tightly regulated by a negative feedback loop at pituitary, hypothalamic and hippocampal levels. There, glucocorticoids bind to the respective receptors, glucocorticoid receptor (GR) and mineralocorticoid receptor (MR), and reinstate the homeostatic equilibrium by shutting down the stress response (de Kloet et al. 2005).

1.8 Stress related disease models in rodents

The molecular and behavioral effects of stress are well studied in rodents by a wide variety of models. This includes both the time of stress (prenatal, postnatal, adult) and the duration (acute or chronic) of the stress as well as a combination of them. Since the CRH gene is one of the main effectors of the stress response, its promoter methylation and RNA expression has been investigated in several different animal models (Figure 9). Conclusively, epigenetic programming of CRH expression occurs in a stressor-, sex-, and tissue-specific manner (Raabe and Spengler 2013).

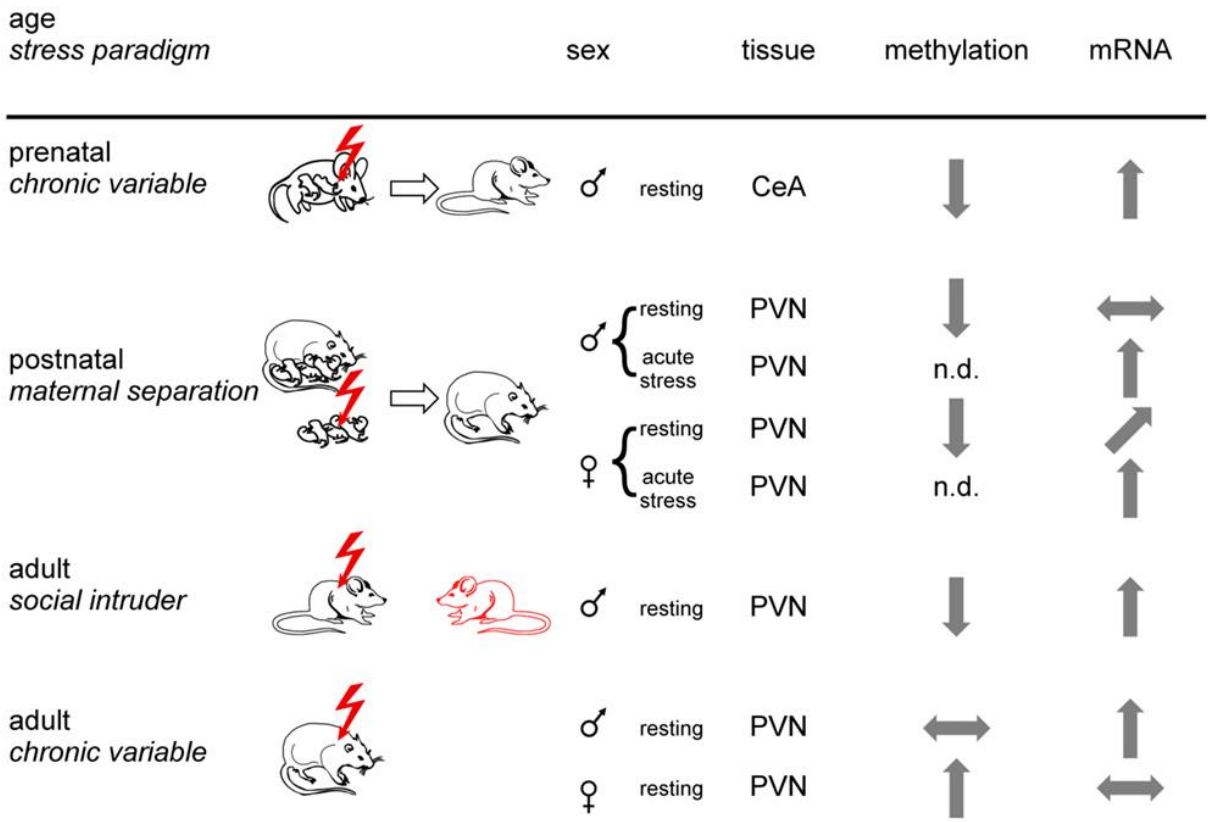

Figure 9: Different experimental stress responses in rodents and their influence on CRH promoter methylation and RNA expression.
Mice and rats were exposed to different stress paradigms at different times of age. CRH promoter methylation and expression changes in the paraventricular nucleus (PVN) and the central amygdala (CeA) are depicted by arrows. ♂: male; ♀: female; n.d.: not determined (Raabe and Spengler 2013).

1.8.1 Animal models of early life stress

Since the postnatal period is critical for the development and maturation of various brain regions like the hippocampus, experimental manipulations in this period are often used to study the long-term consequences of stress exposure (Lucassen et al. 2013). Figure 10 summarizes the most common paradigms to induce early life stress in rodents.

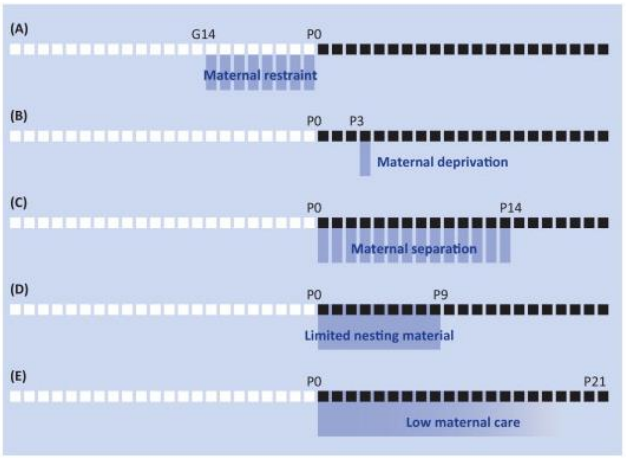

Figure 10: Different paradigms to induce early life stress in rodents.
A: exposure of the pregnant dam to repeated stress; B: a single separation of dam and pups for 24 hours; C: daily separation of dam and pups for 2-5 hours; D: reduced nesting and bedding material; E: selection of the dam based on the natural variation in maternal care (Lucassen et al. 2013).

The overarching principle underlying all these experiments is the alteration of maternal sensory input and care. This includes a disturbed dam-pup interaction, which also affects other key components like warmth, nutrition, and social interaction. Overall, lasting effects of these manipulations on brain structure and function could be shown.

1.8.1.1 Maternal separation

The first of the two early life stress models used in this study was maternal separation. Maternal separation is a well-established model to induce early life stress in rodents and consists of daily 3h separation of the pups from the dam for the first 10-14 days of their life (Pryce and Feldon 2003; Millstein and Holmes 2007). In previous studies, we could already show that early life stress in C57BL/6 mice induces long-lasting changes on all levels of the HPA axis (Murgatroyd et al. 2009; Wu et al. 2014; Bockmühl et al. 2015).

1.8.1.2 Limited nesting material

The second mouse model for early life stress used in this study was the limited nesting and bedding material paradigm. It was first established in rats (Gilles et al. 1996; Ivy et al. 2008) and later transferred to mice (Rice et al. 2008). In both species, a fragmented maternal care was shown to increase corticosterone levels in the pups with long-lasting consequences on CRH expression. In contrast to maternal separation, the overall amount of maternal care is not changed in this paradigm but is rather fragmented and unpredictable. Thus, it might closer resemble the human situation (Molet et al. 2014).

1.8.2 Modeling adult life adversities

In order to test the programming effects of early life stress, mice can be exposed to a second stressor in adulthood. The possible variations of adult stress are numerous, therefore, only the paradigms selected herein will be shortly described.

1.8.2.1 Pharmacological intervention

As a partial surrogate of stress, the injection of corticosterone was chosen in adult mice. Corticosterone was preferred to dexamethasone due to its capability to cross the blood brain barrier. Moreover, corticosterone is the natural ligand to the glucocorticoid receptor in contrast to the synthetic glucocorticoid dexamethasone.

1.8.2.2 Chronic social defeat stress

The chronic social defeat stress paradigm has been well characterized and validated within and outside the institute (Berton et al. 2006; Kinsey et al. 2007; Haenisch et al. 2009; Wagner et al. 2011; Balsevich et al. 2014). Generally, mice are exposed to an aggressive, dominant resident mouse, often represented by a CD1 mouse. After the mouse has been defeated, it is separated from the aggressor but still stays in sensory contact. This is applied either as single defeat stress or chronically for a varying number of days. When defeated chronically, each day an unfamiliar aggressor is presented. Chronic social defeat creates a persistent emotional stress without habituation and results in persistent social avoidance (Hollis and Kabbaj 2014).

1.8.3 The match mismatch hypothesis of cumulative stress

There are two prominent hypotheses about the interaction of stressful events throughout life which are partly conflicting each other. The cumulative stress hypothesis, also called two-hit model, suggests that stressful events in early life predispose for pathological outcomes of adult stress or, generally, that more stress exposure leads to worse outcomes (Walker et al. 2009; Taylor 2010). In contrast, the mismatch hypothesis states that harsh environments in childhood can prepare for adult stress. Therefore, individuals which experienced stressful situations during early life are better off than non-stressed counterparts when facing adverse situations in adulthood. Thereby, the consequences of stressful life events are rather a matter of correct forecast and adaption then the actual stressor (Schmidt 2011; Frankenhuis and Del Giudice 2012). Supportive evidence for this hypothesis could already be gained in our institute (Santarelli et al. 2014).

Even though the two hypothesis seem to be mutually exclusive there has been an effort to reconcile them (Nederhof and Schmidt 2012). A third dimension, in addition to early and adult stress, the programming sensitivity of an individual, has been hypothesized. This variable means that the individuals' ability to respond and adapt to environmental cues is taken into account. Consequently,

individuals with high programming sensitivity would benefit from matching environments even if they were aversive. On the other hand, individuals with low programming sensitivity are not able to adapt to early life adversities and thus have problems dealing with stress in adulthood.

1.9 Bioinformatics methods

1.9.1 Batch correction analysis

The consequences of batch effects in high throughput technologies are often underestimated. Batch effects occur for example when subsets of an experiment are performed by a different experimenter, on different days, or with a new lot of reagent. In contrast to low throughput experiments, where batch effects also occur, the data quantities of high throughput technologies like next generation sequencing allows to detect them and correct for it (Leek et al. 2010). Batch effects are avoided by randomization but the full extent of technical and biological artifacts cannot be rigorously determined. Therefore, various methods to correct for batch effects have been established, including surrogate variable analysis (SVA) (Leek and Storey 2007). SVA seeks to detect expression heterogeneity, which are patterns of variation due to an unmodeled factor, within the expression data and estimates surrogate variables correcting for it. Thereby, not only the disturbances by known factors like age, gender, or extraction date can be identified and resolved but unknown factors or interactions between factors as well. The surrogate variables can then be used as covariates in the differential expression determination. In alternative to the SVA, the use of another batch correction method called ComBat is possible. ComBat removes technical batches known to the user, but only one at a time. Moreover, the batch that should be removed has to be protocolled within the experiment and thus be known to the experimenter. This is not always the case since sometimes small but recurrent technical variations or some biological properties are not completely documented. SVA is superior in this case since it predicts batches from within the data. This, on the other hand, results in the possibility of overcorrection. An unbiased data exploration outside of the experimental question is not possible after such corrections (Jaffe et al. 2015).

1.9.2 Differential gene expression analysis

Differential gene expression analysis was conducted with TruSeq® Targeted RNA sequencing (2.2.7). The advantage of this method is the relative time and cost efficiency when compared to standard methods like qPCR and RNA sequencing. qPCR analysis is advantageous when comparing a limited number of genes (1-10) in a large number of samples. With RNA sequencing, on the other hand, the whole transcriptome is sequenced but the number of samples that can be analyzed is limited by the high costs per sample. With TruSeq® Targeted RNA sequencing, the advantages of both methods are combined. Frequently, a subset of genes e.g. a specific pathway or specific marker genes (around 100

genes) are determined by previous experiments. Thus, it is not necessary to sequence the whole transcriptome; however, a large number of samples is analyzed. In this case, TruSeq® Targeted RNA sequencing offers the possibility to sequence a customized set of genes (12-1000) in up to 384 samples at once.

The data gained by TruSeq® Targeted RNA sequencing is represented in counts per transcript. Therefore, standard methods from RNA sequencing can be adapted. In both cases, the number of sequencing reads that correspond to the transcript of a known gene are counted. Subsequently, differences in the quantity of sequenced transcripts, the gene expression level, are compared between experimental groups (Anders et al. 2013). The analysis of count data is well established and has been proposed to be best modeled by a negative binomial distribution (Whitaker 1914). There have been several R packages developed which facilitate the differential expression analysis of sequencing count data: DESeq (Anders and Huber 2010) and its successor DESeq2 (Love et al. 2014) as well as edgeR (Robinson et al. 2010). These are the most popular ones and all belong to the Bioconductor software development project (Gentleman et al. 2004). Beside these sophisticated packages there are also the basic functions for linear models `lm()` from the stats package (Chambers and Hastie 1993) as well as the generalized linear model with negative binomial distribution `glm.nb()` in the MASS package (Venables and Ripley 2002). The use of these basic functions offers the possibility to adjust the analyzing process dependent on the available data and specific needs of the researcher e.g. the combination with the aforementioned batch correction methods.

1.9.3 Network analysis - partial correlation co-expression networks

Gene co-expression networks are a straightforward representation of the functional connectivity of genes. Network nodes represent genes and edges connect genes which are significantly co-expressed (Zhang and Horvath 2005). Co-expression of genes has been shown to be tightly connected to functional similarity (Eisen et al. 1998). Thus, co-expression networks can provide insight into cellular processes that require orchestrated gene expression.

To measure the co-expression between any two genes the Pearson correlation coefficient is generally used. Genes are connected by edges if the coefficient exceeds a specific threshold, this results in a so called “relevance network”. However, a correlation between two genes can result from several associations in this scenario. Genes can be in direct or indirect interaction or can be regulated by a common gene (Schäfer and Strimmer 2005). Thus, it is more appropriate to use the partial correlation coefficient, which depicts only direct interactions. Partial correlation quantifies the correlation between two genes (A and B) while conditioning for one or more other genes (X, Y, Z, …). The correlation of other genes is regressed out from the correlation between A and B, thus the partial correlation between A and B is the part of gene expression which is uncorrelated with other genes

(Fuente et al. 2004). This idea is implemented by graphical Gaussians models (GGMs) (Dempster 1972). GGMs depict only direct edges in an undirected manner between the genes. The R package GeneNet uses GGMs to infer gene association networks which allow the identification of co-regulated genes (Schaefer et al. 2015).

1.10 GR-response eQTLs associated with major depressive disorder

In a recent study, Arloth et al. investigated the influence of single nucleotide polymorphisms (SNPs) on GR target gene activation on a genome-wide level. In their study, 160 male individuals were administered dexamethasone, a synthetic glucocorticoid, to measure the genome-wide activation of target genes in a genotype dependent manner. Blood samples were taken before and 3 hours after dexamethasone application and genome-wide gene expression was measured by microarray analysis. Additionally, DNA was extracted for genome-wide genotyping. The combination of these data allowed the identification of GR-response cis-eQTLs, which are SNPs regulating the GR-dependent activation of a gene in a genotype specific manner (Figure 11).

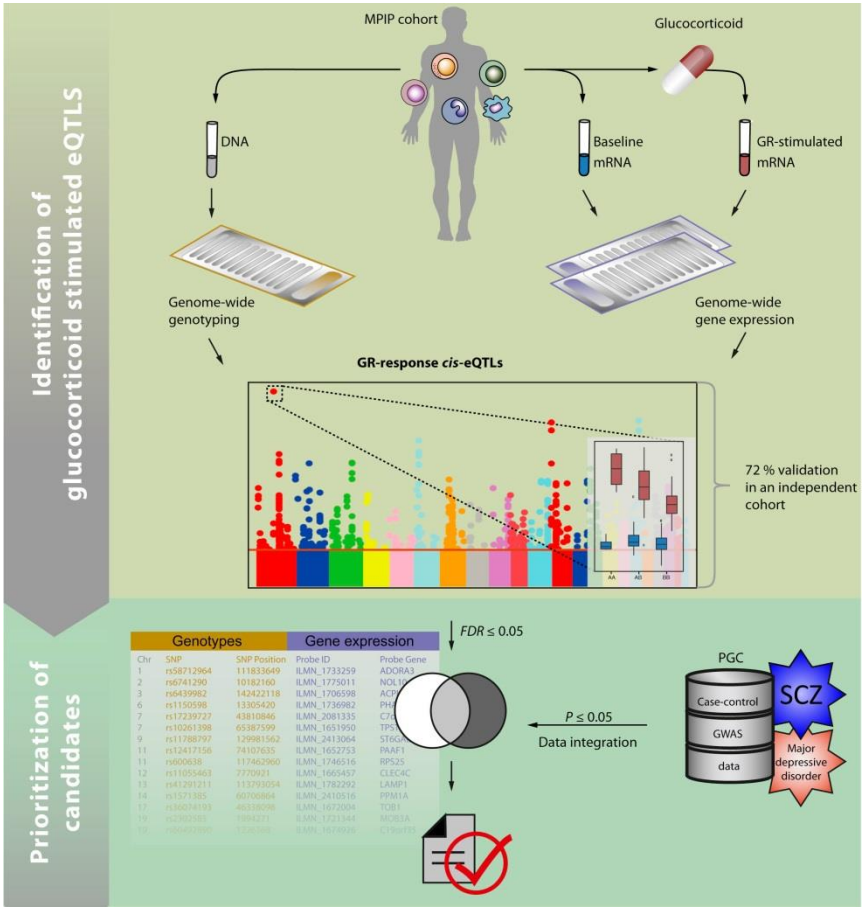

Figure 11: Flow chart summarizing the experimental setup and analysis conducted in the study by Arloth et al.
GR-response expression quantitative trait loci (eQTLs) are identified in whole blood of human males and prioritized by mapping to nominally significant loci from genome wide association studies (GWAS) for major depressive disorder and schizophrenia (SCZ) (adapted from Arloth et al. 2015).

These SNPs were then matched with data from genome-wide association studies (GWAS). GWAS for major depressive disorder (MDD) have so far detected genome-wide significant signals only with limited success (Ripke et al. 2013; Converge Consortium 2015). Therefore, nominally significant hits ($p \leq 0.05$) from Ripke at al. were matched with the identified GR-response eQTLs to obtain 23 MDD-related GR eSNPs. These 23 MDD-related GR-response eQTL genes formed a tightly connected co-expression network (Arloth et al. 2015).

1.11 Aim of the study

Early life stress is a well-established risk factor for depressive disorders later in life. In this study, we wanted to dissect the molecular underpinnings of this relationship with the help of mouse models for depressive disorders on the epigenetic as well as the genetic level (Figure 12).

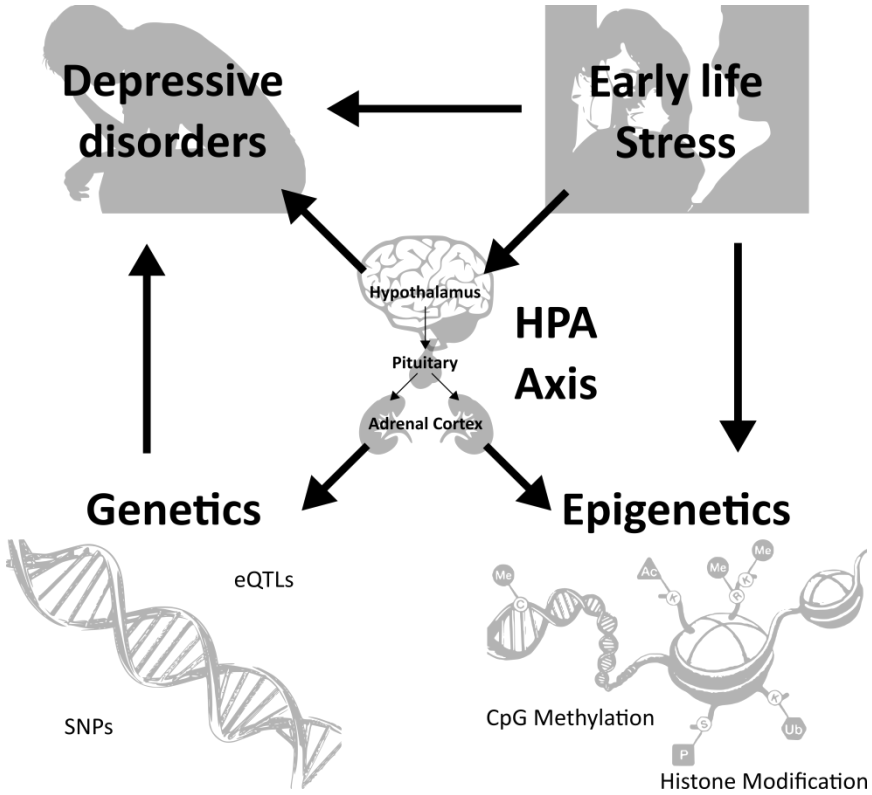

Figure 12: Conceptual framework of the study.
The development of depressive disorders is influenced by early life stress that alters the hypothalamic–pituitary–adrenal (HPA) axis responsiveness via epigenetic programming. Additionally, genetic factors influence the risk of developing psychiatric disorders. Here, the interplay between depressive disorders and early life stress has been investigated on both the epigenetic as well as the genetic level. The first part focuses on epigenetic programming of CRH; the second part investigates the regulation of MDD/SCZ-related GR-response eQTLs.

In the first part, we applied a candidate approach. As the HPA axis is the major stress response system, we investigated one of its main stress hormones, CRH. Previous studies have already shown that AVP, which works in concert with CRH, is epigenetically programmed by early life stress (Murgatroyd et al. 2009) as well as its downstream target POMC (Wu et al. 2014). Further, also the glucocorticoid receptor

gene, which plays an important role in the negative feedback control of the HPA axis, has been shown to be epigenetically programmed in response to early life stress (Bockmühl et al. 2015). In this line, CRH expression and methylation were investigated in adult mice with a history of maternal separation.

In the second part, the gene expression of previously identified eQTL genes was investigated. Based on the study by Arloth et al. (2015) we evaluated the properties of the psychiatric disorders-related GR-response eQTL network in two related mouse models of ELS. The use of these experimental models allowed us manipulations at specific time-points and access to brain tissue. With the help of a new technique, TruSeq® Targeted RNA sequencing, we could pursue an unbiased approach and investigate the expression of the identified eQTL genes in a multitude of stress related brain regions. Further, the long-term effects of early life stress, alone and in conjunction with an adult stressor, could be evaluated.

2 Materials and Methods

2.1 Materials

2.1.1 Equipment

Name	Model	Manufacturer
Bioanalyzer	2100	Agilent
Cryostat	CM3050S	Leica
Desktop Sequencer	MiSeq	Illumina
Dual channel liquid swivel	TCS2-23	Eicom
FEP tubing	i.d. 0.15±0.05 mm	Microbiotech/se AB
Fluorometer	Qubit 3.0	Invitrogen
Gel Documentation System	UVT 2035	Herolab
LightCycler	2.0	Roche
Liquid scintillation counter	LS 6000IC	Beckmann
Microcentrifuge	Microfuge 18	Beckman Coulter
Microcentrifuge (cooling)	5415R	Eppendorf
Microsampler	820	Univentor
NanoPhotometer	P-300	Implen
pH-Meter	inoLab ph720	WTW
Precision Balance	PM2500 DeltaRange	Mettler Toledo
Real Time PCR	MiniOpticon™ MJ mini	Biorad
Scanner	CanoScan 9950F	Canon
SmartSpec Plus Spectrophotometer	170-2525	Biorad
Thermocycler	TGradient 96	Biometra
Thermomixer	Compact	Eppendorf
Ultrapure Water System	PURELAB Ultra	ELGA LabWater
Vortexer	MS2 minishaker	IKA

Table 2: Equipment

2.1.2 Chemicals and consumables

Name	Provider	Cat. Number
0.1 cm Gene Pulser Cuvette	Biorad	165-2083
1kb Plus DNA Ladder	Invitrogen	10787-026
2-propanol	Roth	6752
300 µl microtubes	Microbiotech/se AB	4001048
5-Bromo-4-chloro-3-indolyl β-D-galactopyranoside (X-Gal)	Sigma	B4252
Acetic anhydride	Sigma	A6404
Agar	Roth	5210.2
Agarose	PeqLab	35 1020
BioMax MR film 30x40 cm	Kodak	8929655
Bio-Spin® Columns with Bio-Gel®	BioRad	732-6002
Bromophenol Blue	Sigma	B0126
Chloroform	Sigma	C2432

Corticosterone: HBC complex	Sigma	C174-100MG
Cover slips	DURAN Group	23 550 34
Cresyl Violet acetate	Sigma	C5042
Denhardt's Solution 50x	Sigma	D2532
Dextran sulfate	Sigma	D8906
Dimethyl sulfoxide (DMSO)	Sigma	D8418
di-Potassium hydrogen phosphate trihydrate (K_2HPO_4 x $3H_2O$)	Roth	6878
di-Sodium hydrogen phosphate dihydrate (Na_2HPO_4 x $2H_2O$)	Merck	106576
Dithiothreitol (DTT)	Sigma	D9779
DNA	Sigma	D7656
dNTPs	Thermo Scientific	R0181
Ethanol	Merck	100983
Ethylenediamine tetraacetic acid disodium salt dihydrate (EDTA)	Roth	X986
Formaldehyde	Sigma	F8775
Formamide	Fluka	47670
Glycerol	Roth	3783
Glycogen	Roth	HP51
Insulin Syringe	BD	320801
Isopropyl β-D-1-thiogalactopyranoside (IPTG)	Sigma	I6758
Metacam® (5mg/ml)	Boehringer Ingelheim GmbH	
Microdialysis CMA 11 Guide Cannula	CMA	8309018
Microdialysis Probe (11 Metal Free)	CMA	8011083
Microvette 200 EDTA Tubes	Sarstedt	20.1288
NucleoFast® 96 PCR Plates	Macherey Nagel	743100
Optitran® nitrocellulose membrane	Whatman	10 439 196
Pattern Resin LS	GC America	335201
Phenol/chloroform/isoamylalcohol	Roth	A156
Potassium chloride (KCl)	Sigma	P9541
Potassium dihydrogen phosphate (KH_2PO_4)	Merck	104873
Protein Assay Dye Reagent Concentrate	BioRad	500-0006
Protein marker	Fermentas	SM 1811
Sodium chloride (NaCl)	Roth	9265
Sodium dodecyl sulfate (SDS)	Sigma	436143
ß-mercaptoetanol	Sigma	63689
Superfrost™ Plus microscope slides	Thermo Scientific	J1800AMNZ
Tissue Freezing Medium	Leica	14020108926
Triethanolamine (TEA)	Sigma	T1377
tri-Sodium citrate dihydrate ($Na_3C_6H_5O_7x2H_2O$)	Roth	HN12
Triton X-100	Roth	3051.3
TRIzol® Reagent	Invitrogen	15596-018
Tryptone/Peptone	Roth	8952.2
Tween 20	Roth	9127.1
Uridine 5´-(α-thio) triphosphate [^{35}S]	Perkin Elmer	NEG-039H
Xylene cyanol FF	Sigma	X4126
Yeast extract	Roth	2363.2
Yeast total RNA	Sigma	R6750

Yeast tRNA	Sigma	R9001

Table 3: Chemicals and consumables

2.1.3 Enzymes

Name	Provider	Cat. Number
ABsolute Blue qPCR SYBR Green	Thermo Scientific	AB 4166
DNA Polymerase I, Large (Klenow) Fragment	Invitrogen	18012-021
FastAP Thermosensitive Alkaline Phosphatase	Thermo Scientific	EF0654
HotStarTaq® *Plus*	Qiagen	203601
Proteinase K	Sigma	P2308
Restriction enzymes	Fermentas/New England Biolabs	
RevertAid Premium Reverse Transcriptase	Thermo Scientific	EP0731
RiboLock RNase Inhibitor	Thermo Scientific	E00382
RNAse A	AppliChem	A2760,0100
RQ1 RNase-Free DNase	Promega	M 6101
T4 DNA Ligase	Fermentas	EL0014
T4 Polynucleotide Kinase	Fermentas	EK0031
***Taq* DNA Polymerase**	Thermo Scientific	EP0403
ProtoScript® II Reverse Transcriptase	New England Biolabs	M0368

Table 4: Enzymes

2.1.4 Buffers and solutions

Name	Composition	
10x PBS	NaCl (1.37 M)	80 g
	KCl (27 mM)	2 g
	KH_2PO_4 (20 mM)	2.7 g
	Na_2HPO_4 x $2H_2O$ (100 mM)	17.8 g
	DEPC-Water, fill up to	1000 ml
20x SSC	NaCl	175.3 g
	Na citrate ($Na_3C_6H_5O_7x2H_2O$)	88.2 g
	Dissolve in 800 ml water, adjust pH 7.0 with HCl and fill up to 1 L with a.d.	
SOB Medium	Tryptone	20 g
	Yeast extract	5 g
	NaCl (5 M)	2 ml
	KCl (2.5 M)	1 ml
	DEPC-Water, fill up to	1000 ml
LB-Agar	Tryptone	20 g
	Yeast extract	5 g
	NaCl (5 M)	2 ml
	KCl (2.5 M)	1 ml
	Agar	15 g
	DEPC-Water, fill up to	1000 ml
TB medium	Tryptone	12 g
	Yeast extract	24 g
	Glycerol	0.4% (v/v)
	KH_2PO_4	2.3 g
	K_2HPO_4 x $3H_2O$	16.4 g
IPTG/X-Gal solution	H_2O	105 µl
	DMSO	40 µl
	IPTG (0.1 M)	30 µl

	X-Gal (10%)	25 µl
6x DNA loading dye	bromophenol blue (0.25%) xylene cyanol (0.25%) sucrose (40%) ddH_2O	0.25 g 0.25 g 40 g 100 ml
2 x Hybridization buffer	5 M NaCl 1 M Tris, pH 7.5 0.5 M EDTA, pH 8.0 Sheated and boiled DNA (10 mg/ML) (denaturate 5 min @ 90°C) Yeast total RNA (20 mg/ml) Yeast tRNA (50 mg/ml) Denhardt´s solution 50x Dextran sulfate 50% Sterile water Aliquot and store at –70°C	4.8 ml 0.400 ml 0.080 ml 0.400 ml 1.0 ml 0.080 ml 0.800 ml 8.0 ml 4.44 ml
RNAse buffer	5 M NaCl 1 M Tris-HCl, pH 8.0 0.5 M EDTA, pH 8.0 DEPC-Water	200 ml 20 ml 4 ml 1776 ml
Artificial cerebrospinal fluid (CSF)	145 mM NaCl 2.7 mM KCl 1.2 mM $CaCl_2$ 2 H_2O 1.0 mM $MgCl_2$ 6 H_2O 2.0 mM Na_2HPO_4 pH=7.4	4.2370 g 0.1005 g 0.0880 g 0.1015 g 0.1420 g in 500 ml H_2O
Cresyl Violet Solution	1 g cresyl violet acetate (Sigma) 100 ml H_2O 0.25 ml acetic acid Mix for 1h filter	

Table 5: Buffers and solutions

2.1.5 Molecular biology kits

Name	Provider	Cat. Number
Corticosterone RIA (Rat, Mouse)	DRG Diagnostics	ria-1364
Corticosterone RIA (Rat, Mouse)	MP Biomedicals	07120103
EpiTect® Bisulfite Kit	Qiagen	59104
LightCycler® FastStart DNA Master^{PLUS} SYBR Green I	Roche	03 515 869 001
miRNeasy Mini Kit	Qiagen	217004
NucleoBond PC100	Macherey Nagel	740573
NucleoSpin® Plasmid	Macherey Nagel	740.588.250
NucleoSpin® Extract II Kit	Macherey Nagel	740.609.250
PAXgene Blood RNA Kit	PreAnalytiX	762174
pGEM®-T Vector System	Promega	A3600
Riboprobe® Combination System-SP6/T7 RNA Polymerase	Promega	P1460
RNeasy Mini Kit	Qiagen	74104

Table 6: Molecular biology kits

2.1.6 Primer and oligonucleotides

2.1.6.1 qPCR primers

Gene	Froward	Reverse
CRH	GCGGGCTCACCTACCAAG	TTCTTCACCCATGCGGATCAG
HPRT	ACCTCTCGAAGTGTTGGATACAGG	CTTGCGCTCATCTTAGGCTTTG
MAS	TATTGGCCCAGAGTATCAGCA	GGGGTTTGTCGATGACTTCAA

Table 7: qPCR primers

2.1.6.2 Bisulfite specific primers

Position	Froward	Reverse
CRH Promoter	TGTTAATGGATAAGTTATAAGAAATT	ACTCTAAATTTCTCCACACCAAAACCTA

Table 8: Bisulfite specific primers

2.1.7 Software

Name	Manufacturer
BioEdit	Tom Hall, Ibis Biosciences
DesignStudio	Illumina
FV10-ASW 4.0 Viewer	Olympus
GIMP	The GIMP Team
Illumina Experiment Manager	Illumina
ImageJ	Schneider et al. (2012)
Inkscape 0.91	Free Software Foundation, Inc.
MiSeq Reporter	Illumina
Opticon Monitor 3	Bio-Rad
Roche qPCR	Roche
RStudio with R 3.2.3	RStudio, Inc.
SigmaPlot 12.5	Systat Software GmbH
Vector NTI	Invitrogen

Table 9: Software

2.2 Methods

2.2.1 Animal experiments

All procedures on animals were approved by the Regierung von Oberbayern, filed under reference number 55.2-1-54-2532-114-2013, and were in conformity with European Union Directive 2010/63/EU. Standard laboratory animal housing conditions were maintained throughout the experiments, with 3–4 mice per cage and 12 h daily illumination (lights on at 06:00 a.m.).

2.2.1.1 Early life stress

The well-established paradigm of maternal separation was used to induce early life stress (Plotsky and Meaney 1993; Murgatroyd et al. 2009). Time-pregnant C57BL/6N mothers were purchased from Charles River. Maternal separation was conducted from postnatal day (PND) 1-10. Pubs were placed in new clean cage for 3h daily, the mother was left undisturbed in her home cage. Control pups were

reared under normal facility conditions. Pups remained with their mothers until weaning (PND21), when they were housed in sex-matched groups.

2.2.1.2 Determination of the estrous cycle stage

In order to determine the estrous cycle stage of female mice, cytological examination of vaginal smears was used. Vaginal fluid was collected using an inoculation loop filled with water. The inoculation loop was inserted into the vagina of the loosely fixed mice and vaginal secretion was carefully collected. The fluid was placed on glass slides and air dried. For staining, a solution of 1% methylene blue was used. The slides were dipped in the solution for 10 seconds and subsequently rinsed several times in water. The different cellular composition of vaginal secretion was analyzed under a light microscope with 40x magnification. Typical cellular compositions indicative of the respective cycle stage are illustrated in Figure 13.

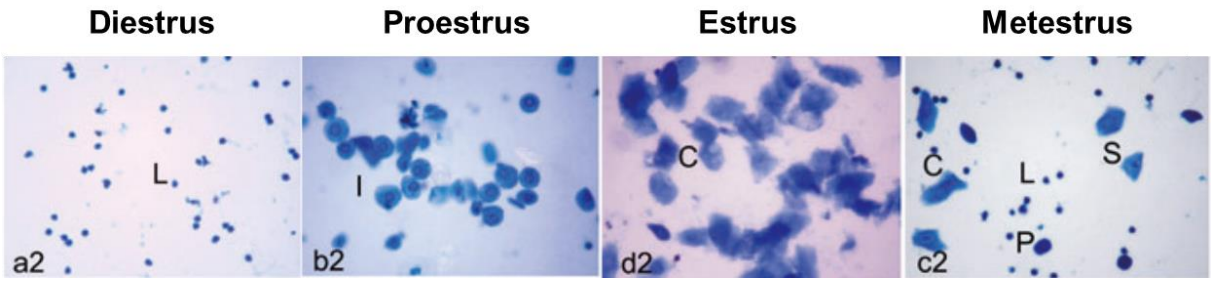

Figure 13: Light microscopy of vaginal smears stained with methylene blue.
The typical cellular composition during the estrous phases in mice are shown. Leucocytes (L), intermediate cell (I), cornified cell (C), parabasal cell (P), and superficial cell (S) are indicated (Yener et al. 2007).

A diestrus smear consists predominantly of leucocytes, often almost exclusively but epithelial cells can also still be present. In proestrus, round nucleated epithelial cells prevail, often in clusters. Anucleated cornified cells are present in estrous which normally last 1 day but can also extend for 2 days. Metestrus is characterized by the same proportion of leucocytes, cornified and nucleated epithelial cells (Yener et al. 2007; Goldman et al. 2007). Vaginal smears were analyzed directly after they were taken. The smears were collected every morning for at least one week before sacrificing the animals in order to assure the correct cycle stage. When estrus or diestrus stage was determined, the respective animals were sacrificed the same morning.

2.2.1.3 Tissue preparation

Mice were sacrificed at 3 month of age by rapid decapitation. Mouse brains were dissected from the scull and snap-frozen in isopropanol (2-propanol) at -80°C.

For in-situ hybridization, frozen brains were sectioned (10 µm) at the level of the PVN under histological control using a cryostat. The sections were collected on microscope slides and stored at -20°C until further use. From the same brains, micropunches were collected with a 0.5 mm diameter punching needle from the brain regions relevant to the specific project under histological control by

cresyl violet staining according to the Mouse Brain Atlas (Paxinos and Franklin 2001) and immediately stored at -80°C.

2.2.1.4 Limited nesting material – chronic social defeat stress mice

Frozen brain samples were kindly provided by Sara Santarelli and Mathias V. Schmidt (Santarelli 2015).

2.2.2 Molecular Biology

2.2.2.1 RNA extraction with RNeasy and miRNeasy

Frozen micropunches from the collected brain regions were lysed immediately in 500 µl Trizol (QIAzol) reagent and the tissue was homogenized by passing through an insulin syringe (29 G) several times. Subsequently, the samples were incubated at room temperature for a minimum of 3 min before adding 100 µl chloroform. The remaining steps were performed according to the manufacturer's protocol. For RNeasy, an equal amount of 70% ethanol was added to the aqueous phase and for miRNAeasy 1.5 volumes of 100% ethanol were added. Elution was performed with 30 µl RNase-free water with a second elution step using the eluate from the first elution.

2.2.2.2 RNA extraction from mouse trunk blood samples with PAX solution

In order to be able to compare the results from human blood samples with mouse blood samples, a modified protocol of the human PAXgene™ blood RNA extraction was used. At least 250 µl of mouse trunk blood were collected in a 1.5 ml Eppendorf tube. Immediately, 2.76 volumes of PAX RNA stabilizer reagent were added to the blood and the tube inverted several times. Tubes were stored at room temperature for at least 2 h but up to 24 h before being stored at -20°C. Further steps were performed according to the manufacturers' protocol using the PAXgene Blood RNA Kit with minor modifications. Incubation at the 55°C shaker was prolonged to 60 minutes and elution was performed with two times 50 µl elution buffer (Krawiec et al. 2009).

2.2.2.3 Plasmid DNA: mini preparations

A single bacterial colony was picked with a sterile tip and inoculated in 2-3 ml SOB (Super Optimal Broth) medium with ampicillin (100-200 µg/ml). The culture was grown for 16 h at 37°C with vigorous shaking before harvesting in in 1.5 ml reaction tubes by centrifugation (14000 rpm/ 1 min/ 4C°). The plasmid DNA was isolated using the NucleoSpin® Plasmid Kit (Macherey-Nagel) according to the manufacturer's instructions.

2.2.2.4 Plasmid DNA: maxi preparations

40 ml TB (Terrific Broth) medium was inoculated with a 2 ml aliquot of a bacterial preculture and was grown at 37°C for 16 h. Plasmid DNA was isolated and purified according to the NucleoBond PC100 (Macherey Nagel) kit manufacturer's protocol. After precipitation with isopropanol, the pellet was dissolved in 200 µl ddH2O and extracted by phenol/chloroform. Therefore, one volume of

phenol/chloroform/isoamylalcohol (25:24:1) was added and vortexed vigorously. After full speed (≥ 15000×g) centrifugation for 3 min at 4°C the supernatant was collected into a new tube, mixed with an equal volume of chloroform/isoamylalcohol (24:1) and centrifuged as before. The supernatant was again collected, mixed with chloroform/isoamylalcohol (24:1) and centrifuged. The supernatant was collected, precipitated with ethanol (2.2.2.5) and resuspended in 100 µl TE-buffer. The DNA concentration was measured using a SmartSpec Plus Spectrophotometer and adjusted to 1 µg/ml.

2.2.2.5 Ethanol precipitation

For ethanol precipitation 2 volumes 99% ethanol with 1/10 volume 3M NaAc and 1/10 volume glycogen (10 mg/ml) were added to 1 volume of reaction. This was mixed thoroughly by vortexing for 1 min and subsequently frozen in liquid nitrogen for 1 min. After centrifugation for 20-30 min at full speed (≥ 15000×g) the supernatant was removed and 300 µl of 70% ethanol added. After another centrifugation for 5-10 min at full speed, the pellet was air dried at 65°C for 5 min. Finally, the DNA was respuspended in 5-10 µl H_2O.

2.2.2.6 Restriction digest of plasmid DNA

Plasmid DNA was cut at selected restriction sites using various restriction enzymes (10 U/µl). Typically, reactions were either 5-25 µg DNA in 50 µl with 2-3 µl restriction enzyme or 300-500 ng DNA in 10 µl with 0.5 µl restriction enzyme. The buffers were chosen according to the manufacturer's instructions. When double digest was performed, the DoubleDigest Calculator[1] was used. When necessary the vector was simultaneously dephosphorylated by adding FastAP Thermosensitive Alkaline Phosphatase.

2.2.2.7 Transformation of DH5α bacteria

An aliquot of 50 µl electrocompetent DH5α E.coli cells was thawed on ice and diluted with 100 µl ice cold ddH2O. An appropriate amount of DNA, either the whole ethanol precipitated ligation mix (5 µl) or 1 ng of purified plasmid of interest, were mixed with 45-50 µl of diluted bacteria and incubated on ice for 1 min. The transformation mix was transferred into an ice cold Gene Pulser Cuvette (Biorad) and incubated for 1 min at RT. Bacteria were transformed at 1.5 kV, 200Ω, 2.5 µF. Immediately after pulse delivery, 700 µl of SOB medium were added to the bacteria and incubated for 1 h at 37°C. 5-100 µl of transformed bacteria were plated on agar-plates containing ampicillin (50 µg/ml) for 16 h at 37°C.

2.2.2.8 Blue/White selection

pGEM-T and pBluescript vectors contain a multiple cloning site flanked by the coding region of β-galactosidase. Insertion of DNA fragments within the multiple cloning site disrupts transcription of β-galactosidase after the induction by Isopropyl β-D-1-thiogalactopyranoside (IPTG). In the presence of 5-bromo-4-chloro-3-indolyl-β-D-galactopyranoside (X-Gal), it is thus possible to identify colonies

[1] http://www.thermoscientificbio.com/webtools/doubledigest/

with religated (blue) versus recombinant (white) vectors. Ampicillin containing LB (lysogeny broth)-agar plates were therefore coated with 200 µl IPTG/X-Gal solution prior to application of bacteria. Blue-white discrimination is best after 24 h at 4°C.

2.2.3 Bisulfite sequencing

In order to determine the methylation status of specific CpGs within regions of interest, sequencing of bisulfite converted DNA was conducted. This method is based on the consideration that 5-methylcytosine is protected from bisulfite conversion; therefore, only unmethylated cytosine nucleotides are converted to uracil. Sequencing of bisulfite converted DNA and comparison with the reference sequence shows methylated cytosine remaining cytosine and unmethylated cytosine converted to thymidine. The workflow of the whole procedure is depicted in Figure 14.

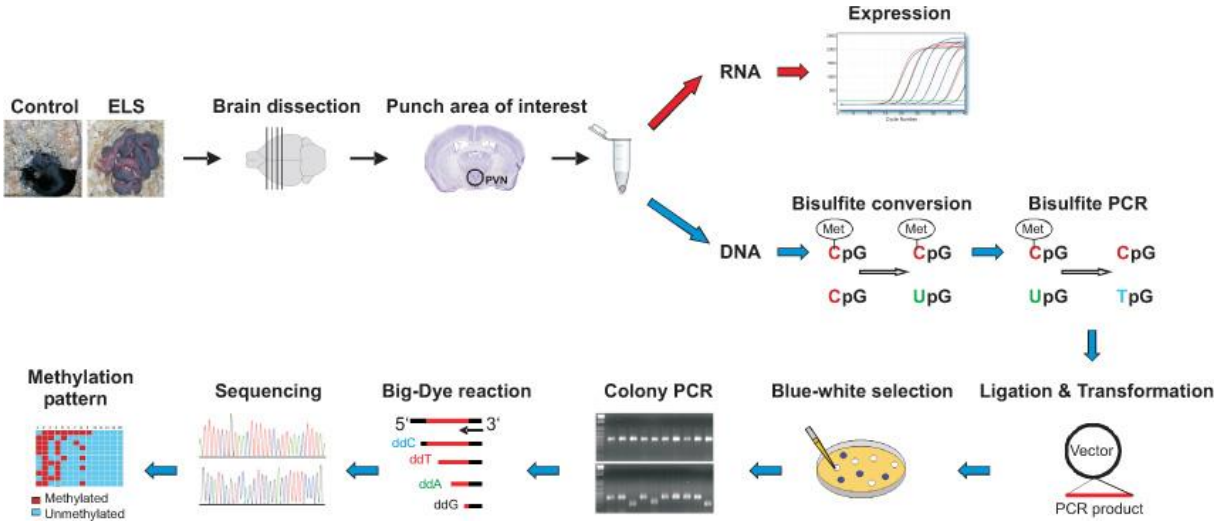

Figure 14: Workflow of the bisulfite sequencing procedure.
Mouse brains were microdissected and areas of interest were punched (here PVN). Further, DNA and/or RNA were extracted from the micropunches. The DNA was bisulfite converted and the region of interest amplified by bisulfite specific PCR. PCR fragments were then ligated into pGEM-T vector for blue-white selection. White colonies were screened on an agarose gel for the correct insert site and subsequently sequenced by Sanger sequencing. Lastly, methylation pattern were determined (Bettscheider et al. 2012).

2.2.3.1 Bisulfite conversion

For sodium bisulfite conversion of genomic DNA, 500 ng DNA extracted from tissue punches were converted using the EpiTect Bisulfite Kit (Qiagen) according to the manufactures instructions.

2.2.3.2 Bisulfite specific PCR

Bisulfite converted DNA was amplified using primers specific for bisulfite converted DNA (Table 8). The amplification was conducted with HotStar Taq Polymerase (Qiagen) according to the manufactures instructions. Primer specific $MgCl_2$ concentrations were evaluated prior to the experiment. Subsequently, successful amplification was verified by gel electrophoresis and the PCR product was purified using Nucleospin® Extract II Kit (Macherey-Nagel).

2.2.3.3 pGEM-T cloning

Purified PCR products were ligated into the pGEM-T vector system (Promega) following the manufacturer's instructions. The ligation reaction was purified by ethanol precipitation (2.2.2.5), transformed into DH5α bacteria (2.2.2.7) and plated on ampicillin containing LB-agar plates pre-coated with 200 µl IPTG/X-Gal solution (2.2.2.8) and incubated 16 h at 37°C.

2.2.3.4 Colony PCR

Recombinant, white colonies were picked with a sterile pipet tip and resuspended in 25 µl PCR reaction mixture containing 1x *Taq* buffer with $(NH_4)_2SO_4$, 3.0 mM MgCl2, 0.6 mM dNTP, 0.4 µM Sp6 and T7 Primers and 0.04 U/µl *Taq* DNA Polymerase final concentration. The reaction was incubated in a thermocycler with a program consisting of 5'/ 95°C + 10x (30''/ 94°C + 30''/ 56°C + 30''/ 72°C) + 30x (30''/ 94°C + 30''/ 48°C + 30''/ 72°C) + 5'/ 72°C. 5 µl of each PCR reaction were loaded on a 2% agarose gel to determine if the cloned inserts were of the correct size. For positive colonies, the remaining reaction was transferred to NucleoFast® 96 PCR Plates (Macherey Nagel). After 20 min 4000 rpm centrifugation at 4°C, 100 µl ddH_2O were added to each well and again centrifuged 20 min 4000 rpm at 4°C. The DNA was recovered in 20 µl ddH_2O on a shaker for 10 min. 2 µl of purified DNA was used directly for sequencing (2.2.3.5) or the plates were stored at -20°C. Sequences were analyzed using the BiQ Analyzer[1] or QUMA[2] .

2.2.3.5 Sanger Sequencing

100 ng purified PCR product or 300 ng Plasmid DNA were mixed in a total volume of 7.5 µl with 5 pmol Sequencing Primer (T7 or SP6) and sent for sequencing to the Biochemistry Core Facility at the MPI of Biochemistry, Martinsried, Germany.

2.2.4 mRNA expression analysis

2.2.4.1 Quantitative real time PCR (qPCR)

RNA samples were reverse transcribed using RevertAid Premium Reverse Transcriptase with oligo(dT) primer according to the manufacturer's instructions. The cDNA was analyzed in a Roche LightCyder using the LightCycler® FastStart DNA Master^{PLUS} SYBR Green I Kit. The relative expression levels were calculated using the ΔΔCT Method (Pfaffl 2001). The relative expression of the target gene was normalized against the housekeeping genes HPRT and MAS as reference while considering the PCR efficiencies.

[1] http://biq-analyzer.bioinf.mpi-sb.mpg.de/
[2] http://quma.cdb.riken.jp

2.2.4.2 In-situ hybridization

CRH transcripts were detected by riboprobes synthesized from *p*Gem4zPST578 (Seasholtz et al. 1991) which contains a 578-bp *Pst*I fragment (330-907bp from ATG) of the mouse CRH exon II. The plasmid was linearized with *Hind*III and in-situ probes radiolabeled with Uridine 5´-(α-thio) triphosphate [^{35}S] were synthesized with SP6 Polymerase using the Riboprobe® Combination System-SP6/T7 RNA Polymerase kit. After template digestion with RQ1 DNAse (1 U/µg template DNA) for 15 min at 37°C, yeast tRNA (0.25 µg/ml) was added and the reaction was purified with RNeasy Mini Kit according to the manufacturer's instructions. Lastly, 2 µl of DTT (5 M) were added to 100 µl eluate. Radioactive incorporation was measured using a liquid scintillation counter. Both, the labeled probes and the 2x hybridization buffer were denatured for 10 min at 80°C. The probes were then diluted to 20 000 cpm/µl with hybridization buffer mixed 1:1 with deionized formamid containing 0.1% SDS, 0.1% sodium thiosulfate and 100 mM DTT. 25 µl of this solution were applied to each section, covered with coverslips and incubated overnight at 55°C in a humid chamber with 4x SSC/50% formamide. Before incubation, the slides were pretreated. First, the tissue was fixed for 5 min with 4% formaldehyde in PBS (phosphate-buffered saline) at room temperature followed by a two times rinse in PBS. Then, the slides were incubated for 10 min in freshly prepared 0.25% acetic anhydride in 0.1 M TEA/HCl. Afterwards, the slides were placed in a series of ethanol (70%, 1 min; 80%, 1 min; 95%, 2 min; 100%, 1min), treated with chloroform for 5 min and again incubated in ethanol baths (100%, 1 min; 95%, 1min) before air drying (Whitfield Jr et al. 1990). The next day, after the incubation with the probe, the coverslips were removed in 1x SSC and the slides underwent the following washing procedure. After two incubations in 1x SSC at room temperature for 20 min, the slides were incubated in 2x SCC/50% form-amide at 52°C for 30 min another 2 times. Incubation in 2x SSC for 10 min at room temperature was followed by RNAse (10 mg/ml in RNAse Buffer) treatment for 30 min at 37°C. Afterwards the slides were rinsed in room temperature 2x SSC and incubated for 30 min in 2x SSC at 52°C. After another rinse in room temperature 2x SSC the slides were incubated for 20 min in H_2O at room temperature. Before drying, the slides were first dipped in 70% ethanol followed by 100% Ethanol. The slides were placed in a metal cassette and exposed to a BioMax film for 5-7 days. The autoradiography films were scanned and semiquantitative densiometric analysis was performed with ImageJ (Schneider et al. 2012).

2.2.5 Microdialysis

All microdialysis experiments were performed within the Microdialysis Laboratory of the MPIP under the supervision of Dr. Anderzhanova as described before (Anderzhanova et al. 2013; Yen et al. 2015).

In this experiment, 16 male C57BL/6 mice aged 2.5 month were single housed for at least one week prior to stereotactic surgery. At the day of surgery, animals were weight and premedicated with the

appropriate dose of the analgesic drug Metacam® (0.5 mg/kg body weight). During the surgery, animals were anesthetized with 2% isoflurane v/v in O_2 at a flowrate of 1.2-1.4 NI/min and fixed in a stereotaxic apparatus. The microdialysis guide cannula was implanted into the right hippocampus at stereotactic coordinates AP -3.10, ML 3.00 DV-1.80 in accordance to the Mouse Brain Atlas (Paxinos and Franklin 2001). The guide cannula, two small (2 mm) custom-made stainless steel anchoring screws, and a metal peg were glued onto the bone surface and fixed with fast drying acrylic Pattern Resin LC. Animals were allowed one week of recovery with Metacam supplemented in the drinking water at 0.25mg/100ml for the first three days. After the surgery and during the experiment mice were housed in square Plexiglas chambers (16 cm×16 cm) on sawdust bedding. The day before the experiment, the microdialysis probe was inserted into the guide cannula under short (30-90 sec) isoflurane anesthesia. The perfusion lines consisting of FEP tubing were connected with the help of a dual channel liquid swivel to allow free movement of the animals and continuously perfused with sterile artificial cerebrospinal fluid at a flow rate of 0.3 µl/min. At the beginning of each experimental day, the flow rate was increased to 1.5µl/min and microdialysis fractions of 20 min each were collected in a refrigerated microsampler. After equilibration (80 min), four baseline fractions were collected followed by the intervention (stress or injection), and then nine consecutive fractions (3 h) were collected. In order to minimize the number of animals, the experiment was designed to last three consecutive days and included a crossover of the pharmacological treatment procedure for each animal. On the first day, all animals were confronted with a physiological stressor, the elevated platform stress (Degroot et al. 2004). During the 5th collection period (each 20 min), the animals were placed on a small round-shaped platform with a diameter of 10 cm which was mounted on top of a vertical pole (40 cm) in the middle of a non-transparent white plastic box (45 cm×45 cm). The illumination at the level of the platform was 600-700 Lux. Within the microdialysis protocol, the elevated platform exposure was performed around 11 am during the light phase of a diurnal cycle. On the second and third day, all the animals were first injected with saline after the baseline period and subsequently (after 3 h) with either 1 mg/kg or 10 mg/kg corticosterone and another nine fractions were collected. Every day half of the animals were injected with either dose and the next day, the dose was opposite. At the end of each experimental day, the flow rate was reduced to 0.3µl/min overnight. Each run consisted of a batch of four animals that were analyzed in parallel. In the first batch, the physiological stress also included a tail vein cut for blood collection before and after the elevated platform, which was omitted in the consecutive batches due to technical difficulties.

2.2.6 Corticosterone radioimmunoassay (RIA)

Corticosterone RIA, either from DRG Diagnostics or MP Biomedicals, were performed according to the manufacturers' protocol with minor adjustments. The samples (plasma, serum or artificial CSF) were diluted in Steroid-Diluent in respect to the expected corticosterone concentration depending on the

experiment. Further, the samples were processed according to the manufacturer's protocol with halved volumes. For microdialysis' artificial CSF, 25 µl sample were diluted 1:2 with 25 µl Steroid-Diluent. Blood samples were diluted 1:200 (5 µl in 1 ml), 1:100 (10 µl in 1 ml) or 1:50 (10 µl in 500 µl) depending on the experiment.

2.2.7 TruSeq® Targeted RNA sequencing

For the assessment of gene expression from several genes in a huge number of samples, TruSeq® Targeted RNA sequencing was chosen. This method allows the parallel processing of 12-1000 genes in 48-384 different samples in a single sequencing run on the MiSeq Sequencer (Illumina).

In order to avoid batch effects, we took care to assign samples randomly distributed during RNA extraction and library preparation. We used 8 samples per group from our 4 experimental groups and 12 brain regions examined which summed up to a total number of 384 samples. During RNA-extraction, 24 samples were extracted at once, whereas the library preparation was done in four 96-well plates. Each 96-well plate contained 3 brain regions which were distributed randomly into the columns of the plate. Each plate column contained 2 samples each from the 4 experimental groups randomly distributed over the rows. 3 columns of a 96-well plate were assigned to one RNA-extraction from each of the 3 brain regions on that plate.

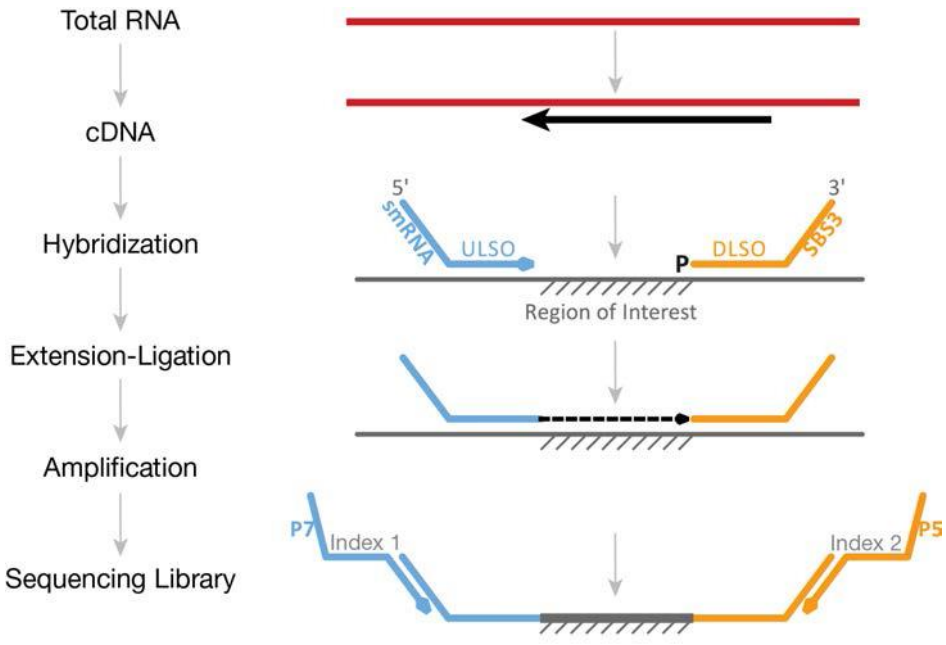

Figure 15: Workflow of the TruSeq® Targeted RNA sequencing library preparation protocol. First, the total RNA is reverse transcribed into cDNA. The specific primers for the transcripts of interest are then hybridized to the cDNA and connected by the extension-ligation step. Through the addition of the indexing primers the samples are marked, amplified and finally pooled to make up the sequencing library. ULSO: Upstream Locus-Specific Oligo, smRNA: small RNA sequencing primer binding site, DLSO: Downstream Locus-Specific Oligo, SBS3: Read 2 sequencing primer binding site; P7: Flow cell binding site, P5: Flow cell binding site (Illumina).

The library preparation was conducted according to the manufacturer's protocol, which is summarized in Figure 15. Briefly, at first, specific assays for the genes of interest have to be chosen in the DesignStudio[1]. The specific primers for these assays are combined and produced by Illumina and result in a targeted oligo pool (TOP). This TOP is applied to the reverse transcribed RNA whereby 50 bp long sequences of the specific genes are amplified. Through the application of two indexing primers, samples are marked, which allows all samples to be combined in one library and sequenced at once.

For the blood samples, a separate library preparation was performed. Thereby the specific properties of the blood RNA samples could be taken into account. The protocol for degraded samples with an initial amount of 200 ng RNA was used. These adjustments and separate library preparation of blood samples in respect to brain samples provided improved sequencing results.

After sequencing with the MiSeq Sequencer, all FastQ files were analyzed with FastQC (Andrews 2010) and reads with Phred Scores lower than 20 or a length smaller than 25 bp were filtered out with PRINSEQ (PReprocessing and INformation of SEQuence data) lite Version 0.20.4 (Schmieder and Edwards 2011). Subsequently, the reads were aligned with Burrows-Wheeler Aligner (BWA) Version 0.7.12 (Li and Durbin 2009) with the manifest file provided by Illumina as reference. The number of reads per gene were summed up in every sample and reads from multiple runs were summed together.

2.2.8 GeneMANIA network analysis

GeneMANIA is an online tool available at http://www.genemania.org. It integrates a vast variety of genomic and proteomic data from GEO, BioGRID, Pathway Commons and I2D as well as well as organism-specific functional genomics data sets from nine different species including human and mouse (Warde-Farley et al. 2010). Co-expression of human genes has been evaluated by selecting all co-expression data sets without the addition of related genes or attributes.

2.2.9 Statistical analysis of CRH data

The statistical analysis of CRH expression data and corticosterone levels in maternal separated females was conducted with SigmaPlot 12.5. Data were analyzed by two-way ANOVA with post-hoc Tukey test. Significant differences are marked with stars: * $p<0.05$; ** $p<0.01$; *** $p<0.001$. All data are plotted as mean±SEM (standard error of mean).

2.2.10 Statistical analysis in R

The statistical analysis of the sequencing data was done in R version 3.2.3 (2015-12-10) (R Core Team 2016) following an in-house pipeline including several different packages:

Bioconductor packages: Rgraphviz (Hansen et al.), DESeq2 (Love et al. 2014), SVA (Leek et al. 2016), limma (Ritchie et al. 2015).

[1] http://designstudio.illumina.com/

CRAN packages: pheatmap (Kolde 2015), RColorBrewer (Neuwirth 2014), ggplot2 (Wickham and Chang 2016), MASS (Ripley et al. 2016) GeneNet (Schaefer et al. 2015), iGraph (Csardi and Nepusz 2006), NetIndices (Soetaert et al. 2014), colorspace (Ihaka et al. 2015), corrplot (Wei and Simko 2016), gtools (Warnes et al. 2015), calibrate (Graffelman 2013)

2.2.10.1 Normalization, outlier detection and batch correction of the data

Filtering genes: Before the analysis, the 10% lowest expressed genes over all samples were excluded. Thereby, genes that were very low or not expressed were removed.

Normalization: DESeq2 was used to normalize the raw counts.

Filtering outliers: Variance stabilizing transformation and rlog transformation were applied to the data and clustered by similarity in heatmaps. Additionally, the similarity of the samples was visualized in a multi-dimensional scaling (MDS) plot. Samples that clustered separately in the heatmap as well as the MDS plot were excluded as outliers.

Batch correction: The DESeq normalized data was examined by principal component analysis (PCA). Technical batch effects such as RNA extraction or library preparation plate and biological effects like treatment group were inspected by coloring the samples accordingly in the plots. To correct for batch effects, surrogate variable analysis (SVA) from the R/Bioconductor package sva was applied. The sva package includes the specific function `svaseq()` for the use with count data (Leek 2014). Significant surrogate variables were calculated according to Leek and Storey (2007). The model matrix of the full model included the experimental groups (adult and early life treatment) and was compared to the null model containing all the other adjustment variables (e.g. RNA extraction, preparation plate). In the next step, the significant surrogate variables were associated to all sample properties in a correlation matrix. The residuals after applying the sva variables were again examined in PCA plots. If there were still samples detected that were more than four standard deviations away from the mean in either of the first two principal components, the samples were excluded.

2.2.10.2 Differential expression analysis

For differential expression analysis, first, a generalized linear model with negative binomial distribution (function `glm.nb()` of package MASS) was used since count data is generally expected to be negative binomial distributed. In our case however, the data for some genes was not following a negative binomial distribution. Therefore, we tested for non-normal distribution with a Shapiro-Wilk test first and given this was not significant ($p \geq 0.05$) we tested for differential expression with a linear model (function `lm()`). To note, in the Shapiro-Wilk test the null hypothesis is normal distribution, thus it has not to be significant to allow tests that assume the data to be normally distributed. If a non-normal distribution was detected, the generalized linear model with negative binomial distribution was used and afterwards tested for its goodness of fit. All reported p-values were calculated either by the linear

model with normally distributed data or by the generalized linear model with negative binomial distribution that passed the goodness of fit test. In all tests, the normalized data was used and the model formula included the surrogate variables as covariates. The interaction effect as well as the specific treatments (early life, adult) were tested separately with the alternative treatment as additional covariate. Significance is reported after controlling for multiple testing with a false discovery rate (FDR) lower than 10% (q-value< 0.1)

Differentially expressed genes were visualized in volcano plots using gtools and calibrate.

2.2.10.3 Network analysis

Networks were built with GeneNet and visualized with Rgraphviz. From the normalized and batch corrected gene expression residuals a partial correlation matrix was built. The networks were then built from the significant edges (qval ≤ 0.2) for every condition in each of the brain regions. The network properties were analyzed using iGraph and visualized in pheatmaps.

3 Results – Epigenetic regulation of CRH in the PVN

No differential CRH expression in adult male mice with a history of maternal separation had been detected in our previous experiments. However, initial experiments with female mice analyzed with respect to the specific stage of their estrous cycle (2.2.1.2) were promising.

3.1 Corticosterone Measurements

Corticosterone levels of female mice exposed to maternal separation were measured at the time of sacrifice (Figure 16).

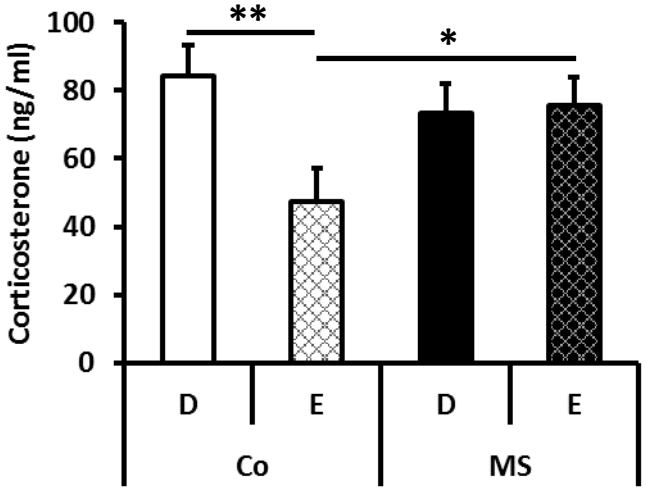

Figure 16: Corticosterone levels of 3-month-old maternal separated female mice.
Corticosterone levels were measured in plasma collected from trunk blood during sacrifice The ANOVA showed a significant interaction effect ($F=4.778$, $p=0.032$). All values are mean±SEM, Co: Control; E: Estrus; MS: maternal separated; D: Diestrus. * $p<0.05$; ** $p<0.01$. (Experiments conducted in collaboration with Florian Raabe)

The corticosterone levels of control mice were significantly different between mice in estrus and diestrus. This suggests a reciprocal link between estrogen levels, which are higher in estrus, and the secretion of corticosterone. This difference in corticosterone levels was not detected in females after maternal separation suggesting that estrogen levels and HPA axis activity were disconnected.

3.2 CRH mRNA expression

The mRNA expression of CRH, one of the main stress hormones of the HPA axis, was measured in the PVN where it is highly expressed.

3.2.1 CRH mRNA expression at 3 months

Female mice with a history of maternal separation were sacrificed after 3 months. At this time-point, mice are well in their adulthood. In-situ hybridization for CRH in the PVN revealed an estrous cycle dependent expression of CRH in control mice (Figure 17).

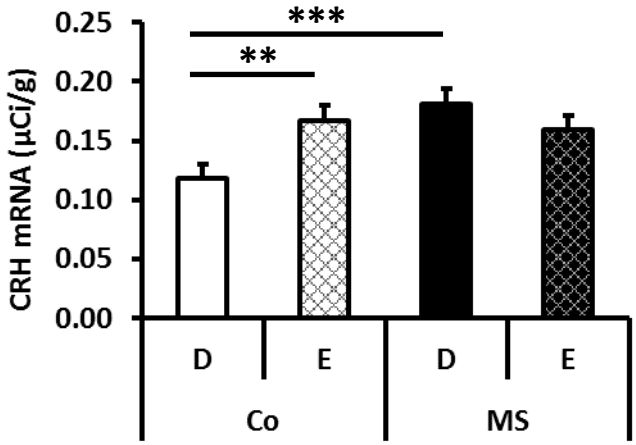

Figure 17: In-situ hybridization for CRH expression in the PVN of 3-month-old maternal separated female mice.
The ANOVA showed a significant effect of early life stress ($F=5.071$, $p=0.032$) and interaction effect ($F=8.494$, $p=0.007$). All values are mean±SEM, Co: Control; E: Estrus; MS: maternal separated; D: Diestrus. ** $p<0.01$; *** $p<0.001$. (Experiments conducted in collaboration with Florian Raabe)

Similar to the corticosterone levels, differences in CRH expression between estrous cycle phases was not present in maternal separated females. A highly significant difference between control and maternal separated mice in the diestrus phase was detected. This suggests that, at the level of the PVN, CRH expression is uncoupled from estrogen levels in maternal separated mice.

3.2.2 CRH mRNA expression at 1 year

In another cohort, maternal separated female mice were 1-year-old; an age that is usually not reached in wild life and can only be achieved in captivity.

Due to the limited availability of material, CRH expression was assessed in these mice using qPCR. At this time-point, no differences in CRH expression were identified between the different groups (Figure 18). This partly resulted from the high variability of the measurements and possibly from dilution effects.

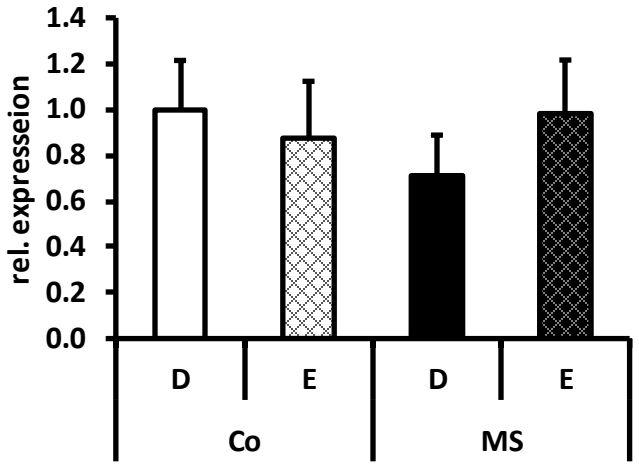

Figure 18: qPCR for CRH expression in the PVN of 1-year-old maternal separated female mice.
Relative expression compared to control diestrus is plotted. All values are mean±SEM, Co: Control; E: Estrus; MS: maternal separated; D: Diestrus

3.3 CRH promoter methylation

CRH expression differences could occur due to different reasons. Differences in synaptic plasticity could result in altered transcription factor modifications or differences in the expression of transcription factors themselves. Furthermore, innervations from connected brain regions could be changed or neurons could undergo morphological changes. Nevertheless, we wanted to focus herein on the previously investigated mechanism, the long-term propagation of early life experiences by CpG methylation. Differential methylation could affect the expression of a gene in various ways. The binding of transcription factors or structural proteins could be altered and affect the composition of the transcription initiation complex. The body of the CRH gene is covered by a large CpG Island which is very sparsely methylated (Appendix 8.1, Raabe 2016). Therefore, we concentrated on the 10 CpG sites preceding the transcription start site.

3.3.1 CRH promoter methylation at 3 months

First, we investigated the CRH promoter CpG methylation at 3 months, the time-point where CRH expression as well as corticosterone levels were uncoupled from estrogen cycling in maternal separated mice. No significant differences were detected in either of the CpGs (Figure 19). In addition, no methylation differences were present between estrous cycle stages in both MS and control mice.

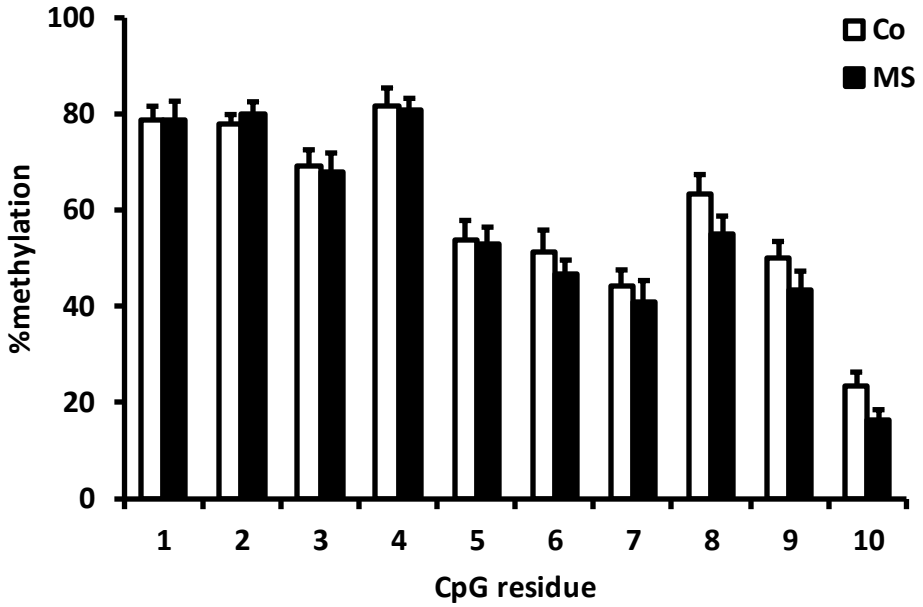

Figure 19: CpG methylation of the CRH promoter region in the first cohort of maternal separated female mice at 3 months.
Co: Control, n=12; MS: maternal separated, n=11.

This result was reproduced in a second cohort of animals (Figure 20).

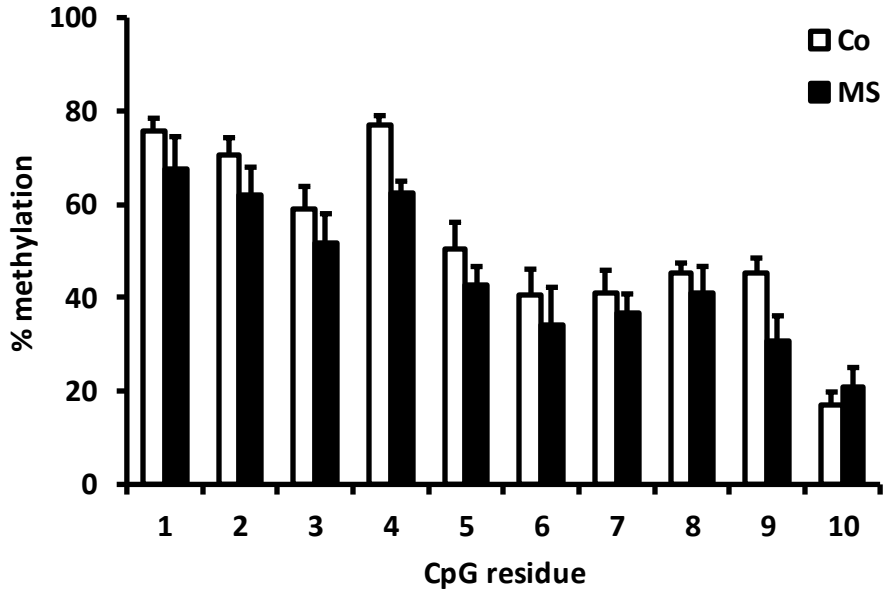

Figure 20: CpG methylation of the CRH promoter region in the second cohort of maternal separated female mice at 3 months.
Co: Control, n=4; MS: maternal separated, n=4

3.3.2 CRH promoter methylation at 1 year

After 1 year, again no differences in CpG methylation at the CRH promoter were detected. Moreover, the methylation pattern resembled the pattern at 3 months without any age dependent changes in DNA methylation (Figure 21).

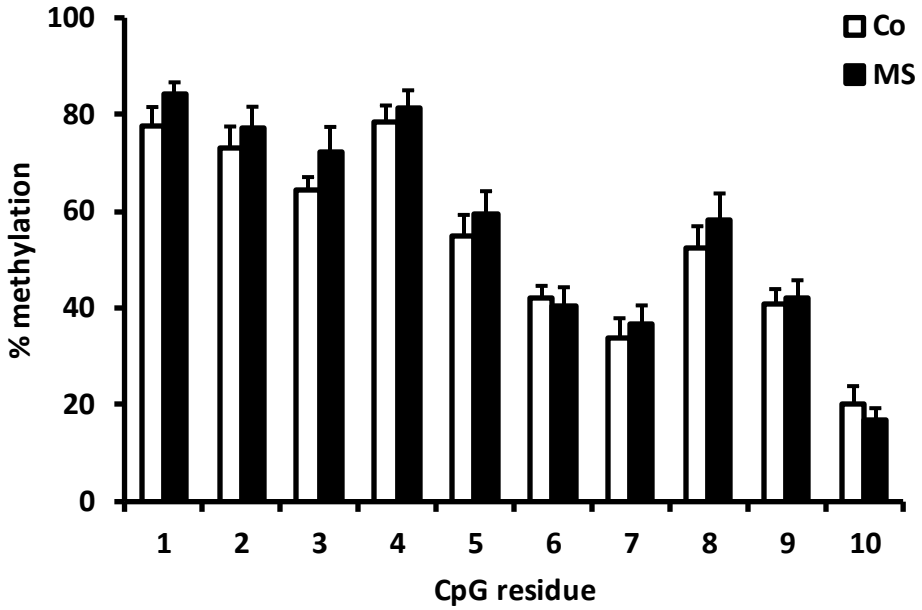

Figure 21: CpG methylation of the CRH promoter region of maternal separated female mice at 1 year.
Co: Control, n=12; MS: maternal separated, n=10

4 Results – GR-response eQTLs associated with MDD and SCZ

In the second part, human GR-response eQTL genes previously identified by Arloth et al. (1.10) were studied in two mouse models of early life stress. In the current study, not only MDD-associated eQTL genes but also GR-response eQTLs which matched nominally significant hits in the latest GWAS for schizophrenia (Schizophrenia Working Group of the Psychiatric Genomics Consortium 2014) were investigated. These disease-related eQTL genes are listed in Appendix 8.2 and form a tightly connected co-expression network as determined from publicly available data obtained through GeneMANIA (Figure 22).

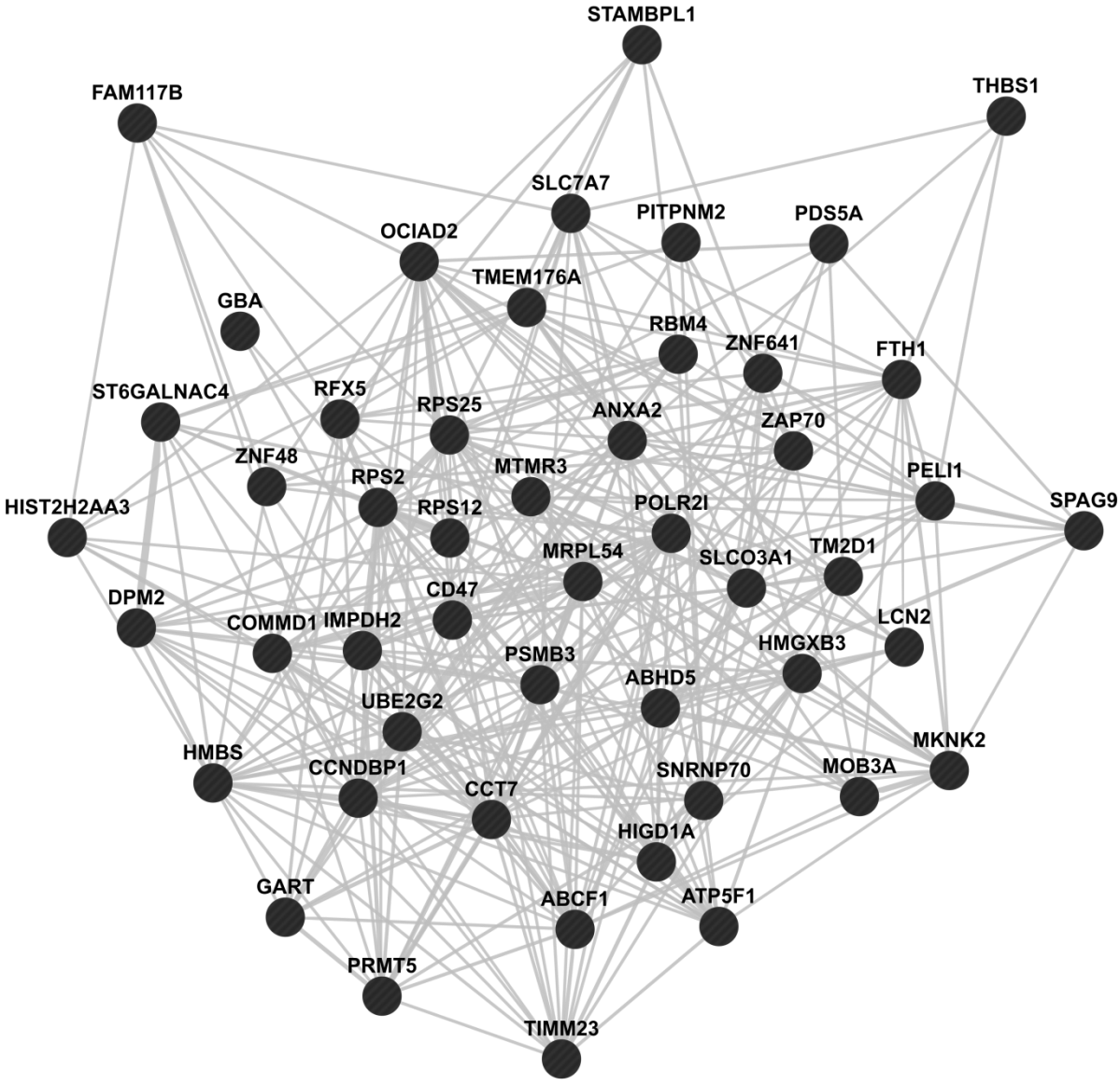

Figure 22: Human GeneMANIA co-expression network.
The MDD/SCZ-related GR-response eQTL genes form a tightly interconnected co-expression network. Edges represent co-expression as determined by GeneMANIA from the literature database.

4.1 TruSeq® sequencing vs microarray expression

Using a new method, TruSeq® Targeted RNA sequencing (2.2.7), we first had to validate its reliability. Therefore, we compared the expression of our genes of interest in three exemplary brain regions from mice sacrificed three hours after dexamethasone (10 mg/kg) injection between TruSeq® sequencing and microarray analysis. Table 10 shows that the expression of the analyzed genes correlates strongly between both techniques.

Table 10: Correlation between TruSeq® sequencing and microarray expression

	Amygdala	dCA3	Pituitary
Correlation all genes	0.75	0.77	0.56
Correlation FC > ±1.1	0.93	0.94	0.81

After filtering out noisy genes with a fold change lower than ±1.1, the correlation becomes even stronger. This illustrates that TruSeq® sequencing produces results comparable to microarrays.

4.2 Microdialysis

In order to assess the kinetics of corticosterone levels in the mouse brain after a single intraperitoneal (IP) injection of corticosterone, we conducted a microdialysis experiment. We aimed at identifying a concentration of corticosterone that best corresponds to a physiological stressor. As exemplary target region, the hippocampus was used. Two doses of corticosterone, 1 mg/kg and 10 mg/kg, were tested and compared to the stress response induced by the elevated platform (2.2.5).

Following treatment (time-point 0), corticosterone levels were increased in all conditions (Figure 23). Only a slight but still detectable increase was observed after injection with saline, as expected. Exposure to the elevated platform resulted only in a mild increase of corticosterone. The combination with a tail vain cut, however, markedly increased the measured corticosterone levels, which peaked in this case at 40 min after the intervention. Corticosterone injection, on the other hand, resulted in an immediate increase, which plateaued between 20 and 40 minutes. After injection of 10 mg/kg corticosterone, levels in the microdialysate increased strongly and reached more than five times the level of the physiological stress response. Moreover, corticosterone levels stayed very high for an extended time period, just returning to the physiological peak level after three hours. After injection of 1 mg/kg corticosterone, levels peaked at around 1.5 times of the elevated platform stress combined with a tail vain cut. Here, the time necessary to reach baseline was similar in both conditions.

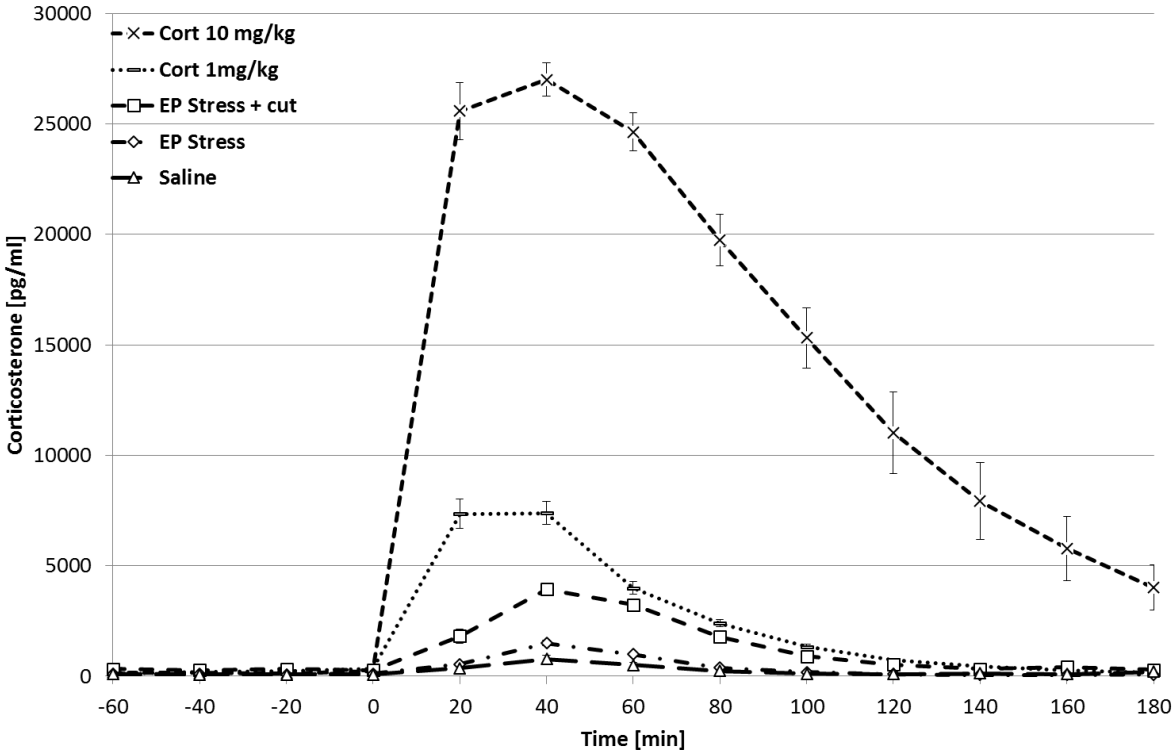

Figure 23: Corticosternme levels in microdialysis fractions from mice hippocampus after exposure to a physiological stressor and compared to corticosterone injection.
Artificial cerebrospinal fluid was collected in fractions of 20 minutes. Four fractions were collected before the treatment (time-point 0) and collections continued until 3 hours after the treatment. Experimental groups: Cort: Corticosterone injection with the respective dose; EP Stress + cut: Elevated platform stress with tail vain cut for blood collection; EP Stress: Elevated platform stress; Saline: Saline injection.

This experiment highlights that the determination of the bioavailability of pharmacological substances in the tissue of interest is crucial after systemic injections to best mimic physiological conditions. Given the results of this experiment, we concluded that a dose of 1 mg/kg best corresponds to a strong physiological stressor. Therefore, this dose was used in the following experiments.

4.3 Maternal separation and corticosterone injection

4.3.1 Animal cohort of maternal separated mice

In the first mouse model, we used male C57BL/6 mice with a history of early life stress due to maternal separation. These mice received a corticosterone injection in adulthood (Figure 24). Maternal separation (MS) was conducted 3 hours daily for the first 10 days of life in the MS groups. At the age of 3 months, the mice were sacrificed either without further treatment (naïve) or following an intraperitoneal injection of 1 mg/kg corticosterone 3 hours before sacrifice.

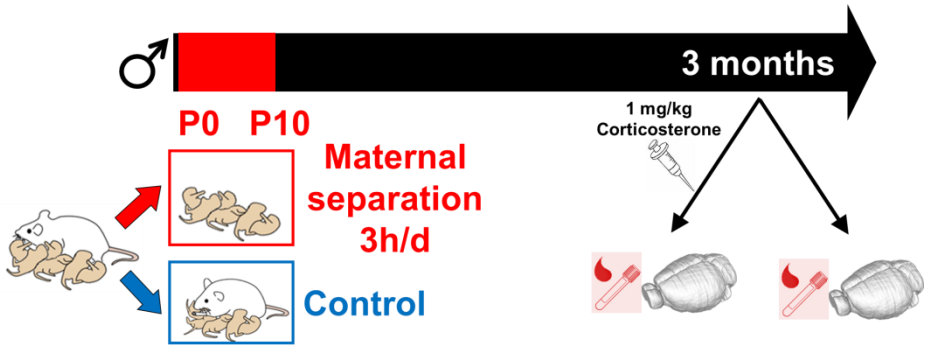

Figure 24: Maternal separation mouse model.
Time-pregnant mothers were assigned to maternal separation (MS) or control groups. The pups of mothers in the MS group were transferred to a new cage for 3 hours per day during the first 10 days. When the mice were aged 3 months, they either received a 1 mg/kg corticosterone injection or were left undisturbed before sacrifice. The blood and brains of all animals were collected.

In total, this resulted in four groups: a control group which did not receive any treatment (Co-naïve); a group which only experienced maternal separation but no adult corticosterone injection (MS-naïve); a group which received only an acute corticosterone injection 3 hours before sacrifice in adulthood (Co-inject); and a group which experienced both, maternal separation and corticosterone injection (MS-inject). From all mice, brains and pituitaries were collected. Additionally, trunk blood for RNA extraction as well as separate blood samples for corticosterone measurements were obtained.

4.3.1.1 Basal corticosterone levels at 5 weeks

To validate the maternal separation procedure, we conducted tail vein bleedings in the 5-week-old mice and assessed the basal corticosterone levels. We could not detect any differences between the corticosterone levels of maternal separated and control mice at this time-point (Figure 25).

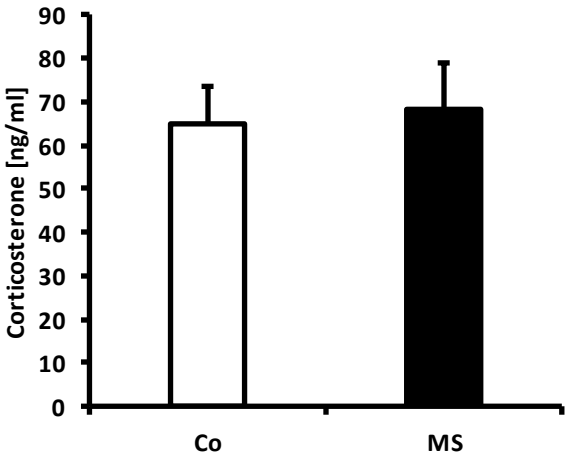

Figure 25: Basal corticosterone levels from 5-week-old maternal separated mice.
Corticosterone levels were measured in serum extracted from tail vein blood collected in the afternoon. All values are mean±SEM, Co: Control; MS: maternal separated

4.3.1.2 Basal corticosterone levels at 3 month

Corticosterone levels were assed in the trunk blood of all mice after sacrifice at 3 months (Figure 26).

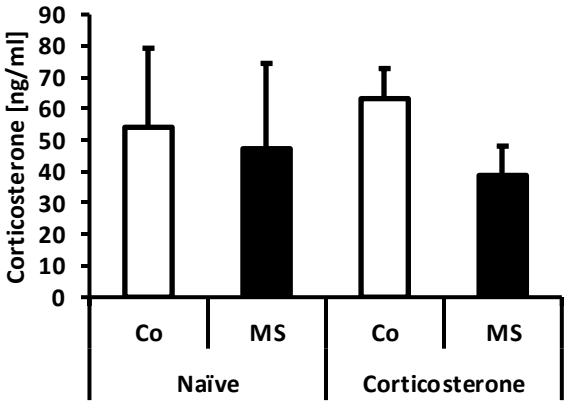

Figure 26: Basal corticosterone levels of 3-month-old maternal separated mice.
Corticosterone levels were measured in serum extracted from trunk blood collected at sacrifice. All values are mean±SEM, Co: Control; MS: maternal separated; Naïve: no adult treatment; Corticosterone: 1 mg/kg corticosterone injection 3 hours prior to sacrifice.

No significant differences between control and MS mice were detected, which is in accord with previous experiments. Interestingly, there were no differences in corticosterone levels between corticosterone injected and naïve mice present. This suggests that the levels of corticosterone in the blood already normalized 3 hours after the injection.

4.3.2 GR-response MDD and SCZ related eQTL gene expression

The gene expression of the mouse orthologues of GR-response MDD- and SCZ-related eQTL genes (8.2) was investigated in 12 different brain regions including amygdala (AMY), bed nucleus of the stria terminalis (BNST), cerebellum (CER), dorsal hippocampal Cornu Ammonis (CA) 1 region (dCA1), dorsal hippocampal CA3 region (dCA3), dorsal dentate gyrus (dDG), prefrontal cortex (PFC), pituitary (Pit), paraventricular nucleus (PVN), ventral hippocampal CA1 region (vCA1), ventral hippocampal CA3 region (vCA3) and ventral dentate gyrus (vDG). These brain regions were selected for their contribution to the regulation of the stress response as well as their role as targets of the stress response. The cerebellum was assessed as negative control, where no stress related expression differences were expected. Additionally, we also investigated the expression of these genes in the blood. This opens the opportunity to directly relate the results to the human analysis.

4.3.2.1 TruSeq Sequencing

The pooled TruSeq library containing 384 brain samples as well as the library for the blood samples were loaded on the Illumina MiSeq sequencer. Table 11 lists the amounts loaded and yield of the specific sequencing runs. For the brain samples, three sequencing runs were performed in order to increase the coverage of single transcripts over all samples. For blood, a second run had to be performed due to the low amount of the clusters passing filter (PF) in the first run. In the second run, the amount of library loaded was halved and thereby nearly 90% clusters PF could be achieved.

Table 11: Quality parameters of sequencing runs from maternal separated mice.

	Load	Cluster density (K/mm2)	Clusters PF (%)	Total reads	Reads past filter	% reads identified
Brain 1	10 pM	1234	68.6	27,616,172	19,561,760	75.86
Brain 2	8 pM	1208	85.6	27,616,220	23,639,608	81.64
Brain 3	8 pM	1048	90.0	25,587,506	23,077,160	83.38
Blood 1	8 pM	1110	35.1	26,117,084	9,214,041	81.09
Blood 2	4 pM	953	89.4	23,932,584	21,401,722	82.94

Generally, the determination of the appropriate amount of sequencing library to be loaded on the MiSeq instrument can be demanding. The protocol suggests 10-15 pM of library to be loaded. However, as depicted in Table 11, much lower quantities are sometimes necessary to receive good results. The actual amount of library depends heavily on the quantification step, typically performed with the Agilent 2100 Bioanalyzer. From our experience, the Bioanalyzer rather underestimates actual sample concentrations. Therefore, it can be helpful to additionally use a second method of quantification, e.g. the Qubit®, to determine the right concentration.

4.3.2.2 Quality control and data assessment

The analysis of heatmaps from rlog and variance stabilizing transformed data as well as MDS plots allowed us the identification of five outlier samples: 109_PVN, 95_PVN, 243_BNST, 229_vDG, 83_vDG (AnimalNr_BrainRegion). Figure 27 presents two principal component (PC) plots of the normalized data after the exclusion of these samples.

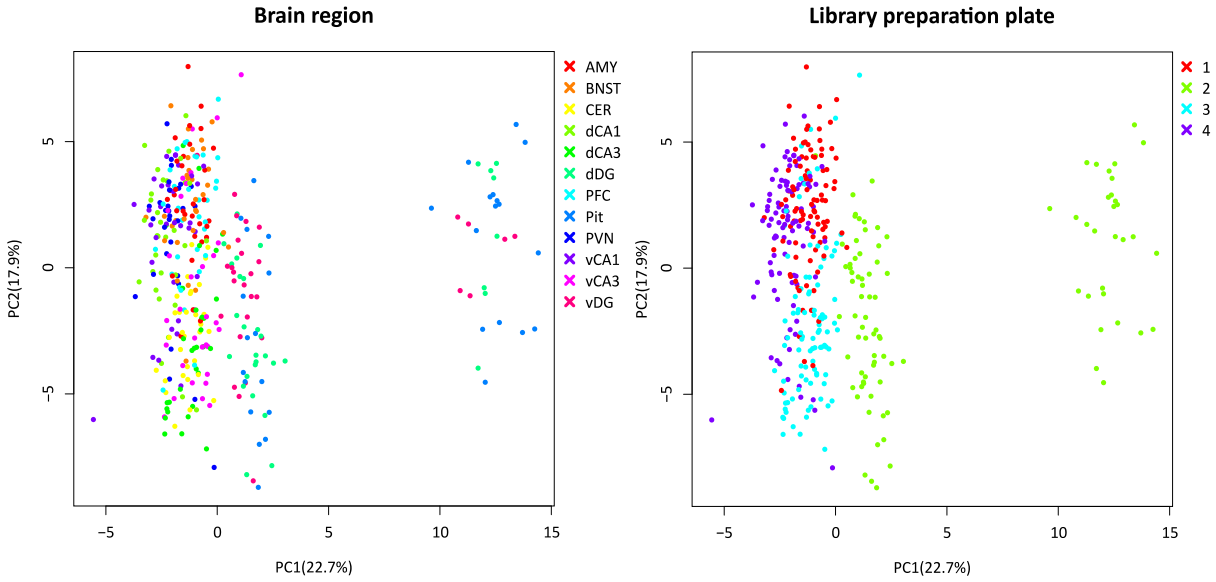

Figure 27: Principal component (PC) plots of normalized count data from maternal separated mice.
In the left plot, the samples are colored by brain region; in the right plot, the samples are colored by library preparation plate.

In the PC plot colored by library preparation plate, a batch caused by this factor was detected. Samples of plate 1 and 4 are mostly overlaying but samples from plate 2 and 3 separate from the other plates. A subset of samples from plate 2 clusters away from all the other samples. We examined the properties of these samples but could not assign the separation to any of our suspected batch effects. The separated samples belong to four specific plate columns which are not adjacent to each other but rather randomly distributed on the plate. Moreover, these samples do not belong to a specific brain region as depicted in the PC plot colored by brain region.

To overcome the problem of hidden batch effects, surrogate variable analysis (SVA) was applied. Four significant surrogate variables (SVs) were determined and their correlation with the sample properties is depicted in Figure 28. The highest correlation of the SVs was present with RNA extraction and library preparation plate, but also plate column and brain region correlated significantly. SV2 and SV4 showed only minor correlations with the suspected batch effects. This illustrates that the SVA also corrects for unknown batch effects in the sample.

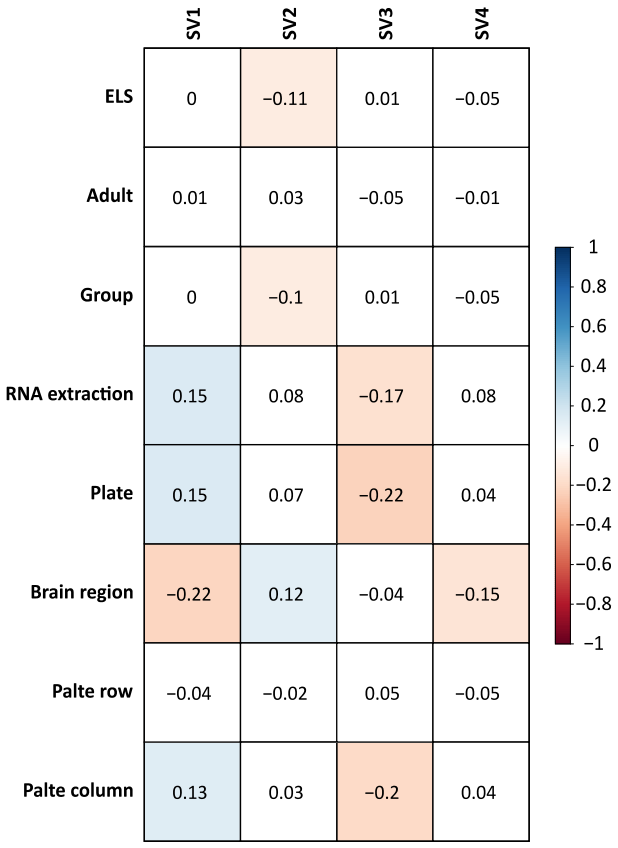

Figure 28: Correlation matrix of surrogate variables (SVs) with sample properties.
Filled colored boxes mark significant associations; positive and negative correlations are marked blue and red respectively.

After the SVA, the corrected dataset has been assessed again by PCA. Two samples, 267_PFC and 81_BNST, had to be excluded due to more than four standard deviations distance from the mean of all samples. The PC plots of the final dataset are presented in Figure 29. The samples from the different

library preparation plates are now much closer together and all samples from plate 2 cluster together. Plate 2 and 3 still cluster rather separately but they overlay much better with plate 1 and 4 compared to the raw data.

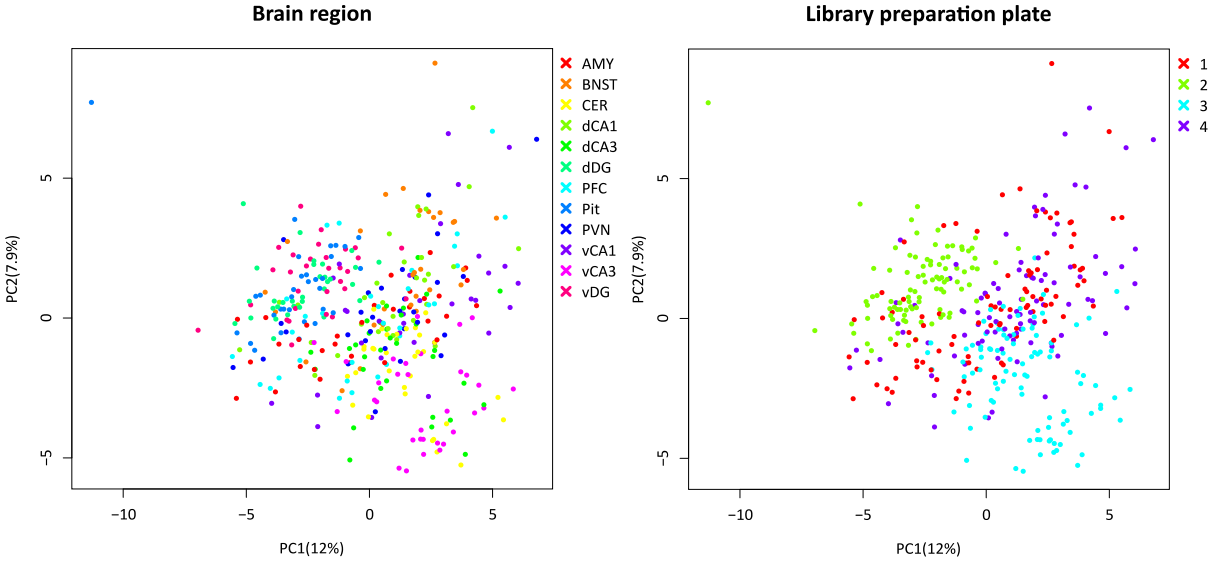

Figure 29: Principal component (PC) plot after batch correction of count data from maternal separated mice. In the left plot, the samples are colored by the brain region; in the right plot, the samples are colored by the library preparation plate.

Overall, this data demonstrates that batch correction is necessary and SVA is suitable to use for this kind of data. The data shown here are only the brain samples, the blood samples have been processed separately in the same way (Appendix 8.3).

4.3.2.3 Differential expression of GR-response MDD- and SCZ-related eQTL genes in the brain

Differential expression analysis in the investigated brain regions of the maternal separated mice revealed only a few significantly different genes after multiple testing correction (Table 12).

Table 12: Differentially expressed genes in brain tissues of maternal separated mice

	ELS	Corticosterone	Interaction
AMY			
BNST			
CER			
dCA1			
dCA3			
dDG			
PFC			Cct7
Pit		Pitpnm2	
PVN	Zfp641	Timm23	
vCA1			
vCA3			
vDG		Abhd5	Zfp641

Acute corticosterone injection had the strongest effect with the regulated genes present in the classic target regions, PVN, pituitary and dentate gyrus. An interaction effect was also detected in the prefrontal cortex.

4.3.2.4 Differential expression of GR-response MDD- and SCZ-related eQTL genes in blood

In the blood, nine genes were significantly regulated after acute corticosterone injection in adulthood (Figure 30). Three genes (Rps25, Spag9, and Impdh2) were down regulated and six genes (Rbm4, Lcn2, Hmbs, Abdh5, Ociad2 and Fth1) were upregulated.

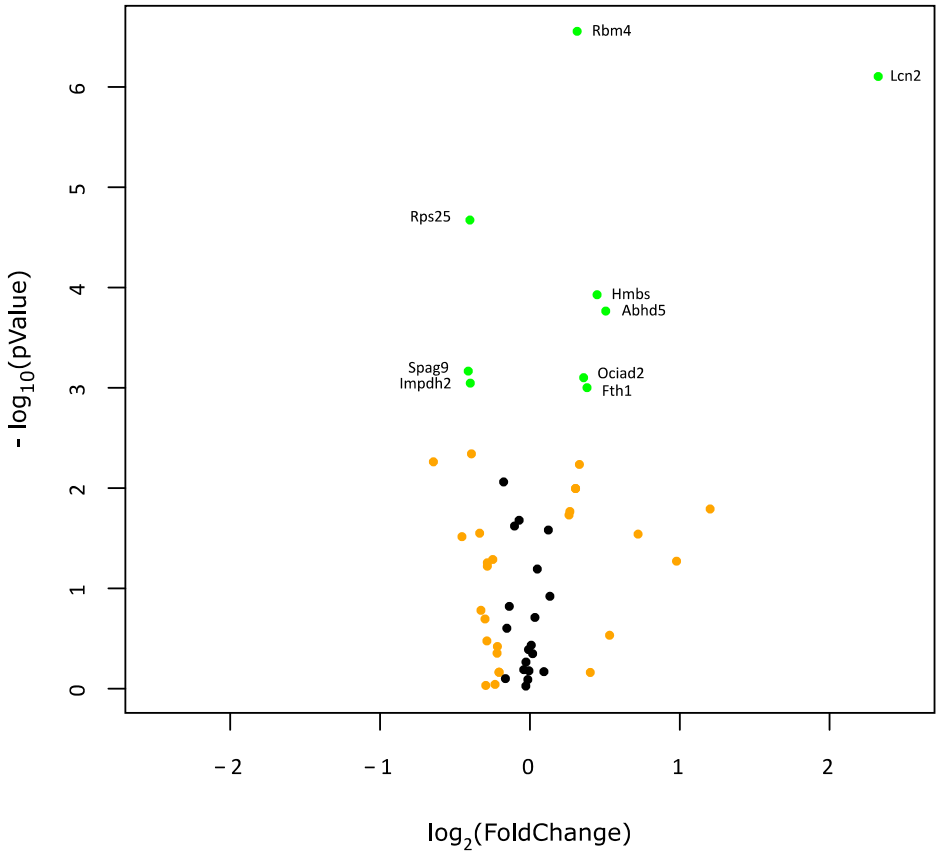

Figure 30: Differentially expressed genes in blood for the effect of acute corticosterone injection in adulthood.
Green dots mark genes which are up- or down-regulated more than 1.15 fold and surpassed the multiple testing threshold (q-value <0.1). The names of the genes are noted beside the dots. Orange dots mark genes that are up- or down-regulated more than 1.15 fold but did not surpass the multiple testing threshold. Black dots mark genes that were not regulated.

There were neither any genes significantly regulated by early life stress nor an interaction effect present in blood.

4.3.3 Network analysis

Network analysis of all brain regions, including blood, revealed region specific co-expression networks in most of the brain regions (Figure 31). In blood, strong networks are present in all experimental groups. Brain regions that present strong network connectivity include vCA3, dCA3, dDG, pituitary, and, interestingly, cerebellum. The network in the control-injected group of the cerebellum is one of

the biggest. This highlights that even though the cerebellum is no classical stress regulatory region, a pharmacological corticosterone stimulus activates this brain region. This is in line with the distribution of the glucocorticoid receptor, which is highly expressed in the cerebral cortex (Morimoto et al. 1996). GR activation in the cerebellum could be important for regulating apoptosis in neuronal progenitors (Noguchi et al. 2008) but the adult function still has to be investigated.

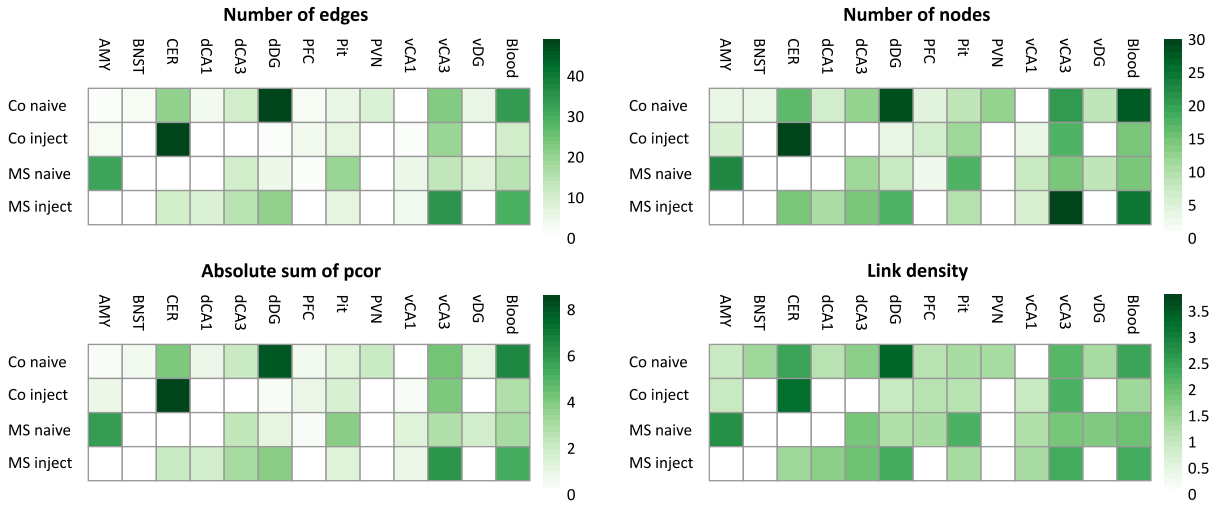

Figure 31: Network properties of co-expression partial correlation networks from maternal separated mice. Depicted are the total number of edges and nodes in the specific networks as well as the absolute sum of the partial correlation coefficient (pcor) and the link density in the respective networks.

In Figure 32, the genes that are part of the specific networks are depicted in a heatmap. The clustering reveals neither clear region specificity nor clustering by experimental conditions. The strongest networks, “CER Co inject”, “DG Co naïve” and “Blood Co naïve” cluster apart from each other as well as the other regions. The four different conditions in blood, which all show substantial network connectivity, do not cluster together as well.

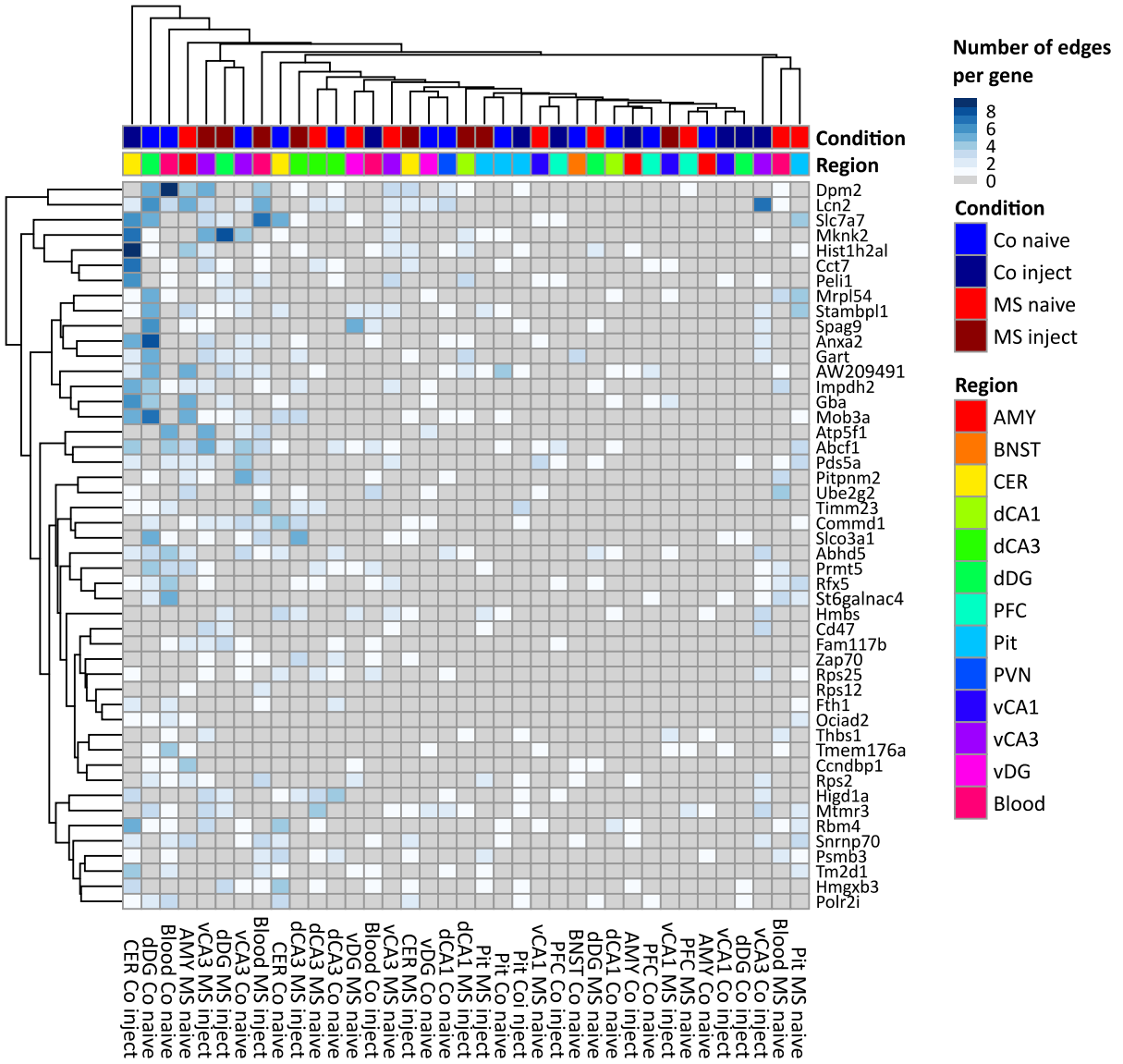

Figure 32: Network node genes and edges per brain region and condition.
On the top, the regions and experimental conditions are color coded and clusterd. On the left side of the matrix, the node genes are presented with the cluster diagram on the right. The colors in the matrix depict the amout of edges established from each gene in the specific networks.

4.4 Limited nesting material and chronic social defeat stress

In the second mouse model, we investigated the interaction between limited nesting material early in life and chronic social defeat stress in adulthood on the expression of the GR-response MDD- and SCZ-related eQTL genes.

4.4.1 Animal cohort

The animal experiments of this cohort were conducted by Sara Santarelli and the group of Mathias Schmidt in Balb/c mice (Santarelli 2015). The experimental timeline and the study groups are summarized in Figure 33. In this experiment, two opposing manipulations were conducted early in life as well as in adulthood. First, early handling (EH), which increases maternal care (Liu et al. 1997; Caldji et al. 1998), in contrast to the limited nesting and bedding material paradigm (LM), which was shown

to induce fragmented maternal care (Rice et al. 2008), was used. Later, in adulthood, mice received either chronic social defeat stress (CD), a paradigm which has been extensively used and validated within and outside the institute (Berton et al. 2006; Kinsey et al. 2007; Haenisch et al. 2009; Wagner et al. 2011; Balsevich et al. 2014) or were housed together with an ovariectomized female mice (OX) as positive social stimulus. Animals either experienced positive or negative conditions in both early life and adulthood (EHOX or LMCD respectively) or experienced opposing conditions in early life and adulthood (EHCD and LMOX). Amygdala, BNST, cerebellum, dCA1, dCA3, dDG, PFC, PVN, vCA1, vCA3, and vDG were collected from frozen brains of these animals. Since there were no pituitaries available from these animals, the nucleus accumbens (Nac) was collected additionally.

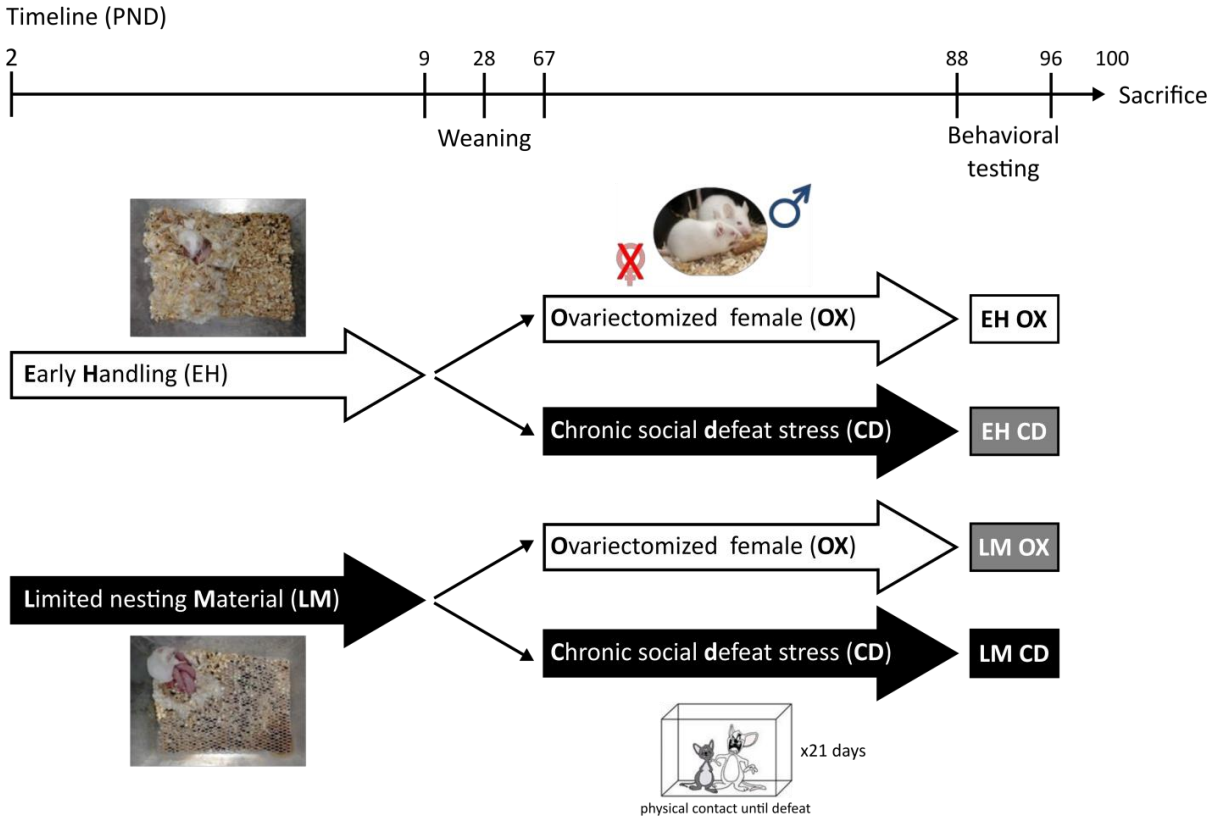

Figure 33: Experimental timeline and conditions of limited nesting material and chronic social defeat stress mice. Between postnatal day (PND) 2 and 9 the litters were randomly exposed to either early handling (EH) or limited nesting material (LM) conditions. Subsequently, they were returned to standard housing conditions until weaning (PND 28) where they were group housed until PND 67. Animals were then randomly assigned to either chronic social defeat stress (CD) or housed with an ovariectomized female (OX) for 21 days. Afterwards behavioral testing was conducted and all animals were sacrificed at PND 100 (addapted from Santarelli 2015).

4.4.2 Library preparation and sequencing

The expression level of the GR-response MDD- and SCZ-related eQTL genes was measured by TruSeq® Targeted RNA sequencing. As before, four sequencing plates with a total of 384 samples were prepared and the pooled library loaded on the MiSeq sequencer (Table 13).

Table 13: Quality parameters of sequencing runs from LMCD mice

	Load	Cluster density (K/mm2)	Clusters PF(%)	Total reads	Reads past filter	% reads identified
Run 1	10 pM	1139	88.84	26.116.940	23.202.998	85.4637
Run 2	10 pM	1126	91.13	26.625.978	24.274.608	86.0245
Run 3	10 pM	1119	88.19	25.438.136	22.434.052	85.0683
Run 4	10 pM	1026	90.12	24.029.084	21.657.320	84.3328

In this experiment, three sequencing runs with all the samples had good yields. However, the index read distribution (Figure 34) was broad in this experiment resulting in some samples being more than 100-times less present in the library than others. Therefore, the lowest 30% of all samples, which were below 0.15% of all index reads identified, were pooled together separately. These samples were than sequenced in a 4th MiSeq sequencing run.

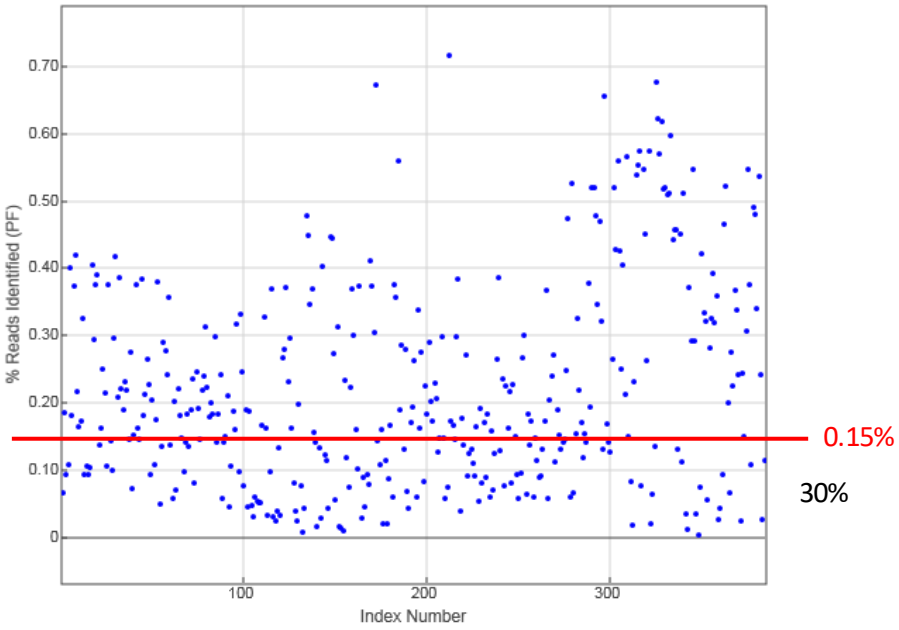

Figure 34: Index read distribution of the first sequensing run.
The percentage of identified reads per index number (sample) is plotted. The lowest 30% of samples have below 0.15% identified reads.

Overall, the sequencing of these libraries was successful with a yield of ~20 million identified reads per run.

4.4.3 Quality control and data assessment

The principle component plots of the normalized raw data illustrate a clustering by brain region (Figure 35). The effect of brain region is stronger compared to the effect of library preparation plate. This is best visible for plates 3 and 4, which both separate into two clusters that correspond to specific brain regions. Otherwise, plate 2, 3, and 4 overlap with each other while plate 1 clusters more separately in the middle between the different regions of plate 3 and 4.

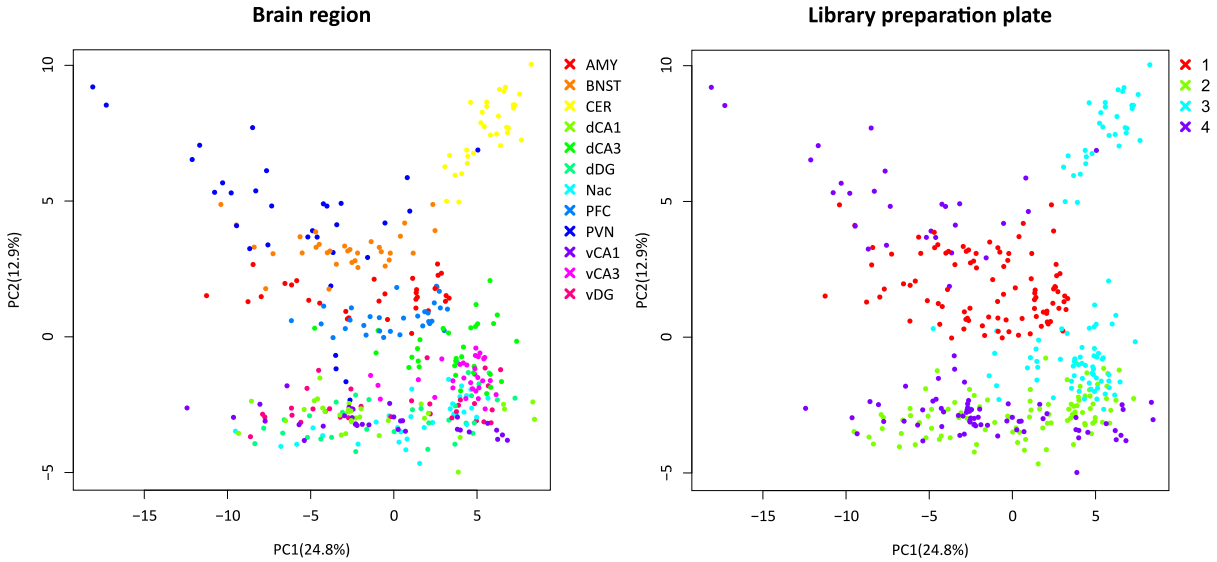

Figure 35: Principal component (PC) plot of normalized count data of LMCD mice.
In the left plot, the samples are colored by the brain region; in the right, plot the samples are colored by the library preparation plate.

Even though a strong brain region effect is present, we decided not to protect this effect in the SVA for several reasons. First, three brain regions always correspond to one library preparation plate. Due to this design, protecting for the brain region effect would make a correction concerning the plate effect not reliable. The plate effect could not be distinguished from the brain region effect by the SVA anymore. Moreover, a comparison between brain regions is only possible after correcting for the brain region effect. In the end, even though we corrected for the brain region effect, the brain regions still cluster together in the principal component plot after the batch correction (Figure 37).

In this experiment, the surrogate variables are highly and significantly correlated only with the suspected batch effects (Figure 36). On the other hand, the experimental conditions, which were protected from the correction, are not correlated with the surrogate variables. Interestingly, SV5 does not correlate with any of the observed parameters. This suggests a hidden batch effect, which the SVA is correcting.

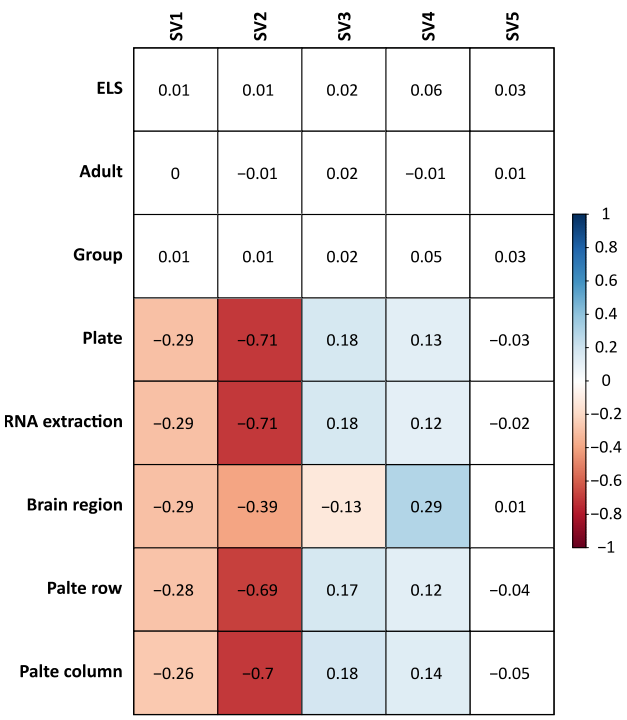

Figure 36: Correlation matrix of surrogate variables (SVs) with sample properties.
Filled colored boxes mark significant associations; positive and negative correlations are marked blue and red respectively.

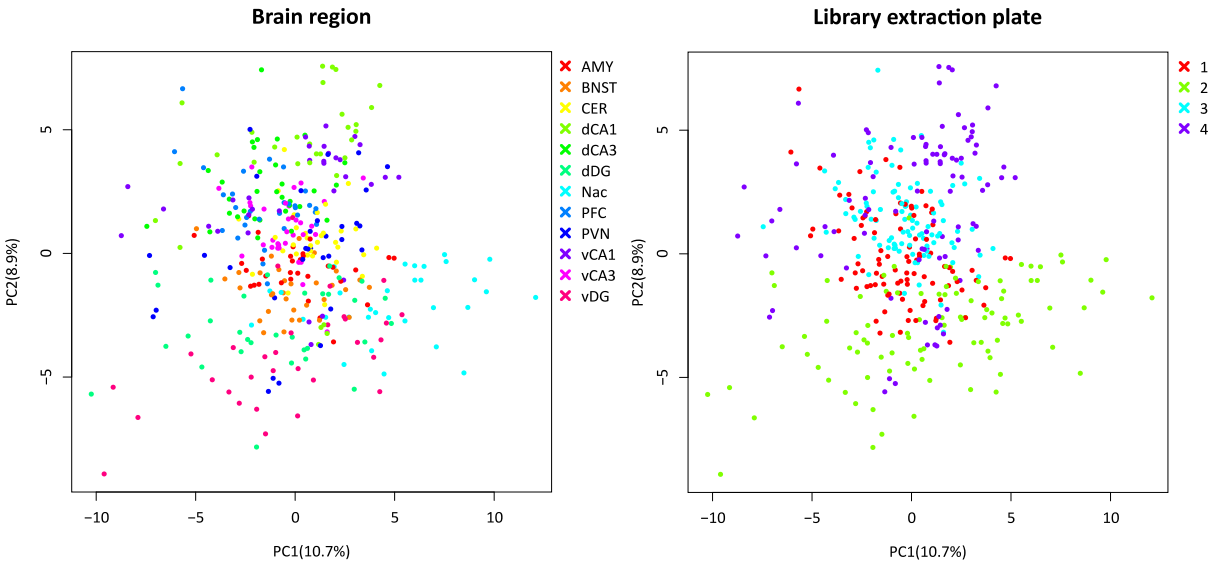

Figure 37: Principal component (PC) plot after batch correction of count data from LMCD mice.
In the left plot, the samples are colored by the brain region; in the right plot, the samples are colored by the library preparation plate.

The SVA corrected data is presented in Figure 37. Two outliers (83_dCA1 and 97_vDG) were excluded due to more than four standard deviations distance from the mean of all samples. The principal component plots illustrate the disappearance of previously detected clusters, especially the different plates are merged together.

4.4.4 Differential expression of eQTL genes

Similar to the previous experiment, differential expression analysis could not detect many significantly regulated genes. The acute stress in adulthood again resulted in the highest number of differentially expressed genes, in this experiment together with the interaction effect (Table 14).

Table 14: Differentially expressed genes in LMCD mice

	ELS	Adult	Interaction
AMY			Higd1a
BNST			
CER			
dCA1		Fth	Ccndbp1
dCA3			
dDG		Hist1h2al	Rps12
PFC			
Nac	Snrnp70	AW209491	Abhd5
PVN			
vCA1		Abhd5	
vCA3			
vDG			

4.4.5 Network analysis

The network analysis of partial correlation co-expression networks revealed strong networks in the PVN as well as the dorsal and ventral CA1 (Figure 38). Other brain regions like the PFC, AMY and BNST, but also other hippocampal subregions, showed only sparse network connectivity. In this experiment, no networks were present in the cerebellum. This suggest that the physiological stress used in this experiment did not activate the GR-response genes in the cerebellum, in contrast to the previous experiment. This would be in line with the concept of different stressful stimuli triggering specific physiological systems. Thus, beside an increase in corticosterone, the context of the stressful situation is critical (Koolhaas et al. 2011).

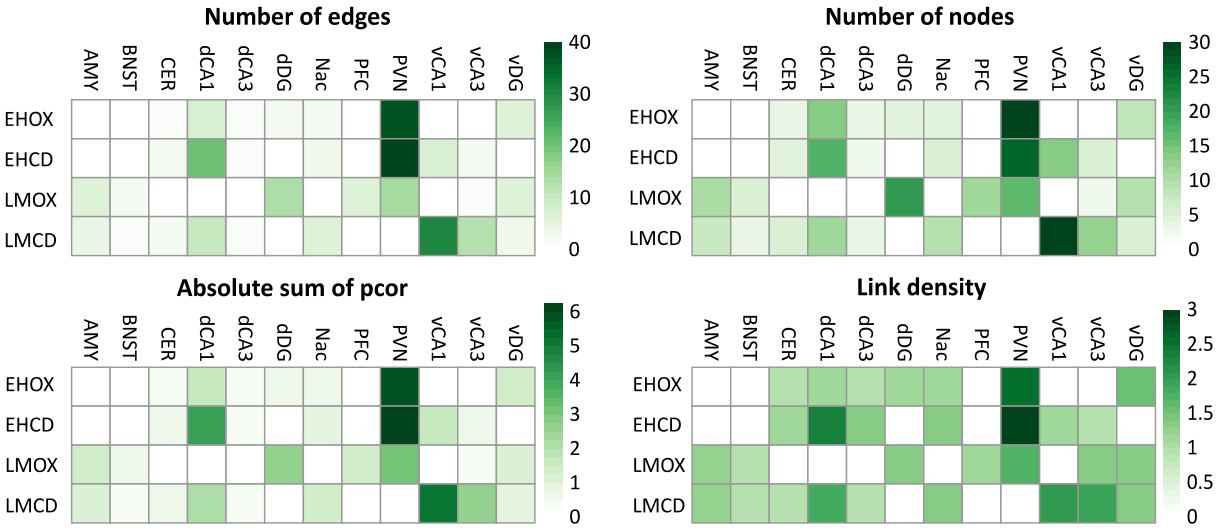

Figure 38: Network properties of co-expression partial correlation networks from LMCD mice.
Depicted are the total number of edges and nodes in the specific networks as well as the absolute sum of the partial correlation coefficient (pcor) and the link density in the respective networks.

The network node genes of the specific networks in the three most connected regions are depicted in Figure 39 and clustered by the number of edges and the betweenness of the genes. The two most connected networks are observed in the early handling groups of the PVN and these cluster together in terms of their edges and genes involved. Notable, the betweenness of the genes is different over all of these highly connected networks, which highlights their structural differences.

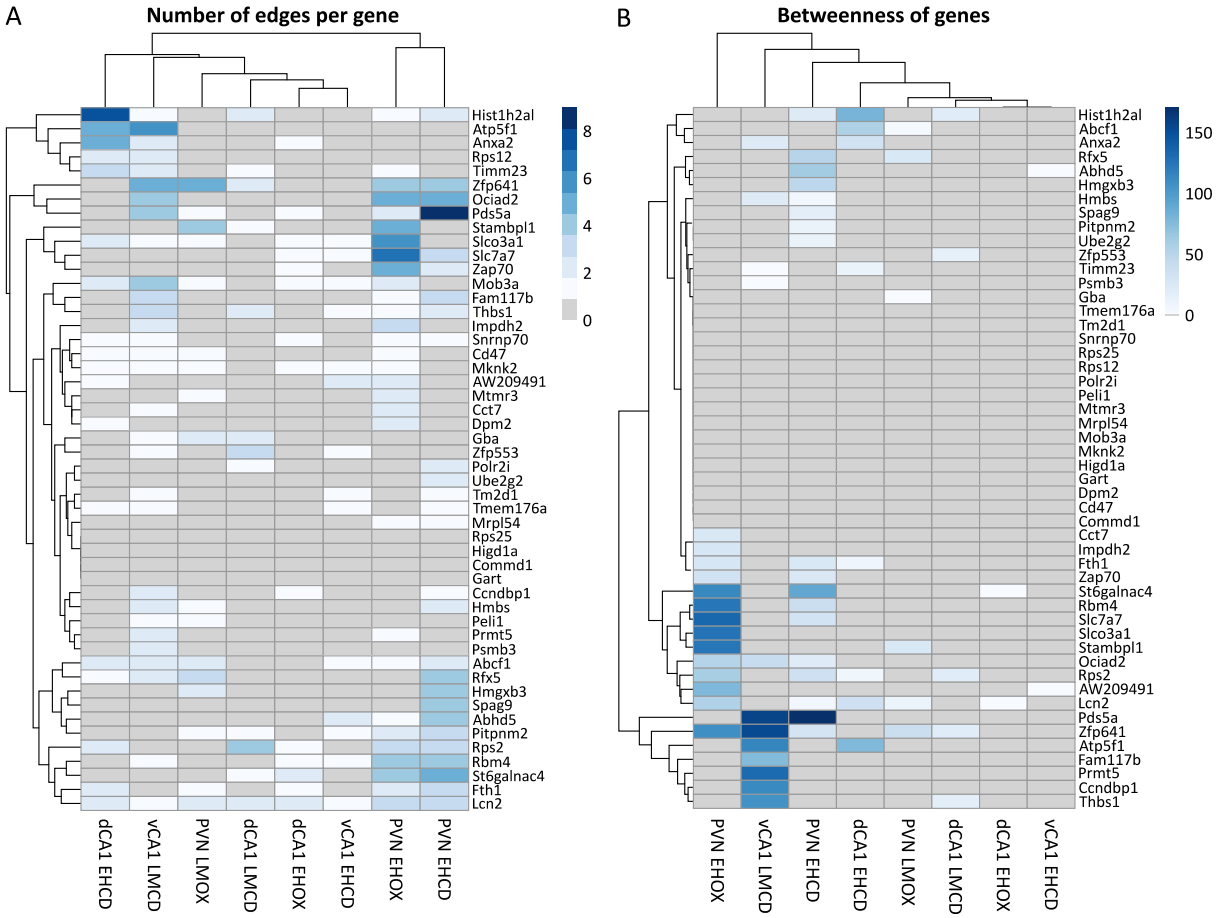

Figure 39: Number of edges and betweenness of network node genes in the most connected regions, PVN, dCA1 and vCA1.

Node genes are clustered by the number of connecting edges (A) or their betweenness (B) in the specific networks.

Specifically in the PVN, the EHOX and EHCD networks have the most node genes and these are connected by the most edges compared to all other networks. Nevertheless, the two networks are very different. Figure 40 presents the network graph of all four experimental groups. The structural differences between the two early handling networks become clearer when focusing on specific genes. One example is the Pds5a gene. It is present in the networks of both groups with a substantial amount of edges but only shows a high betweenness in the EHCD group (Figure 39). In the network graphs, Pds5a is only connected to Ociad2 and Slco3a1 in the EHOX network. In contrast, in the EHCD network, it is connected to many genes and therefore has a central position. Remarkably, the genes which Pds5a is connected to in the two networks are completely different.

Taken together, two strong networks are present in the early handling group in the PVN, with the two networks changing remarkably in response to the adult condition. Interestingly, early life stress seems to disrupt these networks. The network in the LMOX group is rather small and no network is formed in the group exposed to early life and adult stress (LMCD).

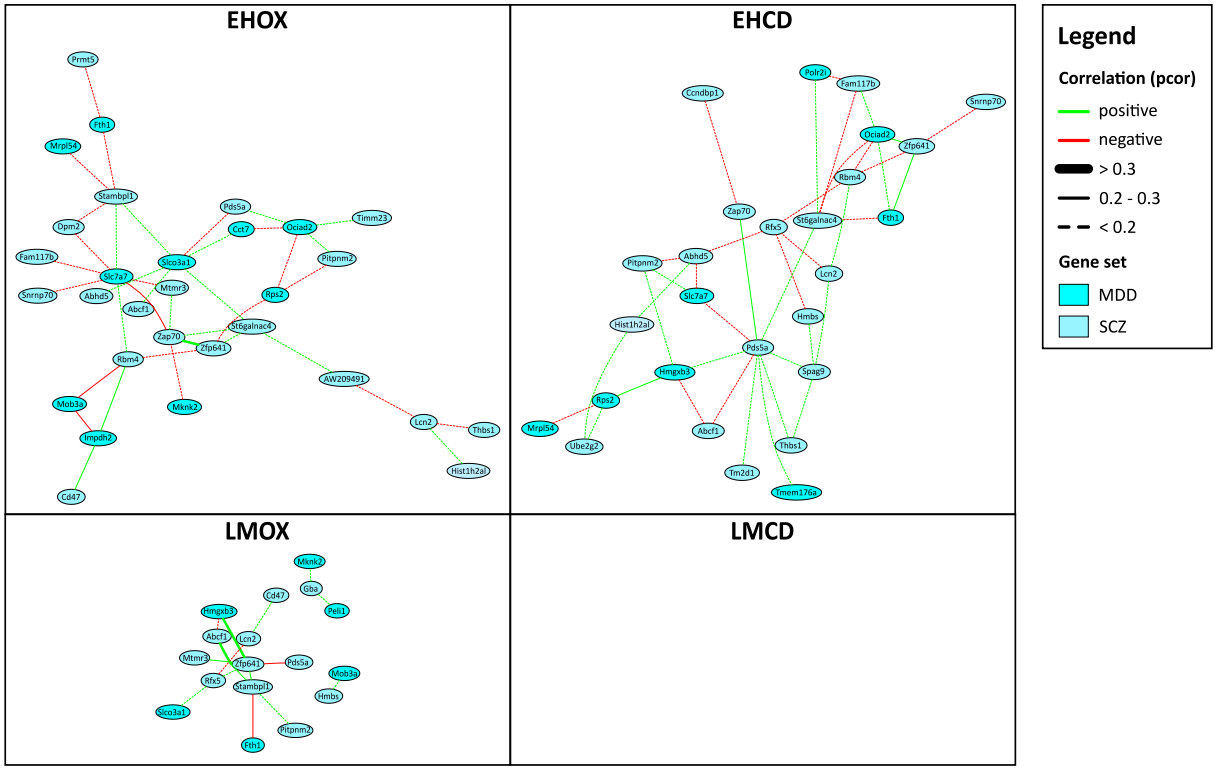

Figure 40: Partial correlation co-expression networks in the PVN.
The specific networks in all experimental groups of the PVN are illustrated. Negative or positive partial correlation is depicted in red or green respectivly. The correlation strength is represented by the edge style.

Figure 41 depicts the network graphs of the dCA1 region. The situation in this brain region is different. Here, the adult condition seems to play the major role with substantial networks present in both chronic social defeat stress groups.

Another large network is present in the LMCD group of the vCA1 (Figure 42). Here, the repeated stress condition seems to activate the co-expression of a large number of genes. Interestingly, Pds5a is one of the major hub genes with a betweenness value comparable to the EHCD group in the PVN (Figure 39B).

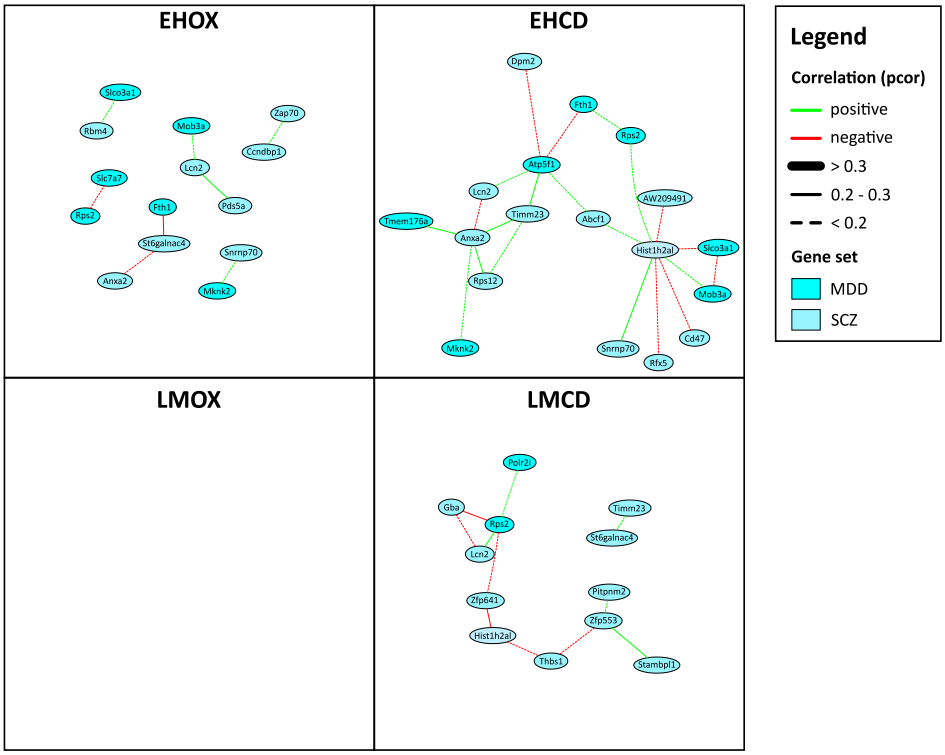

Figure 41: Partial correlation co-expression networks in the dCA1.
The specific networks in all experimental groups of the dCA1 are illustrated. Negative or positive partial correlation is depicted in red or green respectivly. The correlation strength is represented by the edge style.

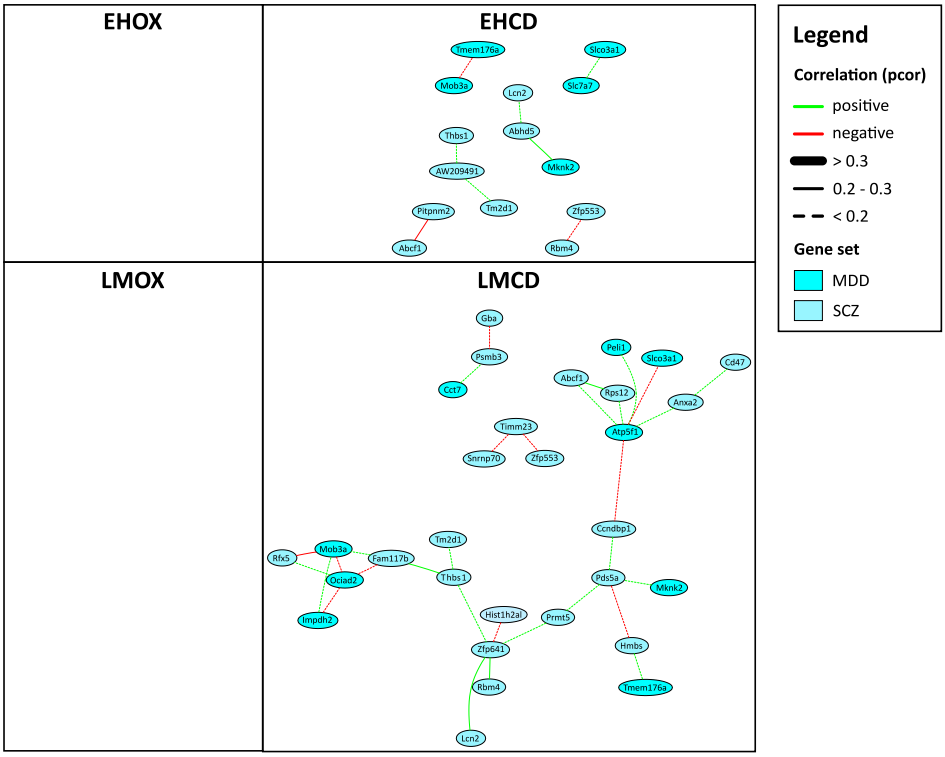

Figure 42: Partial correlation co-expression networks in the vCA1.
The specific networks in all experimental groups of the vCA1 are illustrated. Negative or positive partial correlation is depicted in red or green respectivly. The correlation strength is represented by the edge style.

5 Discussion

In this thesis, the long-term programming effects of early life stress were investigated by two approaches in different animal models. In the first part, a candidate approach was applied. We used maternal separation to investigate the long-term epigenetic regulation of CRH in the PVN. In the second part, a previously in humans established network of GR-response eQTL genes was investigated. In a translational approach, the network properties were evaluated following early life stress alone and in conjunction with adult stress.

5.1 Epigenetic programming of CRH expression

First, long-term programming of gene expression through epigenetic mechanism like DNA methylation was investigated. Based on previous results in the lab, which demonstrated epigenetic programming of various parts of the HPA axis, the expression and promoter methylation of CRH was analyzed. Initial experiments had established sex specific expression differences in adult female mice following maternal separation. Therefore, CRH expression and corticosterone levels were investigated across the estrous cycle in female mice. In control mice, but not in ELS mice, estrous cycle dependent changes in CRH expression and corticosterone levels were detected. The HPA and the hypothalamic–pituitary–gonadal (HPG) axis are interconnected at various levels. Estradiol activates the HPA axis whereas corticosterone suppresses the HPG axis. The sustained CRH and corticosterone levels throughout the estrous cycle in maternal separated mice suggest a disturbed synchronization between the HPA and HPG axis activity by the adverse early life experiences. As underlying mechanism, we were hypothesizing differences in CRH activation due to epigenetic modifications. The proximal CRH promoter contains 10 CpG dinucleotides and numerous transcription factor binding sites (Figure 43).

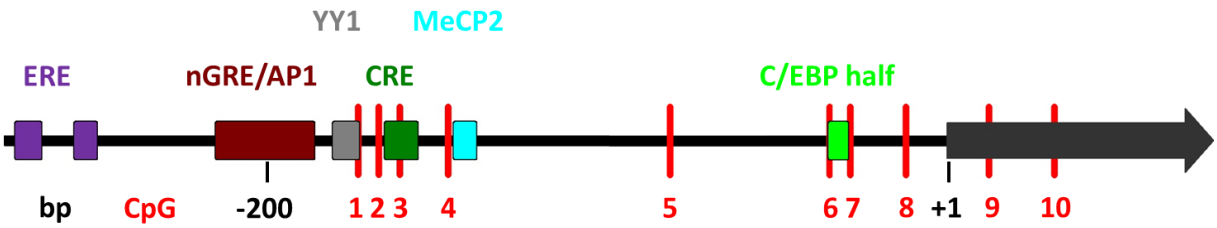

Figure 43: Schematic representation of the CRH Promoter.
Investigated CpG sites are marked by red lines, colored boxes correspond to experimentally validated as well as predicted transcription factor binding sites. ERE: estrogen response element; nGRE: negative glucocorticoid response element; AP1: activator protein 1; YY1: Yin Yang 1; CRE: cAMP response element; C/EBP half: CCAAT/enhancer-binding protein half site; MeCP2: methyl CpG binding protein 2.

The best characterized transcription factor binding sites are the negative glucocorticoid response element (nGRE) and the cAMP response element (CRE) (King et al. 2002; Nicholson et al. 2004). Also estrogen response elements (ERE) are thought to localize at the CRH promoter region (Vamvakopoulos

and Chrousos 1993). Furthermore, alternative pathways of estrogen-dependent activation of the CRH promoter have been proposed (Miller et al. 2004).

The CRH promoter is enriched in CpGs, which also overlap with transcription factor binding sites. Investigation of CpG methylation of this part seemed especially interesting since DNA methylation is known to change the ability of transcription factor binding at its DNA address code. Generally, methylated CpGs are known to impair transcription factor binding. On the other hand, CpG methylation of regulatory sequences can also increase the binding of specific transcription factors (Rishi et al. 2010). However, methylation at the CRH promoter region did not change in maternal separated females. This further highlights the stressor-, sex-, and tissue-specific regulation of CRH gene expression in accord with several related studies (Raabe and Spengler 2013).

Within the framework of thesis, the molecular mechanisms of altered CRH expression in female mice with a history of maternal separation remained unidentified. Future studies need to address a variety of possible mechanisms leading to the observed expression pattern. Beside differences in methylation, posttranslational modifications can modulate transcription factor binding as well. Transcriptional activation at the CRH promoter is a complex interplay between various proteins. Glucocorticoids repress expression through the nGRE whereas the cAMP response element binding protein (CREB) as well as c-Jun–c-Fos heterodimers interact synergistically to activate CRH expression (Nicholson et al. 2004). CREB is a well-studied transcription factor that is involved in the regulation of neuronal plasticity, neuronal growth and survival. Different signaling pathways converge on CREB and regulate its activity by phosphorylation (Lonze and Ginty 2002). Therefore, the regulatory processes that could be affected by early life stress are manifold. In order to comprehensively investigate these regulatory processes, proteomic approaches appear to be necessary.

Additionally, differences in the innervation of the PVN from other brain regions need to be assessed, for example via retrograde tracers. Differences in the cellular composition of the PVN in the response to ELS are another possible source of altered CRH expression. Moreover, dendrite outgrowth and synaptic morphology of CRH neurons could be investigated.

5.2 MDD/SCZ-related GR-response eQTL genes in mice

In a previous study by Arloth et al. (2015), GR-response eQTLs were identified in a cohort of human males. The identified eQTL SNPs were then matched with nominally significant hits from large GWAS for major depressive disorder as well as schizophrenia. The resulting genes from a tightly connected network with some of them associated to both diseases.

In a translational approach, we investigated the network properties of these eQTL genes in mice. Thereby, exposure to stress could be analyzed in a controlled environment. The interplay between early life stress and adult stressors was studied in two mouse models. In the first one, maternal separation was combined with acute corticosterone injection before sacrifice. In the second one, limited nesting material was combined with chronic social defeat in adulthood. In both animal studies, gene expression was measured in stress relevant brain regions. Differential expression analysis on a single gene basis did not reveal many significantly regulated genes. A higher number of differentially expressed genes was detected in blood, which was only available from the first study. In blood, substantial regulation by the acute corticosterone injection was observed. Since the human data was also obtained from blood with a similar stimulus (dexamethasone injection) this highlights the conserved GR responsiveness between species.

As the investigated genes were only weakly regulated on a single gene basis and given the network connectivity established in humans, the network properties were investigated in the different mouse brain regions. Pronounced differences between the two animal models have been found. In the first animal model, a strong activation of genes by acute corticosterone treatment was observed. This can be deduced from the strong network connectivity in the cerebellum, a brain region unrelated to stress regulation. Due to the high abundance of glucocorticoid receptors in the cerebellum (Morimoto et al. 1996) the pharmacological treatment resulted in strong effects in the corticosterone injected control group. Besides that, marked network connectivity was also observed in hippocampal brain regions, with the strongest effects in the ventral CA3 across all conditions. This finding is in accord with the concept that the hippocampus is a major regulator of the stress response and contains a high number of GR. Moreover, peripheral tissues like pituitary and blood showed high network connectivity under all conditions.

In the second animal model, three brain regions stood out in the number of connected nodes and edges: the PVN, the ventral and the dorsal CA1. The highest network connectivity was observed in the early handling groups of the PVN but also the double stress group of the vCA1 showed high connectivity. Especially the PVN but also the CA1 are brain regions well known for their function within the stress response and their involvement in stress regulation. This illustrates the validity of the model and the involvement of the selected genes in stress related regulatory processes.

Pds5a could be identified as particularly interesting gene within all networks. It is located centrally in two networks, the PVN EHCD group and the vCA1 LMCD group. In these networks, it functions as hub gene, influencing the expression of several neighboring genes. This matches well with its potential function as cohesin regulatory factor (Zhang et al. 2009). Cohesin works in concert with CTCF to form and stabilize chromosomal loops, thereby changing the access to DNA regulatory sequences. As a

result, gene regulatory elements either can interact with each other or are insulated from the associated genes. However, the details of the underlying regulatory processes are complex, with a vast variety of involved factors and the exact role of Pds5a seems difficult to decipher. Pds5a and its homologue, Pds5b, have so far been mostly implicated in causing Cornelia de Lange syndrome, a rare developmental disorder that is characterized by mental retardation among other deficits. Pds5a knockout mice, however, lacked any obvious defects in central nervous system development (Zhang et al. 2009).

The central function of Pds5a is observed in different conditions in the two brain regions. In the PVN, the Pds5a hub is activated by chronic social defeat in previously unstressed individuals whereas in the vCA1 the activation occurs only after a history of early life stress. This highlights the regional specificity and distinct underlying regulatory processes. The ventral hippocampus, especially the CA1 region, has been implicated in the tonic regulation of the PVN (Herman et al. 1992). It can be speculated that early life stress triggers long-term programming processes in the hippocampus leading to structural changes which result in the activation of Pds5 and its co-regulated genes after chronic adult stress. This could disturb the regulatory properties of the hippocampus and result in the disruption of the PVN network under stressful conditions, which would explain the absence of the PVN LMCD network.

Overall, the network analysis showed a region specific and stimulus dependent activation of the MDD/SCZ-related GR-response eQTL genes. Early life stress, a major risk factor for psychiatric diseases, modulates the responsiveness of the co-expression networks. This suggests an involvement of the identified genes within stress relevant processes in these psychiatric diseases. Moreover, genes related to either MDD or schizophrenia are always intertwined within the network architecture. Therefore, the identified genes possibly share regulatory processes that are affected in both diseases.

To further evaluate the importance of the identified genes in the context of psychiatric disorders, several experiments could be conducted in the future. In primary cultures of mouse hippocampal cells, regulatory processes could be further evaluated. The use of cultured cells allows the convenient addition and depletion of various cofactors. Using cells from knockout animals, regulatory influences of specific genes could be analyzed quickly. Further, the use of human induced pluripotent stem cells (iPSC) cells could help to translate the insights gained herein back to humans. Human iPSCs could be differentiated into neurons and then stimulated with glucocorticoids. The use of the CRISPR/Cas system (Clustered Regularly Interspaced Short Palindromic Repeats) would allow further manipulations of promoter or enhancer regions. Thereby, the regulatory properties of disrupted transcription factor binding sites or structural inhibitions could be detected. In order to evaluate the MDD/SCZ-related eQTL genes against the background of the whole transcriptome, microarrays or RNA sequencing could be performed. The most interesting brain regions, like the PVN, could thereby be

analyzed in more detail. Another technique would be in-situ hybridization, which has the advantage of spatial resolution but can only be done for a small number of genes.

The spatial resolution provided by the micro punching technique is already high. Nevertheless, new technical developments include fluorescence-activated cell sorting (FACS) and single-cell RNA sequencing. Thereby, even subpopulations of brain regions can be analyzed in detail. Prior to sequencing, specific cell populations like neurons or even CRH expressing cells can be isolated via FACS. The obtained transcriptomes can further be categorized by gene clustering analysis and rare cell types can be identified. This overcomes the difficulty of cellular heterogeneity, which commonly dilutes experimental effects within punching areas. Via single-cell sequencing, cell type specific effects can be identified with high sensitivity. This opens the possibility of more detailed investigations and enables the identification of the underlying mechanistic properties.

In conclusion, the set of MDD- and SCZ-related genes identified by GR-response eQTL analysis in humans has proven to be relevant in stress related disorders. Two related models of early life stress in mice have shown region specific co-expression networks with stress related brain regions being the most prominent. So far, most of these genes have not been implicated in psychiatric diseases and their functions are largely unknown. Future experiments in animals as well as humans have to strengthen the functional involvement of these genes and the related pathways in psychiatric disorders. The elucidation of the regulatory processes within and beside the gene networks could establish a more thorough understanding of the mechanisms leading to these disorders and pave the development of new treatments.

6 Acknowledgments

This work was carried out in the Department of Translational Research in Psychiatry at the Max-Planck Institute of Psychiatry in Munich. First, I would like to thank Professor Dr. Dr. Dr. Florian Holsboer and Dr. Elisabeth B. Binder for giving me the opportunity to prepare my PhD thesis at this institute.

I would like to thank my supervisor PD Dr. Dietmar Spengler for his guidance and support of this work. He was always available for helpful advice and critical discussions.

I would also like to express my gratitude to my thesis advisor PD Dr. Carsten Wotjak as well as Prof. Dr. Wolfgang Enard and the rest of my thesis committee, who kindly agreed to referee this thesis.

This work would not have been possible without the support of many people. I would like to thank Dr. Janine Arloth and Dr. Peter Weber for their excellent expertise and help with conducting the Biostatistics analysis as well as Simone Röh and Dr. Darina Czamara for their helpful advice; Dr. Elmira Anderzhanova for her support with the microdialysis, Anne Löschner for her great support with RNA extraction and next generation sequencing, Monika Rex Haffner for operating the MiSeq, and Anke Hoffmann for always being available for any technical questions in the lab.

I would also like to thank all former and present members of the AG Spengler and the Binder department as well as Prof. Dr. Osborne Almeida and his group for their support during the years. Especially Yannick Menger and Dr. med. Florian Raabe for their help during the CRH project; Mareen Engel, Stella Iurato, Dr. Arleta Madejska, Dr. Yvonne Bockmühl, Dr. Udo Schmidt-Edelkraut, and Dr. Guillaume Daniel for a great time down in the cellar as well as Dr. Nils C. Gassen, Dr. med. Anthony Zannas, Lilia Papst and Kathrin Hafner for being awesome office mates during the last year.

My greatest gratitude goes to my parents, which were always supporting me throughout all the years, and most importantly to my wife Natalie.

7 References

Allis CD, Caparros M-L, Jenuwein T, Reinberg D (2015) Epigenetics, Second edition. Cold Spring Harbor Laboratory Press, New York

American Psychiatric Association, American Psychiatric Association (eds) (2000) Diagnostic and statistical manual of mental disorders: DSM-IV-TR, 4th ed., text revision. American Psychiatric Association, Washington, DC

Anders S, Huber W (2010) Differential expression analysis for sequence count data. Genome Biol 11:R106. doi: 10.1186/gb-2010-11-10-r106

Anders S, McCarthy DJ, Chen Y, et al (2013) Count-based differential expression analysis of RNA sequencing data using R and Bioconductor. Nat Protoc 8:1765–1786. doi: 10.1038/nprot.2013.099

Anderzhanova EA, Bächli H, Buneeva OA, et al (2013) Strain differences in profiles of dopaminergic neurotransmission in the prefrontal cortex of the BALB/C vs. C57Bl/6 mice: Consequences of stress and afobazole. Eur J Pharmacol 708:95–104. doi: 10.1016/j.ejphar.2013.03.015

Andrews S (2010) FastQC A Quality Control tool for High Throughput Sequence Data. http://www.bioinformatics.babraham.ac.uk/projects/fastqc/. Accessed 30 May 2016

Arloth J, Bogdan R, Weber P, et al (2015) Genetic Differences in the Immediate Transcriptome Response to Stress Predict Risk-Related Brain Function and Psychiatric Disorders. Neuron 86:1189–1202. doi: 10.1016/j.neuron.2015.05.034

Armstrong L (2014) Epigenetics. Garland Science, New York

Balsevich G, Uribe A, Wagner KV, et al (2014) Interplay between diet-induced obesity and chronic stress in mice: potential role of FKBP51. J Endocrinol 222:15–26. doi: 10.1530/JOE-14-0129

Beery AK, Zucker I (2011) Sex bias in neuroscience and biomedical research. Neurosci Biobehav Rev 35:565–572. doi: 10.1016/j.neubiorev.2010.07.002

Bell JT, Pai AA, Pickrell JK, et al (2011) DNA methylation patterns associate with genetic and gene expression variation in HapMap cell lines. Genome Biol 12:R10. doi: 10.1186/gb-2011-12-1-r10

Berton O, McClung CA, DiLeone RJ, et al (2006) Essential Role of BDNF in the Mesolimbic Dopamine Pathway in Social Defeat Stress. Science 311:864–868. doi: 10.1126/science.1120972

Bettscheider M, Kuczynska A, Almeida O, Spengler D (2012) Optimized Analysis of DNA Methylation and Gene Expression from Small, Anatomically-defined Areas of the Brain. J Vis Exp. doi: 10.3791/3938

Bockmühl Y, Patchev AV, Madejska A, et al (2015) Methylation at the CpG island shore region upregulates Nr3c1 promoter activity after early-life stress. Epigenetics 10:247–257. doi: 10.1080/15592294.2015.1017199

Briere J, Elliott DM (2003) Prevalence and psychological sequelae of self-reported childhood physical and sexual abuse in a general population sample of men and women. Child Abuse Negl 27:1205–1222. doi: 10.1016/j.chiabu.2003.09.008

Caldji C, Tannenbaum B, Sharma S, et al (1998) Maternal care during infancy regulates the development of neural systems mediating the expression of fearfulness in the rat. Proc Natl Acad Sci 95:5335–5340. doi: 10.1073/pnas.95.9.5335

Chambers JM, Hastie TJ (eds) (1993) Statistical models in S. Chapman & Hall, New York

Chapman DP, Whitfield CL, Felitti VJ, et al (2004) Adverse childhood experiences and the risk of depressive disorders in adulthood. J Affect Disord 82:217–225. doi: 10.1016/j.jad.2003.12.013

Converge Consortium (2015) Sparse whole-genome sequencing identifies two loci for major depressive disorder. Nature 523:588–591. doi: 10.1038/nature14659

Cortellino S, Xu J, Sannai M, et al (2011) Thymine DNA Glycosylase Is Essential for Active DNA Demethylation by Linked Deamination-Base Excision Repair. Cell 146:67–79. doi: 10.1016/j.cell.2011.06.020

Cross-Disorder Group of the Psychiatric Genomics Consortium (2013) Genetic relationship between five psychiatric disorders estimated from genome-wide SNPs. Nat Genet 45:984–994. doi: 10.1038/ng.2711

Csardi G, Nepusz T (2006) The igraph software package for complex network research. InterJournal Complex Systems:1695.

de Kloet ER, Joëls M, Holsboer F (2005) Stress and the brain: from adaptation to disease. Nat Rev Neurosci 6:463–475. doi: 10.1038/nrn1683

Degroot A, Wade M, Salhoff C, et al (2004) Exposure to an elevated platform increases plasma corticosterone and hippocampal acetylcholine in the rat: reversal by chlordiazepoxide. Eur J Pharmacol 493:103–109. doi: 10.1016/j.ejphar.2004.04.011

Dempster AP (1972) Covariance Selection. Biometrics 28:157–175. doi: 10.2307/2528966

Dohrenwend BP, Dohrenwend BS (1976) Sex Differences and Psychiatric Disorders. Am J Sociol 81:1447–1454. doi: 10.1086/226229

Dube SR, Anda RF, Felitti VJ, et al (2001) Childhood Abuse, Household Dysfunction, and the Risk of Attempted Suicide Throughout the Life Span: Findings From the Adverse Childhood Experiences Study. JAMA 286:3089–3096. doi: 10.1001/jama.286.24.3089

Edwards VJ, Holden GW, Felitti VJ, Anda RF (2003) Relationship between multiple forms of childhood maltreatment and adult mental health in community respondents: results from the adverse childhood experiences study. Am J Psychiatry 160:1453–1460. doi: 10.1176/appi.ajp.160.8.1453

Eisen MB, Spellman PT, Brown PO, Botstein D (1998) Cluster analysis and display of genome-wide expression patterns. Proc Natl Acad Sci 95:14863–14868. doi: 10.1073/pnas.95.25.14863

Felitti VJ, Anda RF, Nordenberg D, et al (1998) Relationship of Childhood Abuse and House hold Dysfunction to Many of the Leading Causes of Death in Adults: The Adverse Childhood Experiences (ACE) Study. Am J Prev Med 14:245–258. doi: 10.1016/S0749-3797(98)00017-8

Finkelhor D, Turner HA, Shattuck A, Hamby SL (2015) Prevalence of Childhood Exposure to Violence, Crime, and Abuse: Results From the National Survey of Children's Exposure to Violence. JAMA Pediatr 169:746–754. doi: 10.1001/jamapediatrics.2015.0676

Frankenhuis WE, Del Giudice M (2012) When do adaptive developmental mechanisms yield maladaptive outcomes? Dev Psychol 48:628–642. doi: 10.1037/a0025629

Fuente A de la, Bing N, Hoeschele I, Mendes P (2004) Discovery of meaningful associations in genomic data using partial correlation coefficients. Bioinformatics 20:3565–3574. doi: 10.1093/bioinformatics/bth445

Gentleman RC, Carey VJ, Bates DM, et al (2004) Bioconductor: open software development for computational biology and bioinformatics. Genome Biol 5:R80. doi: 10.1186/gb-2004-5-10-r80

Gibney ER, Nolan CM (2010) Epigenetics and gene expression. Heredity 105:4–13. doi: 10.1038/hdy.2010.54

Gilles EE, Schultz L, Baram TZ (1996) Abnormal corticosterone regulation in an immature rat model of continuous chronic stress. Pediatr Neurol 15:114–119. doi: 10.1016/0887-8994(96)00153-1

Goldman JM, Murr AS, Cooper RL (2007) The rodent estrous cycle: characterization of vaginal cytology and its utility in toxicological studies. Birth Defects Res B Dev Reprod Toxicol 80:84–97. doi: 10.1002/bdrb.20106

Graffelman J (2013) calibrate: Calibration of Scatterplot and Biplot Axes. https://cran.r-project.org/web/packages/calibrate/index.html. Accessed 30 May 2016

Gratten J, Wray NR, Keller MC, Visscher PM (2014) Large-scale genomics unveils the genetic architecture of psychiatric disorders. Nat Neurosci 17:782–790. doi: 10.1038/nn.3708

Green J, McLaughlin KA, Berglund PA, et al (2010) Childhood adversities and adult psychiatric disorders in the national comorbidity survey replication i: Associations with first onset of dsm-iv disorders. Arch Gen Psychiatry 67:113–123. doi: 10.1001/archgenpsychiatry.2009.186

Haenisch B, Bilkei-Gorzo A, Caron MG, Bönisch H (2009) Knockout of the norepinephrine transporter and pharmacologically diverse antidepressants prevent behavioral and brain neurotrophin alterations in two chronic stress models of depression. J Neurochem 111:403–416. doi: 10.1111/j.1471-4159.2009.06345.x

Häfner H, Maurer K, Trendler G, et al (2005) Schizophrenia and depression: Challenging the paradigm of two separate diseases—A controlled study of schizophrenia, depression and healthy controls. Schizophr Res 77:11–24. doi: 10.1016/j.schres.2005.01.004

Hansen KD, Gentry J, Long L, et al Rgraphviz: Provides plotting capabilities for R graph objects. http://bioconductor.org/packages/Rgraphviz/. Accessed 30 May 2016

He Y-F, Li B-Z, Li Z, et al (2011) Tet-Mediated Formation of 5-Carboxylcytosine and Its Excision by TDG in Mammalian DNA. Science 333:1303–1307. doi: 10.1126/science.1210944

Heim C, Binder EB (2012) Current research trends in early life stress and depression: Review of human studies on sensitive periods, gene–environment interactions, and epigenetics. Exp Neurol 233:102–111. doi: 10.1016/j.expneurol.2011.10.032

Heim C, Nemeroff CB (2001) The role of childhood trauma in the neurobiology of mood and anxiety disorders: preclinical and clinical studies. Biol Psychiatry 49:1023–1039. doi: 10.1016/S0006-3223(01)01157-X

Heim C, Nemeroff CB (2002) Neurobiology of early life stress: Clinical studies. Semin Clin Neuropsychiatry 7:147–159. doi: 10.1053/scnp.2002.33127

Herman JP, Cullinan WE, Young EA, et al (1992) Selective forebrain fiber tract lesions implicate ventral hippocampal structures in tonic regulation of paraventricular nucleus corticotropin-releasing hormone (CRH) and arginine vasopressin (AVP) mRNA expression. Brain Res 592:228–238. doi: 10.1016/0006-8993(92)91680-D

Hirschfeld RMA (2001) The Comorbidity of Major Depression and Anxiety Disorders: Recognition and Management in Primary Care. Prim Care Companion J Clin Psychiatry 3:244–254. doi: 10.4088/PCC.v03n0609

Hodes GE, Pfau ML, Purushothaman I, et al (2015) Sex Differences in Nucleus Accumbens Transcriptome Profiles Associated with Susceptibility versus Resilience to Subchronic Variable Stress. J Neurosci 35:16362–16376. doi: 10.1523/JNEUROSCI.1392-15.2015

Hoffmann A, Zimmermann CA, Spengler D (2015) Molecular epigenetic switches in neurodevelopment in health and disease. Front Behav Neurosci 120. doi: 10.3389/fnbeh.2015.00120

Holden C (2005) Sex and the Suffering Brain. Science 308:1574–1574. doi: 10.1126/science.308.5728.1574

Hollis F, Kabbaj M (2014) Social Defeat as an Animal Model for Depression. ILAR J 55:221–232. doi: 10.1093/ilar/ilu002

Ihaka R, Murrell P, Hornik K, et al (2015) colorspace: Color Space Manipulation. https://cran.r-project.org/web/packages/colorspace/index.html. Accessed 30 May 2016

Illumina TruSeq Targeted RNA Expression. http://www.illumina.com/content/dam/illumina-marketing/documents/products/datasheets/datasheet_truseq_targeted_rna_expression.pdf. Accessed 27 Jun 2016

Ito S, D'Alessio AC, Taranova OV, et al (2010) Role of Tet proteins in 5mC to 5hmC conversion, ES-cell self-renewal and inner cell mass specification. Nature 466:1129–1133. doi: 10.1038/nature09303

Ito S, Shen L, Dai Q, et al (2011) Tet Proteins Can Convert 5-Methylcytosine to 5-Formylcytosine and 5-Carboxylcytosine. Science 333:1300–1303. doi: 10.1126/science.1210597

Ivy AS, Brunson KL, Sandman C, Baram TZ (2008) Dysfunctional nurturing behavior in rat dams with limited access to nesting material: A clinically relevant model for early-life stress. Neuroscience 154:1132–1142. doi: 10.1016/j.neuroscience.2008.04.019

Jaffe AE, Hyde T, Kleinman J, et al (2015) Practical impacts of genomic data "cleaning" on biological discovery using surrogate variable analysis. BMC Bioinformatics 16:372. doi: 10.1186/s12859-015-0808-5

Jeltsch A, Jurkowska RZ (2014) New concepts in DNA methylation. Trends Biochem Sci 39:310–318. doi: 10.1016/j.tibs.2014.05.002

Kareta MS, Botello ZM, Ennis JJ, et al (2006) Reconstitution and Mechanism of the Stimulation of de Novo Methylation by Human DNMT3L. J Biol Chem 281:25893–25902. doi: 10.1074/jbc.M603140200

Katz LC, Shatz CJ (1996) Synaptic activity and the construction of cortical circuits. Science 274:1133–1138. doi: 10.1126/science.274.5290.1133

Kendler KS, Gatz M, Gardner CO, Pedersen NL (2006) A Swedish National Twin Study of Lifetime Major Depression. Am J Psychiatry 163:109–114. doi: 10.1176/appi.ajp.163.1.109

Kessler RC, Berglund P, Demler O, et al (2003) The Epidemiology of Major Depressive Disorder: Results From the National Comorbidity Survey Replication (NCS-R). JAMA 289:3095. doi: 10.1001/jama.289.23.3095

Kessler RC, McGonagle KA, Swartz M, et al (1993) Sex and depression in the National Comorbidity Survey I: Lifetime prevalence, chronicity and recurrence. J Affect Disord 29:85–96. doi: 10.1016/0165-0327(93)90026-G

King BR, Smith R, Nicholson RC (2002) Novel glucocorticoid and cAMP interactions on the CRH gene promoter. Mol Cell Endocrinol 194:19–28. doi: 10.1016/S0303-7207(02)00218-6

Kinsey SG, Bailey MT, Sheridan JF, et al (2007) Repeated social defeat causes increased anxiety-like behavior and alters splenocyte function in C57BL/6 and CD-1 mice. Brain Behav Immun 21:458–466. doi: 10.1016/j.bbi.2006.11.001

Kolde R (2015) pheatmap: Pretty Heatmaps. https://cran.r-project.org/web/packages/pheatmap/index.html. Accessed 30 May 2016

Koolhaas JM, Bartolomucci A, Buwalda B, et al (2011) Stress revisited: A critical evaluation of the stress concept. Neurosci Biobehav Rev 35:1291–1301. doi: 10.1016/j.neubiorev.2011.02.003

Krawiec JA, Chen H, Alom-Ruiz S, Jaye M (2009) Modified PAXgene™ method allows for isolation of high-integrity total RNA from microlitre volumes of mouse whole blood. Lab Anim 43:394–398. doi: 10.1258/la.2008.0070157

Leek JT (2014) svaseq: removing batch effects and other unwanted noise from sequencing data. Nucleic Acids Res 42:e161–e161. doi: 10.1093/nar/gku864

Leek JT, Johnson WE, Parker HS, et al (2016) sva: Surrogate Variable Analysis. https://bioconductor.org/packages/release/bioc/html/sva.html. Accessed 30 May 2016

Leek JT, Scharpf RB, Bravo HC, et al (2010) Tackling the widespread and critical impact of batch effects in high-throughput data. Nat Rev Genet 11:733–739. doi: 10.1038/nrg2825

Leek JT, Storey JD (2007) Capturing Heterogeneity in Gene Expression Studies by Surrogate Variable Analysis. PLoS Genet 3:e161. doi: 10.1371/journal.pgen.0030161

Li H, Durbin R (2009) Fast and accurate short read alignment with Burrows–Wheeler transform. Bioinformatics 25:1754–1760. doi: 10.1093/bioinformatics/btp324

Lister R, Mukamel EA, Nery JR, et al (2013) Global Epigenomic Reconfiguration During Mammalian Brain Development. Science 341:1237905. doi: 10.1126/science.1237905

Lister R, Pelizzola M, Dowen RH, et al (2009) Human DNA methylomes at base resolution show widespread epigenomic differences. Nature 462:315–322. doi: 10.1038/nature08514

Liu D, Diorio J, Tannenbaum B, et al (1997) Maternal Care, Hippocampal Glucocorticoid Receptors, and Hypothalamic-Pituitary-Adrenal Responses to Stress. Science 277:1659–1662. doi: 10.1126/science.277.5332.1659

Lonze BE, Ginty DD (2002) Function and Regulation of CREB Family Transcription Factors in the Nervous System. Neuron 35:605–623. doi: 10.1016/S0896-6273(02)00828-0

Love MI, Huber W, Anders S (2014) Moderated estimation of fold change and dispersion for RNA-seq data with DESeq2. Genome Biol 15:550. doi: 10.1186/s13059-014-0550-8

Lucassen PJ, Naninck EFG, van Goudoever JB, et al (2013) Perinatal programming of adult hippocampal structure and function; emerging roles of stress, nutrition and epigenetics. Trends Neurosci 36:621–631. doi: 10.1016/j.tins.2013.08.002

Lupien SJ, McEwen BS, Gunnar MR, Heim C (2009) Effects of stress throughout the lifespan on the brain, behaviour and cognition. Nat Rev Neurosci 10:434–445. doi: 10.1038/nrn2639

MacMillan HL, Fleming JE, Streiner DL, et al (2001) Childhood Abuse and Lifetime Psychopathology in a Community Sample. Am J Psychiatry 158:1878–1883. doi: 10.1176/appi.ajp.158.11.1878

Maunakea AK, Nagarajan RP, Bilenky M, et al (2010) Conserved role of intragenic DNA methylation in regulating alternative promoters. Nature 466:253–257. doi: 10.1038/nature09165

Menger Y, Bettscheider M, Murgatroyd C, Spengler D (2010) Sex differences in brain epigenetics. Epigenomics 2:807–821. doi: 10.2217/epi.10.60

Miller WJS, Suzuki S, Miller LK, et al (2004) Estrogen Receptor (ER)β Isoforms Rather Than ERα Regulate Corticotropin-Releasing Hormone Promoter Activity through an Alternate Pathway. J Neurosci 24:10628–10635. doi: 10.1523/JNEUROSCI.5540-03.2004

Millstein RA, Holmes A (2007) Effects of repeated maternal separation on anxiety- and depression-related phenotypes in different mouse strains. Neurosci Biobehav Rev 31:3–17. doi: 10.1016/j.neubiorev.2006.05.003

Molet J, Maras PM, Avishai-Eliner S, Baram TZ (2014) Naturalistic rodent models of chronic early-life stress. Dev Psychobiol 56:1675–1688. doi: 10.1002/dev.21230

Morimoto M, Morita N, Ozawa H, et al (1996) Distribution of glucocorticoid receptor immunoreactivity and mRNA in the rat brain: an immunohistochemical and in situ hybridization study. Neurosci Res 26:235–269. doi: 10.1016/S0168-0102(96)01105-4

Murgatroyd C, Patchev AV, Wu Y, et al (2009) Dynamic DNA methylation programs persistent adverse effects of early-life stress. Nat Neurosci 12:1559–1566. doi: 10.1038/nn.2436

Murgatroyd C, Spengler D (2011) Epigenetic programming of the HPA axis: Early life decides. Stress 14:581–589. doi: 10.3109/10253890.2011.602146

Nederhof E, Schmidt MV (2012) Mismatch or cumulative stress: Toward an integrated hypothesis of programming effects. Physiol Behav 106:691–700. doi: 10.1016/j.physbeh.2011.12.008

Neuwirth E (2014) RColorBrewer: ColorBrewer Palettes. https://cran.r-project.org/web/packages/RColorBrewer/index.html. Accessed 30 May 2016

Nicholson RC, King BR, Smith R (2004) Complex regulatory interactions control CRH gene expression. Front Biosci J Virtual Libr 9:32–39.

Noguchi KK, Walls KC, Wozniak DF, et al (2008) Acute neonatal glucocorticoid exposure produces selective and rapid cerebellar neural progenitor cell apoptotic death. Cell Death Differ 15:1582–1592. doi: 10.1038/cdd.2008.97

Ooi SKT, O'Donnell AH, Bestor TH (2009) Mammalian cytosine methylation at a glance. J Cell Sci 122:2787–2791. doi: 10.1242/jcs.015123

Paxinos G, Franklin KBJ (2001) The mouse brain in stereotaxic coordinates, 2nd ed. Academic Press, San Diego

Pfaffl MW (2001) A new mathematical model for relative quantification in real-time RT–PCR. Nucleic Acids Res 29:e45–e45. doi: 10.1093/nar/29.9.e45

Plotsky PM, Meaney MJ (1993) Early, postnatal experience alters hypothalamic corticotropin-releasing factor (CRF) mRNA, median eminence CRF content and stress-induced release in adult rats. Mol Brain Res 18:195–200. doi: 10.1016/0169-328X(93)90189-V

Pryce CR, Feldon J (2003) Long-term neurobehavioural impact of the postnatal environment in rats: manipulations, effects and mediating mechanisms. Neurosci Biobehav Rev 27:57–71. doi: 10.1016/S0149-7634(03)00009-5

R Core Team (2016) R: A Language and Environment for Statistical Computing, R Foundation for Statistical Computing, Vienna, Austria. http://www.R-project.org/

Raabe F (2016) Epigenetische Programmierung von Corticotropin-releasing-Hormon durch frühen Stress. Dissertation zum Erwerb des Doktorgrades der Medizin an der Medizinischen Fakultät der Ludwig-Maximilians-Universität zu München

Raabe FJ, Spengler D (2013) Epigenetic risk factors in PTSD and depression. Front Mol Psychiatry 4:80. doi: 10.3389/fpsyt.2013.00080

Rice CJ, Sandman CA, Lenjavi MR, Baram TZ (2008) A Novel Mouse Model for Acute and Long-Lasting Consequences of Early Life Stress. Endocrinology 149:4892–4900. doi: 10.1210/en.2008-0633

Ripke S, Wray NR, Lewis CM, et al (2013) A mega-analysis of genome-wide association studies for major depressive disorder. Mol Psychiatry 18:497–511. doi: 10.1038/mp.2012.21

Ripley B, Venables B, Bates DM, et al (2016) MASS: Support Functions and Datasets for Venables and Ripley's MASS. https://cran.r-project.org/web/packages/MASS/index.html. Accessed 30 May 2016

Rishi V, Bhattacharya P, Chatterjee R, et al (2010) CpG methylation of half-CRE sequences creates C/EBPα binding sites that activate some tissue-specific genes. Proc Natl Acad Sci 107:20311–20316. doi: 10.1073/pnas.1008688107

Ritchie ME, Phipson B, Wu D, et al (2015) limma powers differential expression analyses for RNA-sequencing and microarray studies. Nucleic Acids Res 43:e47–e47. doi: 10.1093/nar/gkv007

Robinson MD, McCarthy DJ, Smyth GK (2010) edgeR: a Bioconductor package for differential expression analysis of digital gene expression data. Bioinformatics 26:139–140. doi: 10.1093/bioinformatics/btp616

Santarelli S (2015) The molecular and behavioral function of SLC6A15, a novel candidate gene for depression. Dissertation an der Fakultät für Biologie der Ludwig-Maximilians-Universität München

Santarelli S, Lesuis SL, Wang X-D, et al (2014) Evidence supporting the match/mismatch hypothesis of psychiatric disorders. Eur Neuropsychopharmacol 24:907–918. doi: 10.1016/j.euroneuro.2014.02.002

Saxonov S, Berg P, Brutlag DL (2006) A genome-wide analysis of CpG dinucleotides in the human genome distinguishes two distinct classes of promoters. Proc Natl Acad Sci U S A 103:1412–1417. doi: 10.1073/pnas.0510310103

Schaefer J, Opgen-Rhein R, Strimmer K (2015) GeneNet: Modeling and Inferring Gene Networks. https://cran.r-project.org/web/packages/GeneNet/index.html. Accessed 30 May 2016

Schäfer J, Strimmer K (2005) Learning Large-Scale Graphical Gaussian Models from Genomic Data. Sci Complex Netw Biol Internet WWW 776:263–276. doi: 10.1063/1.1985393

Schizophrenia Working Group of the Psychiatric Genomics Consortium (2014) Biological insights from 108 schizophrenia-associated genetic loci. Nature 511:421–427. doi: 10.1038/nature13595

Schmidt MV (2011) Animal models for depression and the mismatch hypothesis of disease. Psychoneuroendocrinology 36:330–338. doi: 10.1016/j.psyneuen.2010.07.001

Schmieder R, Edwards R (2011) Quality control and preprocessing of metagenomic datasets. Bioinformatics 27:863–864. doi: 10.1093/bioinformatics/btr026

Schneider CA, Rasband WS, Eliceiri KW (2012) NIH Image to ImageJ: 25 years of image analysis. Nat Methods 9:671–675. doi: 10.1038/nmeth.2089

Schübeler D (2015) Function and information content of DNA methylation. Nature 517:321–326. doi: 10.1038/nature14192

Seasholtz AF, Bourbonais FJ, Harnden CE, Camper SA (1991) Nucleotide sequence and expression of the mouse corticotropin-releasing hormone gene. Mol Cell Neurosci 2:266–273. doi: 10.1016/1044-7431(91)90054-R

Soetaert K, Kones JK, van Oevelen D (2014) NetIndices: Estimating network indices, including trophic structure of foodwebs in R. https://cran.r-project.org/web/packages/NetIndices/index.html. Accessed 30 May 2016

Spruijt CG, Gnerlich F, Smits AH, et al (2013) Dynamic Readers for 5-(Hydroxy)Methylcytosine and Its Oxidized Derivatives. Cell 152:1146–1159. doi: 10.1016/j.cell.2013.02.004

Sullivan PF, Daly MJ, O'Donovan M (2012) Genetic architectures of psychiatric disorders: the emerging picture and its implications. Nat Rev Genet 13:537–551. doi: 10.1038/nrg3240

Sullivan PF, Neale MC, Kendler KS (2000) Genetic Epidemiology of Major Depression: Review and Meta-Analysis. Am J Psychiatry 157:1552–1562. doi: 10.1176/appi.ajp.157.10.1552

Tahiliani M, Koh KP, Shen Y, et al (2009) Conversion of 5-Methylcytosine to 5-Hydroxymethylcytosine in Mammalian DNA by MLL Partner TET1. Science 324:930–935. doi: 10.1126/science.1170116

Taylor SE (2010) Mechanisms linking early life stress to adult health outcomes. Proc Natl Acad Sci 107:8507–8512. doi: 10.1073/pnas.1003890107

The Network and Pathway Analysis Subgroup of the Psychiatric Genomics Consortium (2015) Psychiatric genome-wide association study analyses implicate neuronal, immune and histone pathways. Nat Neurosci 18:199–209. doi: 10.1038/nn.3922

The WHO World Mental Health Survey Consortium (2004) Prevalence, severity, and unmet need for treatment of mental disorders in the world health organization world mental health surveys. JAMA 291:2581–2590. doi: 10.1001/jama.291.21.2581

Thurman RE, Rynes E, Humbert R, et al (2012) The accessible chromatin landscape of the human genome. Nature 489:75–82. doi: 10.1038/nature11232

U.S. Department of Health and Human Services, Administration for Children and Families, Administration on Children, Youth and Families, Children's Bureau (2013) Child Maltreatment 2012.

U.S. Department of Health and Human Services, Administration for Children and Families, Administration on Children, Youth and Families, Children's Bureau (2011) Child Maltreatment 2010.

Vamvakopoulos NC, Chrousos GP (1993) Evidence of direct estrogenic regulation of human corticotropin-releasing hormone gene expression. Potential implications for the sexual dimophism of the stress response and immune/inflammatory reaction. J Clin Invest 92:1896–1902. doi: 10.1172/JCI116782

Venables WN, Ripley BD (2002) Modern Applied Statistics with S. Springer New York, New York, NY

Wagner KV, Wang X-D, Liebl C, et al (2011) Pituitary glucocorticoid receptor deletion reduces vulnerability to chronic stress. Psychoneuroendocrinology 36:579–587. doi: 10.1016/j.psyneuen.2010.09.007

Walker AK, Nakamura T, Byrne RJ, et al (2009) Neonatal lipopolysaccharide and adult stress exposure predisposes rats to anxiety-like behaviour and blunted corticosterone responses: Implications for the double-hit hypothesis. Psychoneuroendocrinology 34:1515–1525. doi: 10.1016/j.psyneuen.2009.05.010

Warde-Farley D, Donaldson SL, Comes O, et al (2010) The GeneMANIA prediction server: biological network integration for gene prioritization and predicting gene function. Nucleic Acids Res 38:W214–W220. doi: 10.1093/nar/gkq537

Warnes GR, Bolker B, Lumley T (2015) gtools: Various R Programming Tools. https://cran.r-project.org/web/packages/gtools/index.html. Accessed 30 May 2016

Weber M, Hellmann I, Stadler MB, et al (2007) Distribution, silencing potential and evolutionary impact of promoter DNA methylation in the human genome. Nat Genet 39:457–466. doi: 10.1038/ng1990

Wei T, Simko V (2016) corrplot: Visualization of a Correlation Matrix. https://cran.r-project.org/web/packages/corrplot/index.html. Accessed 30 May 2016

Weissman MM, Bland R, Joyce PR, et al (1993) Sex differences in rates of depression: cross-national perspectives. J Affect Disord 29:77–84. doi: 10.1016/0165-0327(93)90025-F

Whitaker L (1914) On the Poisson Law of Small Numbers. Biometrika 10:36–71. doi: 10.2307/2331739

Whiteford HA, Degenhardt L, Rehm J, et al (2013) Global burden of disease attributable to mental and substance use disorders: findings from the Global Burden of Disease Study 2010. The Lancet 382:1575–1586. doi: 10.1016/S0140-6736(13)61611-6

Whitfield Jr HJ, Brady LS, Smith MA, et al (1990) Optimization of cRNA probe in situ hybridization methodology for localization of glucocorticoid receptor mRNA in rat brain: A detailed protocol. Cell Mol Neurobiol 10:145–157. doi: 10.1007/BF00733641

Wickham H, Chang W (2016) ggplot2: An Implementation of the Grammar of Graphics. https://cran.r-project.org/web/packages/ggplot2/index.html. Accessed 30 May 2016

Wu H, Zhang Y (2014) Reversing DNA Methylation: Mechanisms, Genomics, and Biological Functions. Cell 156:45–68. doi: 10.1016/j.cell.2013.12.019

Wu Y, Patchev AV, Daniel G, et al (2014) Early-life stress reduces DNA methylation of the Pomc gene in male mice. Endocrinology 155:1751–1762. doi: 10.1210/en.2013-1868

Yen Y-C, Gassen NC, Zellner A, et al (2015) Glycogen synthase kinase-3β inhibition in the medial prefrontal cortex mediates paradoxical amphetamine action in a mouse model of ADHD. Front Behav Neurosci 67. doi: 10.3389/fnbeh.2015.00067

Yener T, Turkkani Tunc A, Aslan H, et al (2007) Determination of Oestrous Cycle of the Rats by Direct Examination: How Reliable? Anat Histol Embryol 36:75–77. doi: 10.1111/j.1439-0264.2006.00743.x

Zhang B, Chang J, Fu M, et al (2009) Dosage Effects of Cohesin Regulatory Factor PDS5 on Mammalian Development: Implications for Cohesinopathies. PLOS ONE 4:e5232. doi: 10.1371/journal.pone.0005232

Zhang B, Horvath S (2005) A General Framework for Weighted Gene Co-Expression Network Analysis. Stat Appl Genet Mol Biol. doi: 10.2202/1544-6115.1128

Zimmermann CA, Hoffmann A, Raabe F, Spengler D (2015) Role of Mecp2 in Experience-Dependent Epigenetic Programming. Genes 6:60–86. doi: 10.3390/genes6010060

Zimmermann CA, Raabe F, Hoffmann A (2016) Epigenetic Programming of the HPA Axis by Early Life Adversity. In: Spengler D, Binder E (eds) Epigenetics and Neuroendocrinology. Springer International Publishing, pp 115–133

8 Appendix

8.1 Methylation of the CRH gene region

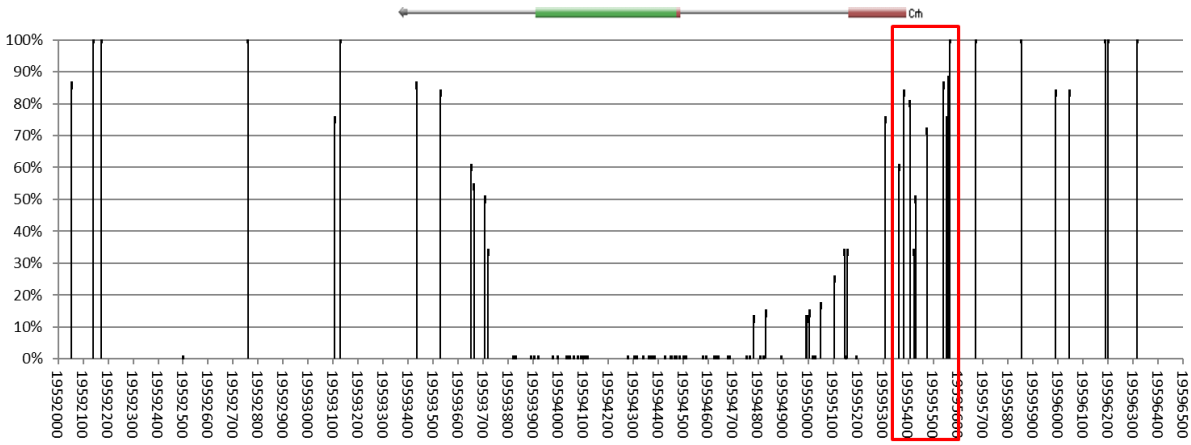

Figure 44: CpG density and methylation level around the CRH gene.
The corticotrophin releasing hormone (Crh) gene is schematically represented at the top (red: untranslated region, green: coding region). The percentage of methylation is depicted according to the genomic position on mouse chromosome 3. Data are derived from NeuN$^+$ cells of 6-week old female mice (http://neomorph.salk.edu/brain_methylomes/browser_mm.html). The red square marks the promoter region with the ten CpGs investigated in this study.

8.2 GR-response eQTL Genes associated with major depressive disorder or schizophrenia

Mouse Gene	Gene Name	Transcript ID	Ensembl Gene ID	Entrez Gene ID	Human Orthologue	GWAS	GWAS p-Value	GWAS SNP
Abcf1	ATP-binding cassette, sub-family F	NM_013854	ENSMUSG00000038762	224742	ABCF1	SCZ	0.000005966	rs885950
Abhd5	abhydrolase domain containing 5	NM_026179	ENSMUSG00000032540	67469	ABHD5	SCZ	0.004019	rs7622109
Anxa2	annexin A2	NM_007585	ENSMUSG00000032231	12306	ANXA2	SCZ	0.01452	rs8041381
Atp5f1	ATP synthase, H+ transporting, mitochondrial F0 complex, subunit B1	NM_009725	ENSMUSG00000000563	11950	ATP5F1	MDD	0.0211	rs1981294
AW209491	expressed sequence AW209491	NM_001104646	ENSMUSG00000039182	105351	C7orf25	SCZ	0.04897	rs639459
Ccndbp1	cyclin D-type binding-protein 1	NM_010761	ENSMUSG00000023572	17151	CCNDBP1	SCZ	0.0007651	rs524908
Cct7	chaperonin containing Tcp1, subunit 7	NM_007638	ENSMUSG00000030007	12468	CCT7	MDD	0.0216	rs12620091
Cd47	CD47 antigen (Rh-related antigen, integrin-associated signal transducer)	NM_010581	ENSMUSG00000055447	16423	CD47	SCZ	0.02181	rs11707455
Commd1	COMM domain containing 1	NM_144514	ENSMUSG00000051355	17846	COMMD1	MDD	0.01837	rs6545924
Dpm2	dolichol-phosphate (beta-D)	NM_010073	ENSMUSG00000026810	13481	DPM2	SCZ	0.0401	rs4075428
Fam117b	family with sequence similarity 117,	NM_001037725	ENSMUSG00000041040	72750	FAM117B	SCZ	0.03867	rs6709463
Fth1	ferritin heavy chain 1	NM_010239	ENSMUSG00000024661	14319	FTH1	MDD	0.03206	rs2956993
Gart	phosphoribosylglycinamide	NM_010256	ENSMUSG00000022962	14450	GART	SCZ	0.002387	rs724208
Gba	glucosidase, beta, acid	NM_008094, NM_001077411	ENSMUSG00000028048	14466	GBA	SCZ	0.0002636	rs11264449
Higd1a	HIG1 domain family, member 1A	NM_019814	ENSMUSG00000038412	56295	HIGD1A	SCZ	0.04127	3-43101876
Hist1h2al	histone cluster 1, H2al	ENST00000613174		667728	HIST2H2AA3, HIST2H2AA4	MDD SCZ	0.01333 0.000000001178	1-148440425
Hmbs	hydroxymethylbilane synthase	NM_001110251, NM_013551	ENSMUSG00000032126	15288	HMBS	SCZ	0.0002048	rs538645
Hmgxb3	HMG box domain containing 3	NM_134134	ENSMUSG00000024622	106894	HMGXB3	MDD	0.02882	rs917585
Impdh2	inosine 5'-phosphate dehydrogenase 2	NM_011830	ENSMUSG00000062867	23918	IMPDH2	MDD	0.01812	rs1873625
Lcn2	lipocalin 2	NM_008491	ENSMUSG00000026822	16819	LCN2	SCZ	0.02056	rs13285411
Mknk2	MAP kinase-interacting serine/threonine kinase 2	NM_021462	ENSMUSG00000020190	17347	MKNK2	MDD	0.03063	rs2395891
Mob3a	MOB kinase activator 3A	NM_172457	ENSMUSG00000003348	208228	MOB3A	MDD	0.03063	rs2395891
Mrpl54	mitochondrial ribosomal protein L54	NM_025317	ENSMUSG00000034932	66047	MRPL54	MDD	0.02239	rs12611262
Mtmr3	myotubularin related protein 3	NM_028860	ENSMUSG00000034354	74302	MTMR3	SCZ	0.005103	rs42931
Ociad2	OCIA domain containing 2	NM_026950	ENSMUSG00000029153	433904	OCIAD2	MDD	0.04318	rs10002500
Pds5a	PDS5, regulator of cohesion maintenance, homolog A (S. cerevisiae)	NM_001081321	ENSMUSG00000029202	71521	PDS5A	SCZ	0.03074	rs6531673
Peli1	pellino 1	NM_023324	ENSMUSG00000020134	67245	PELI1	MDD	0.03645	rs2422008
Pitpnm2	phosphatidylinositol transfer protein, membrane-associated 2	NM_011256	ENSMUSG00000029406	19679	PITPNM2	SCZ	0.0009596	rs12423255
Polr2i	polymerase (RNA) II (DNA directed) polypeptide I	NM_027259	ENSMUSG00000019738	69920	POLR2I	MDD	0.001129	19-40883657

Prmt5	protein arginine N-methyltransferase 5	NM_013768	ENSMUSG00000023110	27374	PRMT5	SCZ	0.02411 rs8015121
Psmb3	proteasome (prosome, macropain) subunit, beta type 3	NM_011971	ENSMUSG00000069744	26446	PSMB3	SCZ	0.008982 rs6607302
Rbm4	RNA binding motif protein 4	NM_009032	ENSMUSG00000096370, ENSMUSG00000094936	19653	RBM4	SCZ	0.01732 rs11227523
Rfx5	regulatory factor X, 5 (influences HLA class II expression)	NM_017395	ENSMUSG00000005774	53970	RFX5	SCZ	0.02759 rs7556661
Rps12	ribosomal protein S12	NM_011295	ENSMUSG00000061983	20042	RPS12	SCZ	0.0218 rs6904470
Rps2	ribosomal protein S2	NM_008503	ENSMUSG00000044533	16898	RPS2	MDD	0.02056 rs7194275
Rps25	ribosomal protein S25	NM_024266	ENSMUSG00000009927	75617	RPS25	SCZ	0.0429 rs10790231
Slc7a7	solute carrier family 7 (cationic amino acid transporter, y+ system), member 7	NM_011405	ENSMUSG00000000958	20540	SLC7A7	MDD	0.008192 rs12432242
Slco3a1	solute carrier organic anion transporter family, member 3a1	NM_023908	ENSMUSG00000025790	108116	SLCO3A1	MDD	0.04023 rs2269799
Snrnp70	small nuclear ribonucleoprotein 70 (U1)	NM_009224	ENSMUSG00000063511	20637	SNRNP70	SCZ	0.03631 rs1559155
Spag9	sperm associated antigen 9	NM_001199203, NM_027569, NM_001025428, NM_001025429, NM_001025430,	ENSMUSG00000020859	70834	SPAG9	SCZ	0.03252 rs2277628
St6galnac4	ST6 (alpha-N-acetyl-neuraminyl-2,3-beta-galactosyl-1,3)-N-acetylgalactosaminide alpha-2,6-sialyltransferase 4	NM_011373	ENSMUSG00000079442	20448	ST6GALNAC4	SCZ	0.03018 rs4075428
Stambpl1	STAM binding protein like 1	NM_029682	ENSMUSG00000024776	76630	STAMBPL1	SCZ	0.0001133 rs10881678
Thbs1	thrombospondin 1	NM_011580	ENSMUSG00000040152	21825	THBS1	SCZ	0.002172 rs4924398
Timm23	translocase of inner mitochondrial membrane 23 homolog (yeast)	NM_016897	ENSMUSG00000013701	53600	TIMM23	SCZ	0.03044 rs4253082
Tm2d1	TM2 domain containing 1	NM_053157	ENSMUSG00000028563	94043	TM2D1	SCZ	0.02172 rs425181
Tmem176a	transmembrane protein 176A	NM_025326, NM_001098271	ENSMUSG00000023367	66058	TMEM176A	MDD	0.03427 rs2072443
Ube2g2	ubiquitin-conjugating enzyme E2G 2	NM_019803	ENSMUSG00000009293	22213	UBE2G2	SCZ	0.04937 rs2329844
Zap70	zeta-chain (TCR) associated protein kinase	NM_009539	ENSMUSG00000026117	22637	ZAP70	SCZ	0.02912 rs17031905
Zfp553	zinc finger protein 553	NM_146201	ENSMUSG00000045598	233887	ZNF48	SCZ	0.01043 rs12443981
Zfp641	zinc finger protein 641	NM_173769	ENSMUSG00000022987	239652	ZNF641	SCZ	0.02616 rs1859441

Table 15: GR-response eQTL Genes associated with major depressive disorder or schizophrenia.

8.3 Batch correction blood

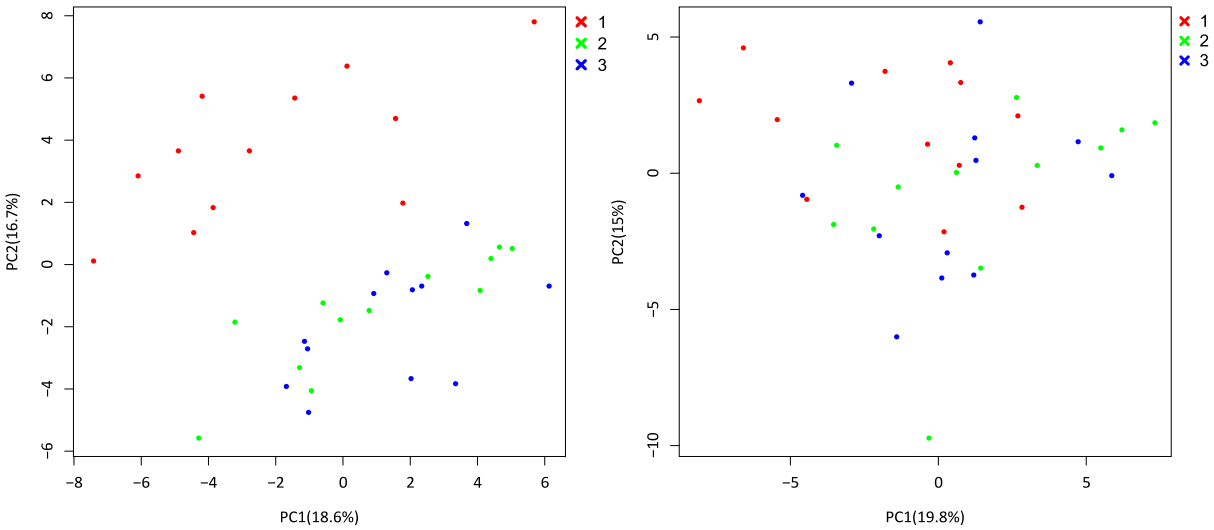

Figure 45: Principal component (PC) plots of the batch correction for MS/Co blood samples.
In the left plot, the samples are colored by RNA extraction batch before surrogate variable analysis; in the right plot, the samples are colored by RNA extraction batch after surrogate variable analysis

9 List of Abbreviations

Abbreviation	
5caC	5-carboxylcytosine
5fC	5-formylcytosine
5hmC	5-hydroxymethylcytosine
5hmU	5-hydroxyuracil
5mC	5-methylcytosine
ACTH	adrenocorticotropic hormone
ADHD	attention deficit hyperactivity disorder
AMY	amygdala
AN	anorexia nervosa
ANOVA	analysis of variance
AP	anterior-posterior
AP1	activator protein 1
ASD	autism spectrum disorder
AVP	arginine vasopressin
BER	base excision repair
BNST	bed nucleus of the stria terminalis
BPD	bipolar disorder
C/EBP	CCAAT/enhancer-binding protein
CA	cornu ammonis
CD	chronic social defeat stress
CD	Crohn's disease
CER	cerebellum
CH_3	methyl group
Co	control
CRE	cAMP response element
CREB	cAMP response element binding protein
CRH	corticotrophin releasing hormone
CRISPR	Clustered Regularly Interspaced Short Palindromic Repeats
CSF	cerebrospinal fluid
DALYs	disability-adjusted life years
dCA1	dorsal hippocampal CA 1 region
dCA3	dorsal hippocampal CA 3 region
dDG	dorsal dentate gyrus
ddH_2O	double-distilled water
DNA	Deoxyribonucleic acid
DNMT	DNA methyl transferase
DV	dorsal-ventral
EH	early handling
ELS	early life stress
eQTL	expression quantitative trait locus
ERE	estrogen response element
FACS	fluorescence-activated cell sorting
FC	fold change
FDR	false discovery rate
GGMs	graphical Gaussians models

GR	glucocorticoid receptor
GWAS	genome-wide association study
HPA	hypothalamic–pituitary–adrenal
HPG	hypothalamic–pituitary–gonadal
IBD	inflammatory bowel disease
IP	intra peritoneal
iPSC	induced pluripotent stem cells
IPTG	isopropyl β-D-1-thiogalactopyranoside
LB	lysogeny broth
LM	limited nesting material
MDD	major depressive disorder
MDS	multidimensional scaling
MeCP2	methyl CpG binding protein 2
ML	medial-lateral
MR	mineralocorticoid receptor
MS	maternal separated
Nac	nucleus accumbens
NER	nucleotide excision repair
nGRE	negative glucocorticoid response element
OCD	obsessive compulsive disorder
OX	ovariectomized female
PBS	phosphate-buffered saline
PC	principal component
PCA	principal component analysis
PF	passing filter
PFC	prefrontal cortex
PND	postnatal day
POMC	proopiomelanocortin
PVN	paraventricular nucleus
RNA	ribonucleic acid
SCZ	schizophrenia
SEM	standard error of mean
SNP	single nucleotide polymorphism
SOB	Super Optimal Broth
SSRI	selective serotonin reuptake inhibitor
SV	surrogate variable
SVA	surrogate variable analysis
TB	Terrific Broth
TDG	thymine DNA glycosylase
TET	ten-eleven translocation
TOP	targeted oligo pool
TS	Tourette's syndrome
vCA1	ventral hippocampal CA 1 region
vCA3	ventral hippocampal CA 3 region
vDG	ventral dentate gyrus
X-Gal	5-bromo-4-chloro-3-indolyl-β-D-galactopyranoside
YY1	transcription factor Yin Yang 1

Eidesstattliche Erklärung

Hiermit erkläre ich, Christoph Andreas Zimmermann, an Eides statt, dass ich die vorliegende Dissertation mit dem Titel „Early Life Stress Regulates Expression Of Risk Genes For Major Depressive Disorder“ selbstständig und ohne unerlaubte Hilfe angefertigt habe. Ich habe weder anderweitig versucht, eine Dissertation einzureichen oder eine Doktorprüfung durchzuführen, noch habe ich diese Dissertation oder Teile derselben einer anderen Prüfungskommission vorgelegt.

München, den 28.06.2017 Christoph Zimmermann .....